UNIVERSITY OF TWENTE.

Faculty of Sciences and Technology

Quantifying pathological synergies in the upper extremity of stroke patients with the use of a multisensory system

Miguel M. C. Bhagubai

M.Sc. Thesis
November, 2019

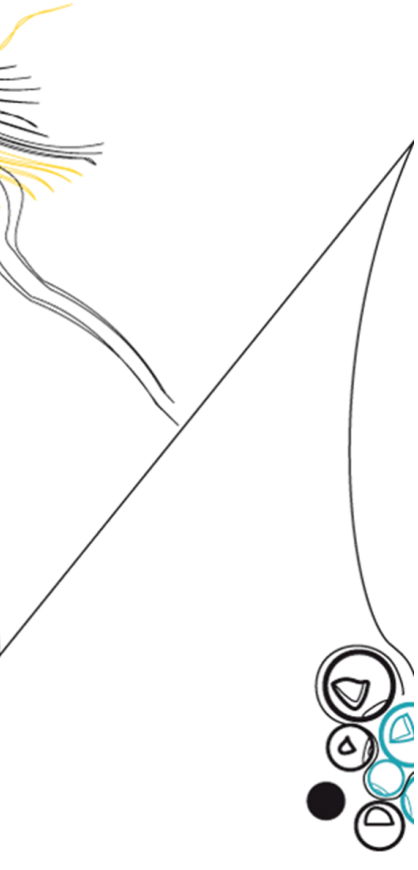

Supervisors:
prof. dr. ir. P. H. Veltink
dr. ir. B. J. F. van Beijnum
G. J. W. Wolterink, MSc
prof. dr. ir. G.J.M. Krijnen

Biomedical Signals and Systems Group
Faculty of Sciences and Technology,
Biomedical Engineering
University of Twente
P.O. Box 217
7500 AE Enschede
The Netherlands

Acknowledgements

The work developed during my master would not be possible without the contribution of a group of people who are or became very significant to me.

First, I would like to thank Prof. Dr. Ir. Peter Veltink for presenting me to the research topic and giving me the opportunity to work on it. I deeply appreciate the guidance and freedom to explore the topic. Moreover, I would like to express my gratitude to Gerjan Wolterink and to Dr. Ir. Bert-Jan van Beijnum for all the support and guidance throughout the work. The constant backup and supervision impacted greatly on my progress as a student and on the quality of the research done.

A special thanks to Anne Schwarz, from the University of Zurich, Switzerland, who prepared and conducted the experiments performed in this research by my side. The shared stress during the experiments period in Zurich was much more enjoyable with your good mood and positivity.

A huge recognition is in order to my close friends who supported me and walked this path alongside me since the beginning of the master. Francisco, who came with me to the Netherlands and shared the office where we worked for several months, with whom I created a bond stronger than I could have imagined. Sara, for showing me that no matter how independent or stubborn I was, help is always needed, and I am so grateful for yours. Joana, for all the friendly fights and crashes, thanks for putting a smile on my face, even in the most stressful times. Inês, for being so attentive and interested in whatever was going on in my life. A huge thanks to all of you, I will forever be grateful for your love and friendship.

I would also like to thank my friends from Portugal for showing me that no matter how far away I am, I will always have someone to lean on.

Last but not least, I would like to express my deepest thankfulness to my family.

≫ Aos meus pais, por todo o apoio e amor incondicional que me deram toda a minha vida. Obrigado por tudo o que fizeram e sacrificaram por mim. Sou quem sou hoje por vossa causa, e espero no futuro chegar a ser mais como vocês. Ao meu irmão que, apesar de nem sempre darmo-nos bem, foi e será o meu protetor e exemplo a seguir. À minha Dadi que nunca deixou de se preocupar e pensar em mim todos os dias. À minha avó que sempre zelou pela minha saúde e bem estar alimentar desde que vim para a Holanda. Um grande obrigado a todos. ≪

Thank you / Dank u wel / Obrigado

Summary

Stroke is the third most common cause of disability in the world, where 5 million patients become permanently disabled. Stroke is caused by a disruption of blood flow in the brain, causing neuronal cell death. Depending on the size and location of the tissue damage, different types of disabilities can be experienced by stroke survivors. Around 80% of stroke patients suffer from motor deficits in the upper extremity, which limits the limbs' functionality. In order to recover motor function, stroke patients resort to rehabilitation.

The rehabilitation process is an extensive and complex procedure due to the diverse and varied types of impairment. In order to increase the efficiency and to evaluate the patients' progress, a proper assessment of motor function is required. The rehabilitation procedure is adapted based on the reassessment of patients through time.

Stroke patients are usually assessed by therapists in a laboratory environment. Several assessment protocols and scales are used to identify and qualify the severity of motor impairments, as well as the level of functional performance of the upper extremity. With the use of assessment scales, therapists are able to score the level of impairment of patients. However, stroke assessment scales are exclusively observer-based, either by a clinician or by self-report. High inter-rater reliability and well defined protocols are required. Inconsistencies in the assessment of the level of impairment can lead to less efficient rehabilitation programs.

Sensor-based technologies have been developed in order to objectively quantify the presence and severity of motor impairments in stroke patients. Kinematic measures of the patient's movement during the assessment procedures provides a detailed and objective measure of motor function and performance. The present thesis focuses on the usability of a multisensory distributed system in measuring abnormal movement patterns in the upper extremity of stroke patients. The main objective of this thesis is the evaluation of a sensor based system that can objectively measure stroke patient's kinematics and identify irregular pathological upper extremity movements.

The multisensory system developed is composed of several Inertial Measurement Units distributed along the trunk, arm and hand. Additionally, force sensors are included in the fingertips of the thumb, index and middle fingers. An electromyographic measuring system is used in parallel in order to measure muscle activity of key muscles of the upper extremity. In this thesis, measurements with the system were performed in stroke patients and a kinematic analysis is presented to extract relevant features for assessing the upper extremity. The system was used in two different scenarios: 1) while stroke patients perform predefined movements of the Fugl-Meyer Assessment scale (a motor function evaluation scale) and 2) while patients

perform reach-grasp-displace tasks of several blocks (with different sizes and weight). The extracted features were used to evaluate the patient's performance and to identify pathological synergistic movements during the movements.

The system's ability of identifying abnormal movements and in characterizing the patient's performance was evaluated. It was found that stereotypical movements related to motor impairments can be measured in both the affected and non-affected upper extremities of stroke patients. The severity of these pathological movements reflected in the kinematic features was also related to the level of impairment of patients according to the severity score given by a therapist (Fugl-Meyer Assessment Score). It was found that the system can measure a higher coupled activity of the shoulder and elbow joints when the tasks are performed with the affected arm (directly related to the level of pathological muscle coupling). In the functional reach-grasp-displace tasks, the more affected patients showed to adopt more compensation strategies in order to successfully displace the different objects. The size of the object was shown to affect the posture of the hand and the way patients grasp it. The weight of the object had an effect on the level of compensation that patients use.

The use of the multisensory system has made it possible to analyse detailed movement patterns and arm postures during the clinical assessment evaluation of the upper extremity of stroke patients. The usage of this system in the clinic can provide a better and objective evaluation of the severity of motor impairments. However, the presented methods need to be further tested in a larger population. The presented kinematic features can also be extended to fully characterize the patient's motor function and performance. Nevertheless, the system has great potential to complement the clinical evaluation of stroke patients.

Contents

Chapter 1

General Introduction

Stroke (or cerebrovascular accident) has been far studied throughout the years, and it can be characterized as an abnormal blood supply to the brain, resulting in irreversible cell death. The most common types of stroke are ischemic (partial or complete blockage of a blood vessel) and haemorrhagic stroke (rupture of a vessel in the brain) [1]. Ischaemic stroke accounts for 85% of of all strokes. The disruption of blood flow in the brain affects the energy consumption processes of neuronal cells, and consequently, tissue damage, leading to its death depending on the duration of the deprivation. The region of reduced blood flow, also referred to as the infarct zone, is where the minimum levels of blood flow are below the required for maintaining cell viability. The brain tissue surrounding the infarct zone is structurally undamaged, but the cell activity is reduced. This region is called penumbra, and if the flow is not restored in time, it will cause cell death, increasing the infarct region [2].

Globally, stroke is the second most common cause of death and the third prevalent cause of disability [3]. According to the World Health Organization, 15 million people suffer from stroke annually. Of these, around 5.5 million die and 5 million become permanently disabled [1]. The disability outcomes caused by stroke can be very different in between patients. The long-term effects depend greatly on the size and location of the brain lesion. Common disabilities present in stroke survivors is lower and upper limbs motor deficits, cognitive dysfunction, impaired consciousness and dysphagia [4]. About 80% of patients suffer from motor impairments, affecting their ability to control movements and limiting mobility [5]. The majority of stroke survivors suffer from unilateral motor deficits. Specific lesions locations are associated with different types of impairments. Many stroke lesions affect several areas from the sensorimotor cortex and, consequently, the patients develop multiple impairments, depending on the size of the damaged area [2]. Muscle weakness or paralysis is the main impairment that leads to non-use of the affected limbs. Increased spasticity, muscle stiffness and stroke-related pain are additional factors that lead to immobility and loss of function [6]. When performing voluntary movements with the affected side of the body, the damages in the neural pathways cause an interruption on the recruitment of muscles, causing a reduced ability to perform coordinated movements. The coordination of muscles is defined as synergy, and due to the impairments caused by stroke, muscle patterns have an abnormal behaviour in patients, where the loss of independent joint control affects the movement pattern [7]. The

loss of fractionated movement has been shown to be a specific type of impairment, and is not related to weakness, muscle co-contraction or spasticity [8]. The presence of multiple impairments lead to a learned bad use of the limb, and give rise to several compensation strategies to complete functional tasks. Although the success in completion of tasks due to the compensatory actions adopted by the patient increases, motor performance decreases and recovery is limited regardless the amount of therapy [9].

Assessment of Motor Function

The recovery process for stroke patients is a very complex process. The level of motor recovery occurs due to several different factors and is highly patient-specific. A majority of stroke patients with motor disabilities resort to rehabilitation in order to recover functional performance, independence and increased quality of life [10]. Stroke rehabilitation has the form of a cyclical process, where the patients are firstly assessed to identify the types of impairments and to quantify its severity, secondly the prospective goal for improvement is defined, thirdly the therapeutic interventions are applied based on the assessments made, and finally a reassessment is done to monitor the patient's progress and to adjust the treatment protocol, if needed [11]. Difficulties that affect the process of motor rehabilitation are related to the non-stationary type and nature of the impairments and to the possible existence of multiple impairments at the same time. The treatment process is then hard to define throughout the progression of the recovery [6]. Assessment of human functioning if of high importance in order to evaluate the different aspects of the pathological motor behaviours and to apply a well structured therapy plan. Several clinical assessments were developed to evaluate the level of the different types of impairments. Their heterogeneity creates difficulties in creating a single standardized assessment method to determine which disabilities, and to what extent, are present after stroke. In order to categorize disabilities of stroke patients, the International Classification of Functioning, Disability and Health (ICF) [12] is of relevance. Disabilities of stroke patients can be differentiated in three categories: body functions and structures, activities and participation (figure 1.1). The ICF model gives context to all human functioning, taking in account personal and environmental factors. Clinical assessment of motor performance is used to evaluate the level of body function and activity [13] [14] [15]. Usually, on the body structure and function level, these types of assessment describe the patient's range of motion, strength and smoothness of the movement. Other clinical tests are used to evaluate the patient's performance in completing certain tasks, which is related to the activity level. This thesis focuses on assessment of motor function of stroke patients, in particular of the upper extremity.

The most common clinical assessment scale used for assessing impairments in body function is the Fugl-Meyer Assessment (FMA) scale [17]. The Fugl-Meyer scale is a stroke specific test designed to assess motor and joint function, sensation qualities and balance in hemiplegic stroke patients [18]. This assessment scale was developed in 1975, and it is still widely used today. It is considered the gold standard scale, and is used as a reference for the validity of other motor function scales. The FMA scale contains five domains: motor function of

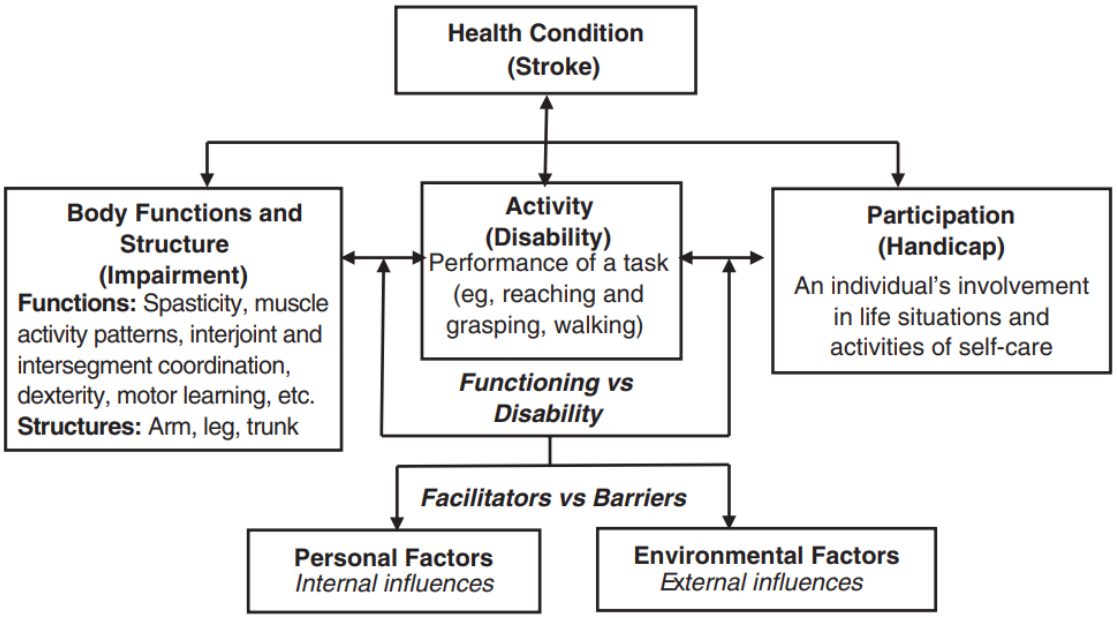

Figure 1.1: ICF core set for stroke [16]

the upper and lower extremity, sensory function, balance, joint range of motion and joint pain. The motor domain is based on Twitchell's [19] and Brunnstrom's [20] description of motor recovery following stroke. It is documented that motor function restoration follows a predictable sequence starting with an initial flaccid paralysis, followed by the restoration and hyperactivity of reflexes, increased muscle tone and spasticity, voluntary movement emerges with the presence of pathological synergies and, finally, normalization of muscle tone and reflexes [21]. The different domains can be evaluated separately, and depending on the evaluated section, different scores can be given to a patient's performance. The motor function domain is subdivided into upper and lower limb. Each item of the test is scored with a three point ordinal scale, where 0 is the equivalent of not being able to perform the movement, 1 is given when the patient performs the movement partially, and 2 when it is fully executed. The upper extremity subsection contains 33 different items, so a maximum of 66 points can be given. The item order is organized from proximal (shoulder) to distal (finger) body segment evaluation, which is the order of recovery described by Twitchell. Although reliability and validity of the FMA scale has been shown to be very high, it is limited by a ceiling effect. Also, it does not evaluate activity levels of patients, and it is recommended to use this scale in conjunction with clinical assessments focused on activity instead of impairments [21].

There are several tests that evaluate motor performance when completing functional tasks. These measures relate to the activity levels of patients. Usually, separate tests for the upper and lower limb are used, but there are scales that cover both upper and lower extremities of the body [15]. A very common assessment test scale for the upper extremity is the Action Research Arm Test (ARAT) [17]. The ARAT was originally developed in 1981 by Lyle [22], and it was derived from the Upper Extremity Function Test (UEFT) proposed by Carroll [23] in 1965. It is composed of 19 items subdivided into four subscales: grasp, grip, pinch and

gross movement. Each item is evaluated with a four point ordinal scale ranging from 0 to 3, where 0 is awarded if the patient cannot produce any movement, and 3 when the task is done completed with normal performance. Scoring takes in account both the duration and functional performance. If the patient completes a task but in a longer period of time, the highest score is not awarded. The order of the items starts with the most difficult task, where if the patient is scored with the maximum value, all the following tasks in the subsection are equally awarded. If not, the easiest task follows. In case the patient is scored with the minimum value on the easiest task, all the subsequent items are discarded and scored the same. The maximum score given to the ARAT scale is 57, and it requires a specific set of objects and a standardized protocol to be applied in the clinic [24]. The ARAT's test reliability and validity has been assessed and compared to the FMA scale [25]. It was found that the ARAT has both a ceiling and floor effects. In patients with severe impairments or near normal performance, the scale is not sensitive enough. It is most appropriate when used in patients with moderate to severe hemiparesis. In another study, it was found that the ARAT measures cannot be transformed into interval scores, showing that the scale only provided a rank evaluation of the patients [26]. The amount of change in score is not equivalent to the amount of functional improvement.

1.1 Motivation

Many of the clinical measurements are exclusively observer-based, either by a clinician or by self-report, and ordinal scales. They mostly describe what movements can be performed and what activities can be completed without taking in account the qualitative value of the task. Time-related assessments, where the duration to complete a task is taken in account, do not consider compensation strategies that increase the completion time, but do not actually translate to improvement of body function. The presence of either ceiling or floor effects is a limiting factor in some scales (in particular the FMA and the ARAT). Additionally, some assessment methods require strict protocols for having a good reliability. The clinician needs to get training in order to evaluate correctly the different patients. The chance for a systematic bias is higher if the training is not performed, or if the protocol is not well defined. More objective and qualitatively methods for evaluation of motor performance are needed.

Objective Assessment of Motor Function and Performance

Many researchers have explored the use of motion capture techniques to evaluate human kinematics and kinetics, either with the use of optical systems in movement laboratories, or with wearable sensors [27]. Optical motion tracking systems are considered to be the gold standard in measuring body movements due to its high accuracy in estimating positions. These types of systems use several infrared cameras and markers to track key positions of the different joints. The movement is reconstructed by estimating the position of the markers. A major drawback is the high cost of the cameras and the need of a special laboratory. The camera's calibration is a long process, and if not done properly, the kinematic reconstruction is affected due to the inability to track the markers. The cameras should also be completely

stable during the movements. More recently, advances in technology created more affordable, markerless, commercial movement cameras. These systems were, however, not designed to be used for clinical assessment. Although affordable camera systems have potential for therapy applications (by gamifying rehabilitation tasks, becoming more user friendly and motivating the patient's participation), the levels of accuracy are not sufficient to precisely measure human movement.

Wearable sensors have been used extensively in clinical research for several different applications. With the use of inertial measurement units, which include accelerometers, gyroscopes and/or magnetometers, it is possible to extract multiple features that help quantifying objectively human motion and its performance. These sensors are relatively small, cheap and portable. Inertial sensing can provide a more sensitive way to evaluate motor control and enhance diagnostic accuracy. The technological advances on this type of sensors has been able to reduce the errors in estimating orientations and positions with the development of calibration methods and sensor fusion algorithms for noise and drift reduction in the measurements [28]–[30].

In addition to kinematics, it is viable to study the interaction of the body with the surrounding environment. In patients, the use of additional sensors can give insight on the way they interact with objects. Force sensors can provide information on how a stroke patient grasps a certain object. Force production on the fingers is affected by stroke and the resulting weakness causes loss of functional performance [31]. Measuring kinetics provides an evaluation of dexterity in the hand and ability to perform different grasping tasks. Kinematic and kinetic measurements can not evaluate spasticity or muscle weakness objectively. There is a correlation of weakness and muscle abnormal co-activation patterns with the movement profile, but kinematic measurement alone can not distinguish the level of these impairments present in patients [32], [33].

To solve the limitations of current clinical assessments, the use of inertial measurement units, force sensors and EMG measurements become a possible solution. To tackle this, a multisensory system was designed, and included: 1) kinematic sensors (inertial measurement units), designed to be distributed along the sternum, shoulder, upper and lower arms, hand and thumb, index and middle fingers; 2) force sensitive resistors intended to be placed on the fingertips of the thumb, index and middle fingers; 3) a separate EMG recording device to measure muscle activity of several arm muscles. The main motivation of the work presented is to find quantitative features to objectively assess upper extremity motor performance and function, to be used in addition to current subjective clinical scales.

1.2 Framework

The presented work is part of the SoftPro European project (European Union's Horizon 2020 research and innovation programme, grant agreement No. 688857), with a research objective of assisting people with upper limb amputations or motor disabilities. A sensing system for assessing motor function was developed at the Biomedical Signals and Systems group of the University of Twente, Netherlands, with the collaboration of the Department of

Neurology of the University Hospital Zurich (UZH), Switzerland. This thesis project focused on the application and clinical evaluation of the system in stroke patients and its usability in objectively quantifying pathological synergies and motor dysfunction.

1.3 Research questions

Following the introductory section, with the development of a multisensory system for assessment of the upper limb of stroke patients, some questions arise:

1. Can the multisensory distributed system differentiate the affected arm from the non-affected in stroke patients while performing defined movements designed to assess motor function (FMA protocol)?
2. Do the objective kinematic features measured by the distributed system during the FMA protocol relate with the level of impairment dictated by the clinical scores of the patients?
3. Can the system differentiate the affected arm from the non-affected in stroke patients while performing functional reach-to-grasp movements?
4. Is the system able to quantify compensation strategies adopted by stroke patients when performing functional movements?
5. Does the size and weight of the objects in reach-to-grasp tasks influence the movement pattern of the patients' upper extremity?
6. Do the objective kinematic features measured by the distributed system during functional tasks relate with level of impairment dictated by the clinical scores of stroke patients?

1.4 Report organization

The following report is organized in 4 different chapters:

- Chapter 1 is intended to give a general overview on stroke and to set an initial understanding on the subject. The problem statement is defined and the motivation for the research done is expressed.
- Chapter 2 includes the detailed description of the methods used in the kinematic reconstruction of the upper extremity and trunk by the distributed IMU system. The main data processing methods used in this work are explained and an evaluation on the system's validity is done.
- Chapter 3 refers to a first approach on the problem. The distributed measuring system is used in a usability study, where the hypothesis that it is possible to use quantitative kinematic features to evaluate upper limb function is tested, and research questions

1 and 2 are answered. The system is used in a clinical setting following the FMA procedure. Conclusions on its ability to differentiate affected and non-affected limbs with the quantitative features are taken, and it is compared to the clinical FMA scores. The structure of this chapter follows the structure of a journal paper, and it is intended to be published. The methodology used for the kinematic reconstruction and for the extraction of the relevant features to analyse the patients' movements is repeated in a summarized way.

- In Chapter 4, the same experimental setup is used but with a different protocol. Here, the ARAT test protocol is used. A reach-to-grasp task is done, with several objects that vary in size and weight. The purpose of this chapter is to answer questions 3, 4, 5 and 6 (questions 3 and 6 are similar to questions 1 and 2 but in a different setting).

- Finally, Chapter 5 includes a general discussion and conclusion, as well as a future perspective on the subject, reflection of the main objectives of this thesis and the work done.

Chapter 2

Kinematic reconstruction

The main part of this thesis is focused on the analysis of movement with the distributed measuring system. Several methods exist to analyse the measures of the sensors in order to reconstruct the movement done by the user of the system. The following chapter describes the methods used in this work to reconstruct the kinematic data of the inertial sensor units of the distributed system and to extract the relevant features used in the analysis of the movement.

The measurement system is composed of 8 inertial measurement units (IMU) that include both accelerometers and gyroscopes. Figure 2.1 shows how the system is mounted onto the sternum and upper extremity of a person.

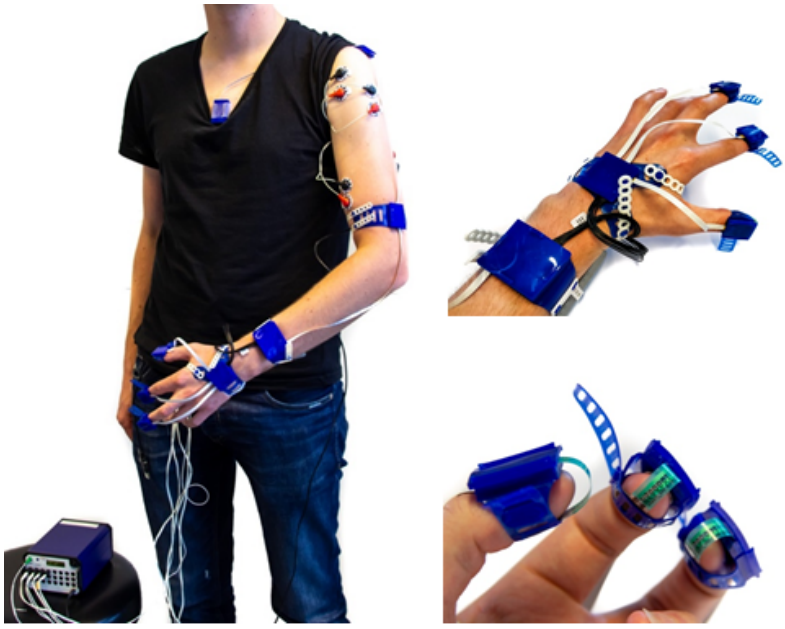

Figure 2.1: Distributed IMU system.

The IMUs allow measuring the acceleration and angular velocity over time. With this data, it is possible to recreate the kinematics of each sensor, and consequently, of each correspondent limb segment where the IMU is placed. The kinematic reconstruction of the movements of the sensors is based on the orientation estimation of each one. The orientation

of the sensors is calculated usually by integrating the angular velocity measurements in order to find the angular change between time points. Several algorithms have been developed in order to optimize the orientation estimation and reduce errors. Here, the Madgwick filter [34] was used in order to extract the sensor's orientation (more details in the following sections of this chapter). However, the sensor's orientation does not correspond exactly to the limb segment's orientation, since its placement is not perfectly aligned with the anatomical frames of the upper extremity. To tackle this problem, a sensor-to-segment calibration is performed. The following flowchart summarizes the steps taken to estimate the limb segment's orientation of the distributed measuring system:

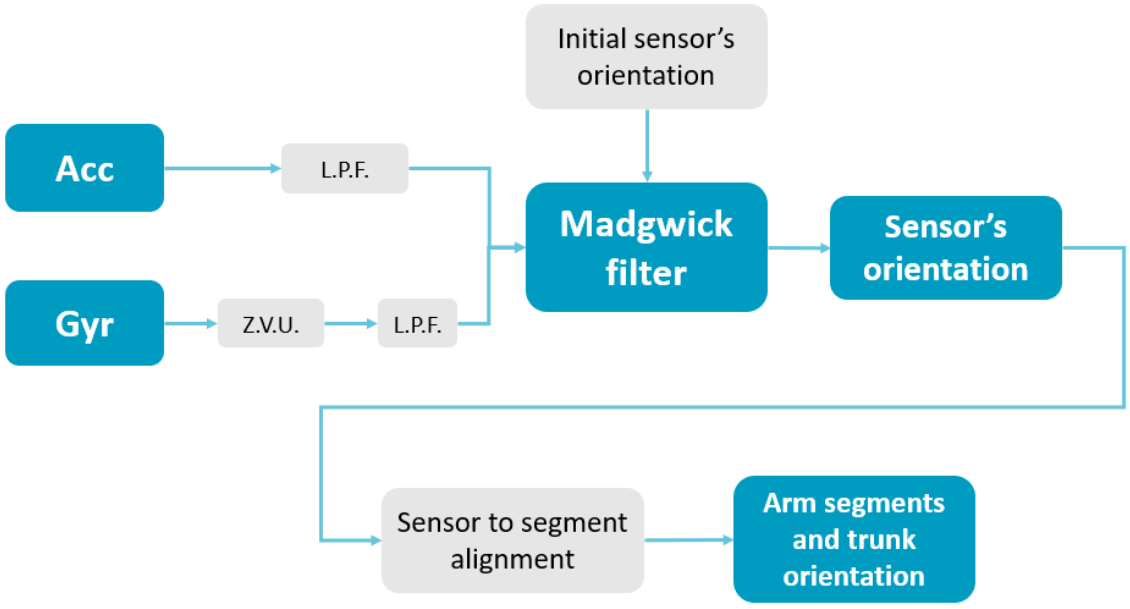

Figure 2.2: Flowchart presenting the steps taken to estimate the limb segment's orientation from the IMU measurements.

The first step taken is the processing of the accelerometer (acc) and the gyroscope (gyr) data. Both are low pass filtered with a Butterworth filter with a cut-off frequency of 10 Hz (L.P.F.). A zero velocities update (ZVU) is also applied to the gyroscope data. Here, if the sensor is considered static (if the norm of the angular velocity is smaller than $3°/s$), the offset is removed. This method was based on the work of Kirking et al. [35]. The beginning and end of the static periods is identified and the linear trend is removed. The zero velocities update is used in order to decrease the effects of drift and noise present in the gyroscope data, which influences the sensor orientation estimation.

2.1 Sensor Orientation Estimation

The inertial sensors used in this study included tri-axial accelerometers and gyroscopes, enabling measuring the acceleration and angular velocity. The gyroscope allows measuring the angular rate change of the sensor. If the angular velocity is integrated over time, by knowing

the initial conditions, the orientation of the sensor is computed. The measurement errors, such as noise and bias caused by physical changes in the environment or non-optimal calibration of the sensors, are accumulated in the orientation estimation when integrating the angular velocity, causing large deviations from the sensors' real orientation. The accelerometers, by measuring the earth's gravitational field, provide information about the inclination of the sensor. In sensors that also incorporate magnetometers, a second reference is available, since they measure the earth's magnetic field. Different types of algorithms have been used in order to correct the orientation estimation via gyroscope integration by optimally fusing the measurements of the different sensors. In this work, the Madgwick filter [34] was used. This filter uses acceleration and magnetometer measurements as a reference to correct for drifts in the orientation estimated by the gyroscopes. For this, a gradient descent algorithm is used to correct the orientational drifts caused by the gyroscope measurement errors. It is computationally efficient and was proven to have a comparable accuracy in estimating orientations as Kalman-based filters [34].

The Madgwick filter estimates the orientation in a quaternion representation, where the rotation of a certain frame A to a different frame B is defined as a rotation of angle θ around an axis $\vec{r}^A$ defined in frame A:

$$ {}^{A}q_{B} = [q_w \; q_x \; q_y \; q_z] = [\cos\frac{\theta}{2} \; -r_x \sin\frac{\theta}{2} \; -r_y \sin\frac{\theta}{2} \; -r_z \sin\frac{\theta}{2}] \tag{2.1} $$

This way, given the initial orientation of the sensor q_{init}, the angular change in time is given by the fusion of the orientation calculated by integrating the angular velocity and optimizing it with the tilt measured with the accelerometers and the heading given by the magnetometers. For every accelerometer and gyroscope measurement at a certain time point t, an associated quaternion q_t is calculated that corresponds to a rotation of the sensor's frame in space in the specific time point.

2.1.1 Global frame definition

As it was said before, the IMUs used in this work did not include magnetometers in all of the sensors. Due to this, only the gyroscope and accelerometer values were used to compute the orientation. Since there is only one reference vector (earth's gravity field), it is not possible to define a common global frame for all sensors. However, this frame is needed to define the initial orientation of the sensors to be used in the kinematic estimation of the whole movement. Without a common global frame, the orientation of the sensors would be independent of each other and it would not be possible to estimate the real orientation of the arm.

The solution is to define the axes of the global frame by performing common movements in all the sensors. The method used was based in [36]. The rotation matrix from the global frame to sensor S can be written as:

$$ {}^{G}\mathrm{R}_{S} = \; {}^{S}\mathrm{R}_{G}^{T} \; = [{}^{s}\vec{x_g} \; {}^{s}\vec{y_g} \; {}^{s}\vec{z_g}]^T \tag{2.2} $$

Where ${}^s\vec{x_g}$, ${}^s\vec{y_g}$ and ${}^s\vec{z_g}$ are the representation of the global frame's axes with respect to the sensor s.

The first action used to define the global frame is static and it involved measuring the acceleration of all sensors when the subject was standing still with the arm fully stretched along the side of the body and the fingers extended, pointing down. The gravity vector measured by the accelerometers defines the vertical axis of the global frame relative to the sensor s:

$$ {}^s\vec{z_g} = \frac{median(\vec{a_s})}{||median(\vec{a_s})||} \tag{2.3} $$

The second action is dynamic and intended to measure a common horizontal axis. The subject was asked to do a trunk flexion movement, with the arm accompanying the flexion as a rigid body. The angular velocity is measured and the horizontal axis of the global frame relative to the sensor s is defined:

$$ {}^s\vec{y_g} = \frac{median(\vec{\omega_s})}{||median(\vec{\omega_s})||} \tag{2.4} $$

The third axis is given by the cross product between the other two:

$$ {}^s\vec{x_g} = {}^s\vec{y_g} \times {}^s\vec{z_g} \tag{2.5} $$

The estimated ${}^s\vec{y_g}$ may not be perpendicular to the vertical axis ${}^s\vec{z_g}$ obtained from the gravity vectors. Therefore, a correction is made by taking the cross product between ${}^s\vec{z_g}$ and ${}^s\vec{x_g}$ (which are two perpendicular axes):

$$ {}^s\vec{y_g} = {}^s\vec{z_g} \times {}^s\vec{x_g} \tag{2.6} $$

Figure 2.3 represents a schematic of the two movements. After the calibration, each sensor will have a rotation matrix ${}^G\mathrm{R}_S$ that represents its orientation relative to the common global frame when the subject is standing still with the arm and fingers stretched and pointing down.

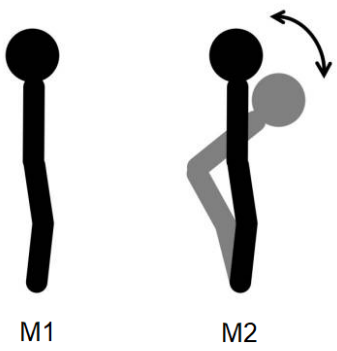

Figure 2.3: Static (M1) and dynamic (M2) movements used in the global frame definition.

2.1.2 Initial orientation

The lack of a horizontal reference, provided by the earth magnetic field, does not allow for the correction of heading errors in the sensors orientation. To reduce these errors caused by drift in the gyroscope, the kinematic reconstruction of each movement in the protocol was done individually. By instructing the subject to start and end the tasks always in the same posture, the orientation estimation is then "reset", eliminating drift errors that could be accumulated.

The subject is asked to immediately go to the initial position after performing the movements used to define the global frame. The orientation of the sensors is estimated in the transition period from the straight static position to the starting pose, using ${}^{G}\mathrm{R}_{s}$ as the initial orientation for the estimation. The orientation of the IMUs at the end of this estimation is used as the initial orientation for the movements ${}^{G}\mathrm{R}_{s_{init}}$.

2.2 Sensor-to-segment Calibration

The sensor-to-segment calibration procedure is based on the acquisition of data while the subject is in defined static postures or during dynamic movements. The principle is that measurements of the gravity vector by the accelerometer when the limb segment is in a defined posture represents an axis of the anatomical frame of the respective limb; likewise, measurements of the sensor's angular velocity during a defined dynamic movement also represent an axis of the anatomical frame of one limb segment. The definition of the anatomical frames is depicted in Figure 2.4.

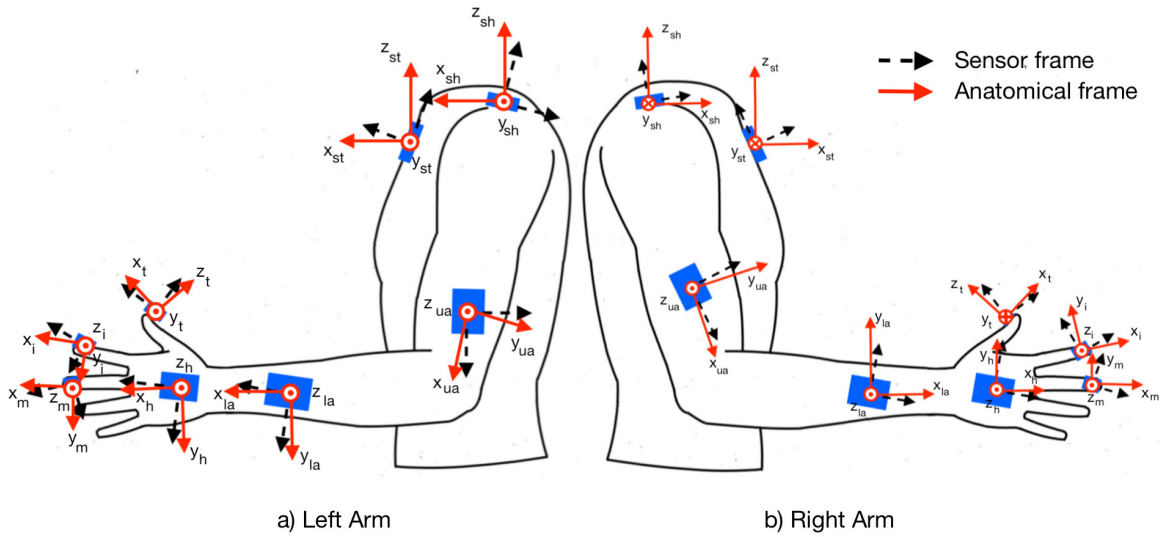

Figure 2.4: Sensor's frames and correspondent anatomical frames of the eight different IMUs of the measurement system. Subfigure a) shows the frames in the left arm, and subfigure b) in the right arm.

The chosen postures/movements for this calibration were based on previous work done

by Luinge et al. [37] and Ricci et al. [38]. Each posture/movement is used to define one of the axes of the respective limb segment. The global frame definition protocol is an alternative way of aligning the sensors to the limb segments. However, it is not accurate enough to find every anatomical frame. The fact that it is a general movement of the trunk and the whole upper extremity causes deviations between the axis measured by the sensors and the anatomical axis. For example, if the elbow, wrist and fingers are not fully extended, the gravity vector measured by the accelerometers will not correspond to the longitudinal axes of these limb segments.

The following table 2.1 indicates which anatomical axis is defined with each calibration movement:

Table 2.1: Anatomical axes of the left and right arms defined by each item of the sensor-to-segment calibration protocol.

	Calibration Position/ Movement	**Anatomical Axis Left Arm**	**Anatomical Axis Right Arm**
1	Static hand flat on a table	$\vec{z_h}$, $\vec{z_i}$, $\vec{z_m}$	$\vec{z_h}$, $\vec{z_i}$, $\vec{z_m}$
2	Static hand sideways, with elbow flexed 90°	$-\vec{y_h}$, $-\vec{y_i}$, $-\vec{y_m}$	$\vec{y_h}$, $\vec{y_i}$, $\vec{y_m}$
3	Static thumb flat on a table	$\vec{z_t}$	$\vec{z_t}$
4	Static thumb sideways, with hand pronated	$\vec{y_t}$	$-\vec{y_t}$
5	Static forearm and hand palm faced down	$\vec{z_{la}}$	$\vec{z_{la}}$
6	Wrist pronation, starting form supinated position	$\vec{x_{la}}$	$-\vec{x_{la}}$
7	Static shoulder adducted, with elbow flexed	$-\vec{x_{ua}}$	$-\vec{x_{ua}}$
8	Static shoulder abducted 90° with elbow flexed	$\vec{z_{ua}}$	$\vec{z_{ua}}$
9	Static straight neutral pose, arm along the body	$\vec{z_{sh}}$, $\vec{z_{st}}$	$\vec{z_{sh}}$, $\vec{z_{st}}$
10	Trunk flexion (arm moving along the upper body)	$\vec{y_{sh}}$, $\vec{y_{st}}$	$-\vec{y_{sh}}$, $-\vec{y_{st}}$

Items 6 and 10 are the only dynamic movements in the calibration protocol. Similarly to the global frame definition, a median filter is applied to the accelerometer data during the static positions or to the gyroscope data during the dynamic movements in order to get the anatomical frame relative to the sensor's frame:

$$\vec{v_{seg}} = \frac{median(\vec{a_s})}{||median(\vec{a_s})||} \qquad \text{or} \qquad \vec{v_{seg}} = \frac{median(\vec{\omega_s})}{||median(\vec{\omega_s})||} \tag{2.7}$$

Where $\vec{v_{seg}}$ is the anatomical axis relative to the sensor s, and $\vec{a_s}$ and $\vec{\omega_s}$ are the accelerometer and gyroscope measurements in the respective calibration static position or dynamic movement respectively. The orientation of the segments' coordinate frame relative to the sensor's coordinate frame is given by a rotation matrix that contains three vectors that correspond to the anatomical axis of the segment, expressed in the sensor:

$$^{S}\mathrm{R}_{Seg} = [\vec{x_{seg}}\ \vec{y_{seg}}\ \vec{z_{seg}}] \tag{2.8}$$

The sensor-to-segment protocol defines two axes by measurements of either the accelerometer or gyroscope. The third axis can be found by taking the cross-product of the two. Because

the two axes of the respective segment are defined by measurements, they may not be exactly orthogonal due to measurement errors. With the items of the calibration protocol chosen, two scenarios can occur: 1) the two axes are defined by accelerometer measurements; 2) one axis is defined by the gyroscope measurement and the other by the accelerometer. In scenario 1, the variance of the two accelerometer measurements is taken, and the one that shows lower variance is considered the more stable and correct. In scenario 2, the gyroscope measurement is taken as the correct one. The other axes is adjusted to ensure an orthonormal coordinate system.

For the hand, thumb, index and middle fingers IMUs, the two axes defined by the measurements are the y- and z-axis. In this case, the x-axis is given by the cross product of of the y-axis with the z-axis:

$$ {}^{S}\mathrm{R}_{Seg} = \begin{cases} \begin{bmatrix} \vec{y_{seg}} \times \vec{z_{seg}} & \vec{y_{seg}} & (\vec{y_{seg}} \times \vec{z_{seg}}) \times \vec{y_{seg}} \end{bmatrix} & \text{if} \quad \sum Var(\vec{y_{seg}}) < \sum Var(\vec{z_{seg}}) \\ \begin{bmatrix} \vec{y_{seg}} \times \vec{z_{seg}} & \vec{z_{seg}} \times (\vec{y_{seg}} \times \vec{z_{seg}}) & \vec{z_{seg}} \end{bmatrix} & \text{if} \quad \sum Var(\vec{y_{seg}}) > \sum Var(\vec{z_{seg}}) \end{cases} \tag{2.9} $$

where $seg = h, i$ or m.

For the lower arm IMU, the anatomical x-axis is given by the angular velocity measurements during movement 6 and the z-axis is given by the accelerometer measurements during 5. The rotation matrix from the sensor s_{la} to the anatomical frame la is then:

$$ {}^{s_{la}}\mathrm{R}_{la} = \begin{bmatrix} \vec{x_{la}} & \vec{z_{la}} \times \vec{x_{la}} & \vec{x_{la}} \times (\vec{z_{la}} \times \vec{x_{la}})) \end{bmatrix} \tag{2.10} $$

The upper arm IMU calibration movements define the x-axis and the z-axis with accelerometer measurements. The sensor-to-segment rotation matrix from the sensor s_{ua} to the upper arm ua is given by:

$$ {}^{s_{ua}}\mathrm{R}_{ua} = \begin{cases} \begin{bmatrix} \vec{x_{ua}} & \vec{z_{ua}} \times \vec{x_{ua}} & \vec{x_{ua}} \times (\vec{z_{ua}} \times \vec{x_{ua}}) \end{bmatrix} & \text{if} \quad \sum Var(\vec{x_{ua}}) < \sum Var(\vec{z_{ua}}) \\ \begin{bmatrix} (\vec{z_{ua}} \times \vec{x_{ua}}) \times \vec{z_{seg}} & \vec{z_{ua}} \times \vec{x_{ua}} & \vec{z_{ua}} \end{bmatrix} & \text{if} \quad \sum Var(\vec{x_{ua}}) > \sum Var(\vec{z_{ua}}) \end{cases} \tag{2.11} $$

Finally, the shoulder and sternum IMUs anatomical frames are defined by the y-axis measured with the gyroscopes and the z-axis measured with the accelerometer. The rotation matrix is given by:

$$ {}^{S}\mathrm{R}_{Seg} = \begin{bmatrix} \vec{y_{seg}} \times \vec{z_{seg}} & \vec{y_{seg}} & (\vec{y_{seg}} \times \vec{z_{seg}}) \times \vec{y_{seg}} \end{bmatrix} \tag{2.12} $$

where $seg = sh$ or st.

2.3 Limb Segment Orientation

With the definition of the global frame, initial orientation and sensor-to-segment alignment rotation matrices, it is finally possible to estimate the limb segment's orientation for each task

of the experimental protocol. Given the initial conditions for the Madgwick filter ${}^{G}\mathrm{R}_{S_{init}}$, with a filter's gain β set to 0.05, and the accelerometer and gyroscope data of the sensor during the movement, the orientation of the sensors is estimated.

The Madgwick filter estimates the orientation in quaternion form, so the initial condition ${}^{G}\mathrm{R}_{S_{init}}$ is converted from rotation matrix to quaternion ${}^{G}q_{S_{init}}$ according to Shepperd's method [39]. The output of the filter is a quaternion for each time point that corresponds to the orientation of the sensor relative to the global frame ${}^{G}q_{S}(t)$.

To get the orientation of the limb segment, the sensor-to-segment calibration parameters are applied. Firstly, the orientation of the sensor is converted from quaternion to rotation matrix by the following formula [40]:

$$ {}^{G}\mathrm{R}_{S}(t) = \begin{bmatrix} 2q_w^2 - 1 + 2q_x^2 & 2q_xq_y - 2q_wq_z & 2q_xq_z + 2q_wq_y \\ 2q_xq_y + 2q_wq_z & q_w^2 - 1 + 2q_y^2 & 2q_yq_z - 2q_wq_x \\ 2q_xq_z - 2q_wq_y & 2q_yq_z + 2q_wq_x & q_w^2 - 1 + 2q_z^2 \end{bmatrix} \tag{2.13} $$

Where ${}^{G}\mathrm{R}_{S}(t)$ is the orientation of the sensor S at time t, and ${}^{G}q_{S}(t) = [q_w\ q_x\ q_y\ q_z]$ is the same orientation in quaternion representation.

Finally, the limb segment orientation at time t is given by:

$$ {}^{G}\mathrm{R}_{Seg}(t) = {}^{G}\mathrm{R}_{S}(t)\ {}^{S}\mathrm{R}_{Seg} \tag{2.14} $$

2.4 Arm Joints and Trunk Compensation Angles Calculation

The arm joint angles can be represented as the angle between the anatomical axes aligned with the respective limb segments. The anatomical frames seen from the global frame are represented by the columns of the rotation matrices calculated in the orientation estimation:

$$ {}^{G}\mathrm{R}_{Seg}(t) = \begin{bmatrix} x_1 & y_1 & z_1 \\ x_2 & y_2 & z_2 \\ x_3 & y_3 & z_3 \end{bmatrix} \tag{2.15} $$

For each limb segment, the x-axis of the anatomical frame corresponds to the first column of the respective rotation matrix, the y-axis is the second column and the z-axis is the third column.

In some cases, to correctly calculate the angle of one degree of freedom, the anatomical axis of one segment of interest is projected onto a plane of another segment. Depending on the joint angle, the plane used in the projection differs. For example, the elbow flexion/extension angle is measured in the xy-plane of the upper arm's anatomical frame. The xy-plane might not always correspond to the actual flexion/extension plane of the elbow. However, the elbow flexion/extension angle does not vary if there is shoulder internal or external rotation, or, in this case, if the sensor does not rotate along with the internal/external rotation of the shoulder. The purpose of projecting the anatomical axis of interest onto the plane of another anatomical frame is to avoid measuring more than one degree of freedom for each joint angle.

The projected vector $\vec{v^p}$ is given by:

$$\vec{v^p} = \vec{v} - \frac{\vec{v} \cdot \vec{n}}{||\vec{n}^2||}\vec{n} \tag{2.16}$$

Where $\vec{v}$ is the axis of the segment's frame and $\vec{n}$ is the plane normal vector.
The angle θ between two vectors $\vec{v_1}$ and $\vec{v_2}$ is given by:

$$\theta = atan2\Big(\frac{||\vec{v_1} \times \vec{v_2}||}{\vec{v_1} \cdot \vec{v_2}}\Big) \tag{2.17}$$

Where $atan2$ is the four-quadrant inverse tangent, outputting angles between $-\pi$ and π.

Shoulder joint angles

The shoulder flexion/extension angle is calculated by firstly projecting the x-axis of the upper arm frame $\vec{x_{ua}}$ onto the zx-plane of the sternum (sagittal plane), by taking equation 2.16, with $\vec{v} = \vec{x_{ua}}$ and $\vec{n} = \vec{y_{st}}$. The flexion/extension angle θ is calculated by taking the angle between $\vec{x_{ua}}^p$ and $-\vec{z_{st}}$. If $\theta = 0°$ means that the shoulder is straight next to the body, pointing down. A positive θ corresponds to a shoulder flexion and a negative θ to a shoulder extension.

The shoulder abduction/adduction angle is calculated by projecting $\vec{x_{ua}}$ to the zy-plane of the sternum's frame (frontal plane, where $\vec{n} = \vec{x_{st}}$). A positive angle indicates an abduction and a negative angle corresponds to an adduction.

Elbow joint angles

The elbow flexion/extension angle is taken by projecting the long axis of the lower arm $\vec{x_{la}}$ onto the xy-plane of the upper arm's frame. A positive angle means flexion of the elbow. If $\theta = 0°$, it indicates that the elbow is fully extended. Negative values for this joint angle mean that there is an over-extension of the elbow.

Wrist joint angles

The wrist flexion/extension angle is calculated the same way as the elbow, but by projecting the x-axis of the hand's frame $\vec{x_h}$ onto the zx-plane of the lower arm's frame. A positive angle indicates wrist flexion and a negative angle wrist extension. If the angle is 0°, it means that the wrist is in the neutral position.

Wrist pronation/supination is calculated by a different method, since there is no plane that accompanies the movement of the hand in order to correctly measure the desired angle. The lower arm IMU is fixed to the distal part of the limb segment, so it pronates and supinates along with the wrist. Comparing its frame to the wrist's frame will not represent the true supination/pronation angle. For this case, the joint angle corresponds to the integration over time of the x component of the gyroscope of the hand IMU. The gyroscope data is firstly aligned to the segment by multiplying it by the sensor-to-segment rotation matrix of the lower arm. A positive angle indicates that the wrist is pronated and a negative angle represents a wrist supination. When $\theta = 0°$, the wrist is in neutral position.

Finger joint angles

The index and middle fingers flexion/extension angles are calculated by projecting the finger's x-axis, $\vec{x_i}$ and $\vec{x_m}$, onto the zx-plane of the hand's frame. Then, the angle between the x-axis of the hand $\vec{x_h}$ and the projected axis of the fingers $\vec{x_i}^p$ and $\vec{x_m}^p$ is calculated.

The thumb flexion/extension angle is calculated by projecting $\vec{x_t}$ onto the xy-plane of the hand, and then calculating the angle between $\vec{x_h}$ and $\vec{x_t}^p$.

A positive angle indicates finger flexion and a negative angle represents extension.

Trunk compensation angles

The trunk compensation angles are defined as the inclination or rotation of the sternum's sensor. It is divided into frontal, lateral and rotational compensation angles.

Firstly, the sagittal, frontal and transverse anatomical planes are defined. Since the trunk is not exactly vertical in the initial position, the definition of the anatomical planes is done by calculating the normal vectors of the three planes using the gravity vector:

$$\vec{x_a} = \vec{y_{st}} \times \begin{bmatrix} 0 \\ 0 \\ 1 \end{bmatrix}, \qquad \vec{y_a} = \begin{bmatrix} 0 \\ 0 \\ 1 \end{bmatrix} \times \vec{x_{st}}\ , \qquad \vec{z_a} = \begin{bmatrix} 0 \\ 0 \\ 1 \end{bmatrix} \tag{2.18}$$

Where x_a is the normal vector to the frontal plane, y_a the normal to the sagittal plane and z_a the normal to the transverse plane. The global frame defined in the start of the movement does not correspond to the anatomical planes because the subject's initial posture can have a different heading than the one of the global frame. The definition of the anatomical planes via the initial orientation of the sternum's axis is more accurate and provides the actual trunk compensation angles for each movement.

The trunk frontal compensation is calculated by firstly projecting the z-axis of the sternum onto the sagittal plane with equation 2.16, with $\vec{n} = y_a$ and $\vec{v} = \vec{z_{st}}$. The angle is calculated between the projected initial vector $\vec{z^p}_{st_i}$ and the current one $\vec{z_{st_t}}^p$ throughout the recording.

The trunk lateral compensation follows the same method by calculating the angle between the vectors $\vec{z_{st_i}}^p$ and $\vec{z_{st_t}}^p$ projected onto the frontal plane, with $\vec{n} = \vec{x_a}$.

For the rotational compensation, the y-axis of the sternum is projected onto the transverse plane, with $\vec{n} = \vec{z_a}$. Then, the angle between $\vec{y_{st_i}}^p$ and $\vec{z_{st_t}}^p$ is calculated.

2.5 Validity of the joint angle estimation method

Different tests where performed in order to evaluate the validity of the sensor's orientation estimation and the consequent joint angles calculation.

2.5.1 Stability tests

The first tests where done to evaluate the presence of drift in the sensor's orientation estimation. Two situations where evaluated: 1) laying one sensor static on the table, rotate

it 90° in the positive z direction and leaving it static in that orientation, and finally rotate it again back to the initial orientation; 2) laying the sensor static on the table, grab it and perform arbitrary movements and rotations in all directions and placing it again in the initial orientation. The kinematic reconstruction was done with two methods. Firstly by only integrating the angular velocity measurements given by the gyroscope and secondly with the method described in the previous sections. The results of the tests are presented in Figures 2.5 and 2.6 for situation 1) and 2) respectively.

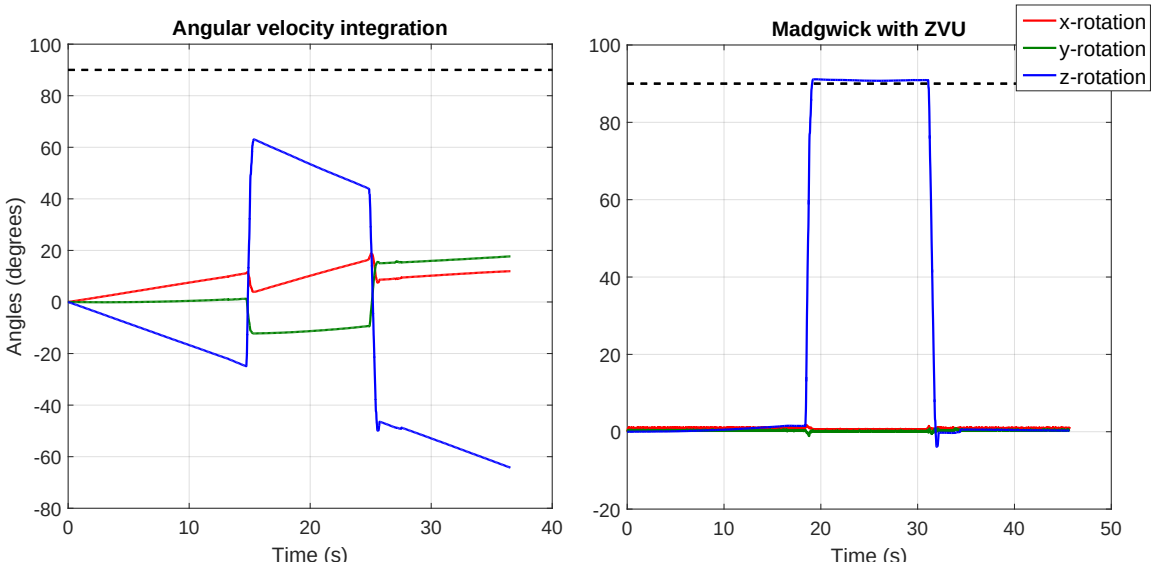

Figure 2.5: Kinematic reconstruction of the test situation 1) by integrating the angular velocity (left) and by using the Madgwick filter and the zero velocities update method (right). The dashed black line indicates the target angle of 90°.

The effect of the accumulated errors in the orientation estimation of the sensors by integrating the gyroscope data is clearly visible when a defined 90° rotation around the z-axis of the sensor is performed, as seen on the left plot of Figure 2.5. The Madgwick filter eliminates the effect of the drift in the inclination of the sensor and the ZVU reduces significantly the drift in the estimation of its heading, where the measured 90° are much more accurate (the measured z-rotation angle was 90.82° in the target position).

If the sensor is rotated in arbitrary directions, the effect of drift is visually noticed when the orientation is estimated by integrating the gyroscope data (as seen in the left plot of Figure 2.6). If the orientation estimation is done with the Madgwick filter and the zero velocity update method, the effect of drift is significantly reduced (as seen in the right plot of Figure 2.6). In the gyroscope integration case, the absolute difference between the x-rotation, y-rotation and z-rotation angles in the start and end of the test is 12.36° , 6.43° and 10.97° respectively. The angular differences between the beginning and ending orientations estimated with the Madgwick filter are 0.18° for the x-rotation, 0.26° for the y-rotation and 0.08° for the z-rotation, which is significantly smaller.

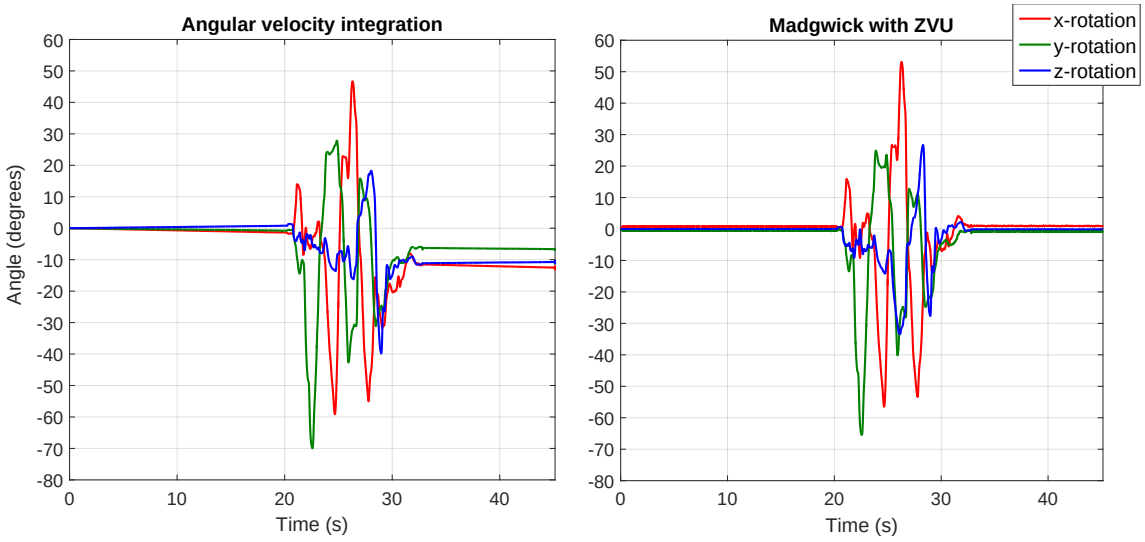

Figure 2.6: Kinematic reconstruction of the test situation 2) by integrating the angular velocity (left) and by using the Madgwick filter and the zero velocities update method (right).

2.5.2 Validity tests

To assess the validity of the distributed system when it is actually mounted onto the trunk and upper extremity of patients, two additional tests were performed. Firstly, by using a rigid model of the arm and secondly by testing the system in healthy subjects.

Rigid model test

The rigid model consists of a wooden replication of the arm, where the simulated shoulder joint is able to flex and abduct and the simulated elbow joint is able to flex from a fully extended posture (elbow flexion angle of 0°). The rigid model validation simulated 90° shoulder flexion and abduction movements, elbow flexion movements, wrist flexion, extension, pronation and supination. The results of the measured joint angles in the target positions of the movements are shown in table 2.2.

The shoulder flexion, abduction, elbow flexion and wrist flexion and extension angles, when the tested movement is a 90° angle of each respective joint, show errors smaller than 3° in the target position. The wrist supination/pronation test with the model shows an overestimation of the joint angle of around 10°. During the tests, the overall angles of the other joints are close to 0°. The fingers flexion angles show a higher deviation from 0° than the other joint angles during the tests.

Table 2.2: Mean measured arm joint angles of the rigid model in the target position during each test movement. (Sh Flex - shoulder flexion; Sh Abd - shoulder abduction; El Flex - elbow flexion; Wr Flex/Ext - wrist flexion/extension; Wr Sup/Pron - wrist supination/pronation; T Flex - thumb flexion; M Flex - middle finger flexion; I Flex - index finger flexion).

	Sh Flex Mov	**Sh Abd Mov**	**El Flex Mov**	**Wr Flex / Ext Mov**	**Wr Sup/Pron Mov**
Sh Flex	87.02°	0.03°	−1.10°	−1.45°	−1.25°
Sh Abd	−1.62°	89.96°	−1.35°	−1.13°	−0.98°
El Flex	0.76°	−0.01°	90.14°	0.02°	−0.04°
Wr Flex/Ext	−4.36°	−4.11°	−3.86°	87.57° / −87.05°	2.86°
Wr Sup/Pron	0.03°	−0.02°	0.99°	−6.10°	−102.10° / 99.26°
T Flex	7.64°	1.12°	−1.42°	3.81°	1.33°
M Flex	7.69°	3.89°	5.20°	4.43°	0.64°
I Flex	7.77°	3.73°	2.43°	2.67°	2.14°

Healthy subjects tests

The experimental protocol done for Chapter 3 was tested in a healthy subject before the experiments in stroke patients. The detailed description of the experimental protocol is defined in the respective chapter. Healthy subjects have the ability of performing more controlled movements, either for the global frame definition and in the sensor-to-segment protocol, but also during the actual movements of the protocol. To summarize the protocol, the subjects were asked to perform 4 different movements that are included in the FMA assessment of the arm and wrist. The first movement of the experimental protocol consisted in a 90° abduction of the shoulder, maximum flexion of the elbow and a 90° degree supination of the wrist. The second movement consisted in a 90° degree flexion of the shoulder while maintaining the elbow fully extended, the wrist in the neutral position (with a 0° flexion and 0° supination angles) and the fingers fully extended as well (with a 0° flexion anfle). The third movement consisted in performing a 90° shoulder abduction with the elbow, wrist and fingers in the same posture as in the second movement. The fourth movement was intended to perform a wrist flexion and extension while the shoulder is flexed around 70° and the elbow fully extended. The results of the joint angles in one repetition of each of the movements performed by one healthy subject are presented in Figure 2.7.

Each movement was done three times. Table 2.3 gathers the mean and standard deviation of the joint angles of the arm when it is in the target posture of each movement performed by the healthy subject.

The measured joint angles in the target position show some variations in the different repetitions. However, the mean joint angles are very close to what was instructed. In movements 2 and 3 (shoulder abduction and shoulder flexion), the mean of the measured angles of these joints are 89.2° and 92.3°, which is very close to the desired 90°. The subjects are instructed to fully extend the elbow in tasks 2, 3 and 4. The measured mean elbow flexion

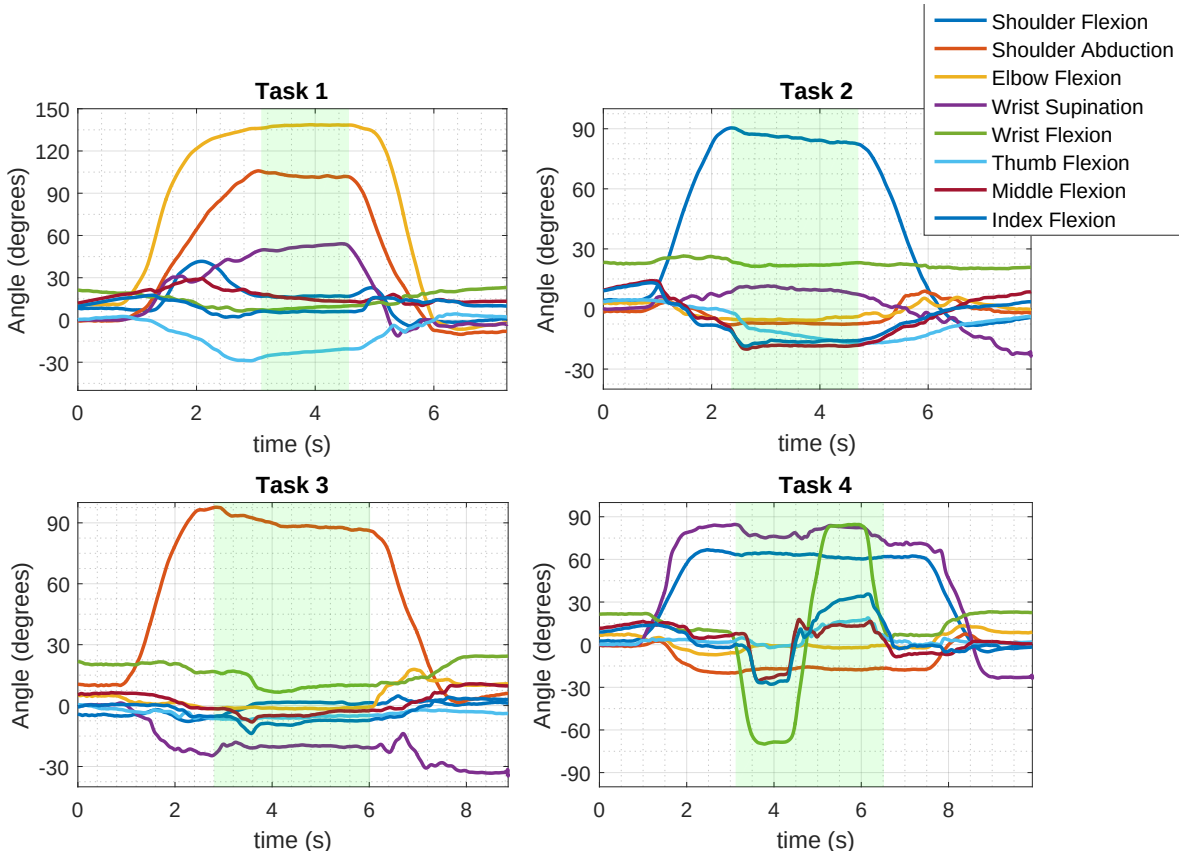

Figure 2.7: Arm joint angles measured in one healthy subject during the movements of the experimental protocol of Chapter 3. The green shaded area indicates the moment where the arm is in the target posture of the movement.

Table 2.3: Mean and standard deviation of the measured arm joint angles of two healthy patients in the target posture of each task of the experimental protocol of Chapter 3. (Sh Flex - shoulder flexion; Sh Abd - shoulder abduction; El Flex - elbow flexion; Wr Flex/Ext - wrist flexion/extension; Wr Sup - wrist supination; T Flex - thumb flexion; M Flex - middle finger flexion; I Flex - index finger flexion).

	Sh Flex	Sh Abd	El Flex	Wr Sup	Wr Flex	Wr Ext	T Flex	M Flex	I Flex
Mov 1	23.8 ± 6.0	104.3 ± 7.4	136.4 ± 4.5	58.2 ± 14.2	15.6 ± 6.0	–	-10.0 ± 11.5	20.8 ± 1.6	10.5 ± 4.0
Mov 2	89.2 ± 0.9	-1.0 ± 5.7	-1.0 ± 4.1	16.5 ± 11.2	21.5 ± 2.1	–	-8.0 ± 6.0	-8.3 ± 10.8	-8.5 ± 9.7
Mov 3	14.9 ± 11.5	92.3 ± 4.1	-7.1 ± 6.2	-18.8 ± 5.2	11.4 ± 4.7	–	-4.7 ± 1.8	-6.4 ± 7.3	-6.5 ± 3.6
Mov 4	60.2 ± 4.1	-5.2 ± 9.1	3.0 ± 5.2	74.5 ± 4.1	88.1 ± 3.1	69.0 ± 0.8	21.0 ± 6.6	9.5 ± 14.9	19.5 ± 9.0

angles are very close to 0°. In movements 2 and 3 this angle is negative, which can be due to overextension of the elbow. The standard deviation of the measure features is not higher than 14.9° (corresponding to the middle finger flexion angle in movement 4). The deviations in these values may be explained by two factors. Firstly, the movement performed is never perfectly the same in different repetitions. Secondly, the sensor-to-segment calibration protocol and the global frame definition may not be perfect, causing deviations between the measured joint angles and the actual arm posture. To accurately assess the validity of the

proposed methods, a reference system should be used, such as optical motion trackers. Nevertheless, the tests done with the rigid model of the arm and in the healthy subject appear to be reliable, but the sources of error have to be taken in account and a further investigation should be done to validate the proposed methods.

Chapter 3

Quantifying pathological synergies in stroke patients with the use of inertial measurement units

3.1 Introduction

Stroke is the third most common cause of disability in the world. Approximately 5 million people suffer from post-stroke impairments every year [1]. Depending on the location and size of damaged cells in the brain, different types of impairments can occur. Around 80% of stroke survivors that suffer from long-term disabilities have impairments related to upper limb motor function [5], [41]. The main impairments that cause loss of motor function are muscle weakness or paresis. Other post-stroke outcomes are increased muscle tone and spasticity, loss of sensation and decreased inter-joint coordination. The presence of different types of motor impairments causes decreased or a learned bad use of the affected limb [6].

The normal muscle co-activation patterns exist in a stable spatiotemporal way across different muscles, and work in the sense of performing complex functional movements. The pattern of muscle recruitment and activation is known as muscle- or motor-synergy. In stroke, the damaged brain cells cause an interruption of the neural pathways. When the cortical cells reorganize, alternative descending pathways emerge [42]. The rearrangement of the descending motor neurons may result in a joint excitation or inhibition of different muscles. The abnormal co-activation muscle patterns are known as pathological synergies, and is associated to a reduced number of degrees of freedom of the motor control. The pathological synergistic movement in stroke patients has been described in the past by Twitchell [19] and Brunnstrom [20]. In the process of motor function recovery, voluntary movement is characterized by two main muscle coupling patterns: the flexor and the extensor synergies. In the flexor synergy, an attempt of movement results in a coupled abduction and external rotation of the shoulder, flexion of the elbow, wrist and fingers, and forearm supination. Similarly, the extensor synergy is characterized by a coupled adduction and internal rotation of the shoulder, elbow extension, wrist and finger flexion, and forearm pronation. These impairments create a learned bad use of the affected extremity, where compensation strategies

are adopted by stroke survivors to increase success in completion of tasks [9].

The importance of assessing motor function rises with the need of proper rehabilitation methods. Motor outcomes due to stroke, and its extent, differ between patients. A subject-specific rehabilitation protocol is needed, and frequent assessment provides better adaptation to the patient's progress [43]. One of the most used assessment scales in the clinic to evaluate motor function is the Fugl-Meyer Assessment scale (FMA) [17]. The FMA scale was developed with the foundations of the motor recovery stages described by Twitchell and Brunnstrom [18]. Although it has been used as a gold standard method of upper extremity motor function assessment, it is an ordinal scale with insufficient sensitivity and has a ceiling effect when evaluating patients with mild impairment [21]. Despite the high values for reliability and validity, the assessment procedure and scoring have to be well defined in order to correctly assess the patient and avoid subjective variation in the score due to the therapist.

More recently, kinematic measurements have been used to objectively quantify motor function in the upper extremity of stroke patients. Kinematic assessment can provide several metrics and features that allow evaluation of both motor function and performance [27], [44]. There is a large variety of kinematic measurement systems and tasks performed used in the different studies. Optical motion capture systems are considered the gold standard system to measure body kinematics. The high cost and the need of a customized laboratory with fixed cameras are big limitations that hamper its usage in the clinic. Various types of exoskeletons or end-effectors and motion capture systems used with arm weight support have also been previously used. These systems obstruct and have influence on the movement, reducing degrees of freedom in some cases. A widely used kinematic type of sensors are inertial measurement units (IMU). These sensors are low-cost and portable, and do not need of specialized labs to perform the measurements. However, IMU sensors show higher errors due to drift and offsets present in the measurements. Developments of sensor fusion algorithms increase validity and reliability when using these types of sensors [28], [30].

The majority of the studies that used wearable IMU sensors evaluated the relation between measuring several tasks associated to activities of daily living and clinical assessment scales, focusing on performance evaluation [27], [29], [44]. Objective assessment of the actual FMA task of the upper limb has been done before with accelerometers and gyroscopes [45], but the extracted features did not take in account the sensor's orientation estimate and did not include measurements of joint angles in the different limb segments. The analysis of the limb segment's orientation is of interest in order to quantify the observations that are done in the clinic while assessing the upper extremity during the FMA. The measurement of the joint angles of the upper extremity are easily translated into the clinic and can be interpreted by therapists.

In this usability study, a custom upper limb IMU system was developed and used to measure upper extremity kinematics of stroke patients while performing items from the FMA upper extremity subscale (FMA-UE). The main objective of the study is to assess the capability of this system in evaluating motor function in stroke patients.

It is hypothesized that the kinematic features measured with the distributed IMU system can objectively distinguish movements done with the affected and the non-affected arms of

stroke patients. Due to the influence of the pathological muscle coupling, the affected upper extremity of stroke patients shows a more stereotypical movement when they volitionally perform different tasks than the non-affected arm. More specifically, the pathological coupling causes the activation of the elbow flexor muscles when the shoulder abductor and flexor muscles are activated (flexor synergy). In the clinical scenario, during the FMA-UE test, patients who have motor impairments due to coupling of the upper extremity muscles, are unable to perform the arm section items without flexing the elbow. The wrist joint is also affected by the pathological coupling. When the shoulder is volitionally abducted or flexed, it is expected that the wrist flexes and supinates in the affected arm of stroke patients. In this study, it is hypothesized that the distributed measuring system measures higher elbow flexion and wrist flexion and supination angles in the affected arm of stroke patients during the FMA-UE protocol. Other types of impairments can also influence motor performance of the patients, such as muscle weakness or paresis. It is also hypothesized that the affected arm joints have a lower range of motion than the non-affected arm. It is expected that impaired patients are unable to reach the target joint angles of the items in the clinical assessment protocol.

Another aim of this study is to relate the features to the FMA-UE score and evaluate if the system can distinguish more affected from less affected patients. It is expected that more affected patients show the effects of the pathological coupling and weakness more than less affected patients. This is translated into a more flexed elbow and wrist during the tasks of the FMA-UE, showing a higher prevalence of pathological synergies in patients with a lower FMA score. The range of motion is also expected to be lower in more affected patients. It is expected that the measurements with the distributed measuring system show the increased difficulty of stroke patients with a lower FMA score to reach the desired arm postures with their affected arm.

The study will provide insight on the usability of the IMU system in conjunction with clinical scales to provide an objective, sensitive and detailed assessment of the upper extremity of stroke patients.

3.2 Methodology

3.2.1 Measurement System

A distributed measurement system was developed at the University of Twente, composed of eight IMUs, with triaxial accelerometers and gyroscopes, and three force sensors. This system was based on the one developed by Kortier et al. [46]. The system is composed of multiple flexible and rigid printed circuit boards (PCB), where each rigid section contains a pair of triaxial gyroscopes and accelerometers (ST LSM330DLC). The system is divided in two subsystems, the arm and the hand string. The arm string consists of four IMUs intended to measure the sternum, shoulder, upper arm and lower arm. The hand string is composed of another four IMUs for the hand, thumb, index and middle fingers. Three force sensitive resistors with the purpose of measuring force produced by the three fingers,

Figure 3.1: Distributed IMU system

connect to the respective IMU modules. Both subsystems are connected to a bus master that enables the collection of data from both subsystems and sends it to the computer via a USB connection. Data is collected by a microcontroller (Atmel XMEGA) at 200 Hz for the gyroscopes and at 100 Hz for the accelerometers. The IMUs are covered by a 3D-printed Thermoplastic polyurethane (TPU) housing and are mounted to the respective body segment using 3D-printed flexible mounting straps. The shoulder and sternum IMU housings do not have straps, and are fixed with medical tape. Figure 3.1 shows the distributed IMU system mounted in the upper extremity and trunk.

3.2.2 Kinematic Reconstruction

The system measures acceleration and angular velocity of the different upper limb segments and the sternum. Several steps are needed in order to estimate the orientation of each sensor, and therefore, each segment. First, a sensor-to-segment calibration was conducted in order to find the orientation of the sensor with respect to the correspondent body segment. Secondly, since magnetometers were not included in the measurements, a common global frame definition is needed for all sensors.

Sensor-to-segment calibration

The IMUs attached to a body segment are not perfectly aligned with the direction of the correspondent anatomical frame. The sternum IMU is placed at the centre of the chest; the shoulder sensor is placed between the superior border of the scapula and the clavicle, near the acromioclavicular joint; the upper arm IMU is placed on the lateral side of the upper

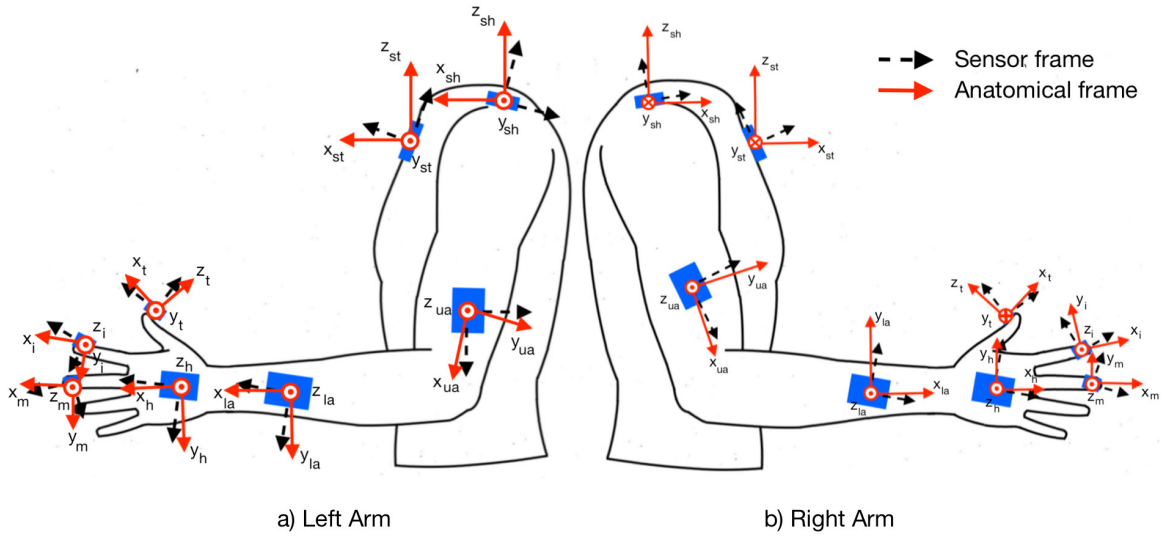

Figure 3.2: Sensor's frames and correspondent anatomical frames of the eight different IMUs of the measurement system. Subfigure a) shows the frames in the left arm, and subfigure b) in the right arm.

arm, near the elbow; the lower arm sensor is placed on the dorsal side of the forearm close to the wrist; the hand IMU is placed on the dorsal side of the hand, roughly in the centre; the fingers sensors are placed in the distal inter phalangeal segments of the thumb, index and middle fingers. The coordinate systems of the sternum, arm and hand were arbitrarily defined in a way that the x-axis of the anatomical frame is in the longitudinal direction of the segment. The sensor's and the anatomical frames defined are shown in Figure 3.2. The alignment of the sensors to the respective limb segments follows a defined protocol that includes static postures and dynamic movements. This protocol was based on Luinge et al. [37] and Ricci et al. [38]. The description of each posture/movement can be found in table 3.1. In the static postures, the gravity vector measured with the accelerometers represents one of the axis. In the dynamic movements, the angular velocity, depending on the rotation direction, also represents an axis. For each sensor, two different axes are measured with the sensors (either by the accelerometer or gyroscope, depending on the segment), and the third axis is calculated with the cross-product of the previous two. A detailed explanation on the definition of the anatomical frames can be found in Chapter 2, in section 2.2.

Global frame definition

In a magnetic and inertial measurement unit sensor, the gravity component measured with the accelerometer and the earth's magnetic field measured with the magnetometer give information on a constant, common reference. The gravity (measured with the accelerometer) and the earth's magnetic north (measured with the magnetometer) correspond to a common vertical and horizontal axis, respectively, for each sensor. In this study, however, there is no reference for the sensors' heading since magnetometers are not used. To define a common

Table 3.1: Description of the sensor-to-segment positions and movements

	Description
1	Static hand flat on a table
2	Static hand sideways, with elbow flexed 90°
3	Static thumb flat on a table
4	Static thumb sideways, with hand pronated
5	Static forearm and hand palm faced down (parallel to the ground)
6	Wrist pronation and supination, starting form supinated position
7	Static shoulder adducted, with elbow flexed 90°
8	Static shoulder abducted 90° with elbow flexed 90°
9	Static straight neutral pose, arm along the body and fingers extended
10	Trunk flexion and extension (arm moving along the upper body)

global frame, the two last movements (static neutral pose and trunk flexion) of the sensor-to-segment calibration protocol are used [36]. The static neutral pose, with the arm stretched along the body and the fingers extended, defines the common vertical axis by measuring the gravity vector in all sensors. The trunk flexion movement is performed with the arm stretched and accompanying the flexion of the hip. The angular velocity defines the horizontal axis of the global frame. The detailed global frame definition is explained in section 2.1.1 of Chapter 2.

Orientation estimation

With the sensor-to-segment alignment and the common global frame for every IMU, it is possible to reconstruct the movement of the chest, arm and hand. Orientation estimation is usually done by integrating the angular velocity over time to get the angular change of the sensor. This method, however, introduces integration drift due to noise and offsets in the gyroscope measurements. Therefore, sensor fusion algorithms are used to correct both the inclination and heading of the sensor. The inclination is corrected with the gravitational component of the accelerometers. The heading is usually corrected with the earth's magnetic field [47]. In this study, a Madgwick filter [34] is used to compensate the IMU's inclination errors due to integration drifts, by fusing data from the gyroscopes and accelerometers. Details on the sensor's orientation estimation can be found in appendix 2.1.

The exclusion of magnetometers was because these sensors are very sensitive to magnetic disturbances of the environment, and can affect the orientation estimation of the heading. In this work, since there is no reference for the heading to be corrected, a zero-velocity update method was used to reduce errors in the orientation estimate. This error correction technique was based on the work of Kirking et al. [35], where if the norm of the angular velocity is

below $3°/s$, the sensor is considered to be static. By instructing the subjects to start and finish the different movements in a static posture, the offset of the gyroscope measurements is taken from the static moments and the linear trend is removed during the movement period. This eliminates the effects of the drift and offset in the gyroscope measures and reduces the integration drift when estimating the sensor's orientation.

The body segment's orientation is then calculated by firstly estimating the sensor's orientation and then rotating them to the anatomical frame with the sensor-to-segment calibration parameters. Appendix 2.3 shows the detailed process to estimate the trunk, arm and hand orientations.

3.2.3 Experimental Design

Participants

Ten moderately affected (FMA-UE scores between 34 and 54) chronic stroke survivors were included in this usability study. The participants were recruited from the University Hospital Zurich, Switzerland. All patients studied suffered from a unilateral lesion resulting from either an ischemic or a hemorrhagic stroke. The participants included in this study were required to be at least 18 years old, with a diagnose of stroke in the chronic stage (>6 months). All had to have stroke-associated impairments of the upper limb and at least partial ability to move the arm against gravity and to perform finger movements for basic grasp function. Exclusion of subjects was done if they had pre-existing impairments of the upper limb, for example orthopaedic impairments, severely increased muscle tone and sensory deficits. Participants were also excluded if severe communication or cognitive deficits that cause inability to follow the procedures and to give informed consent were present, or if there were contraindications on ethical ground. The FMA-UE test was performed before the start of the protocol. Detailed demographic characteristics are presented in table 3.2.

All participants gave written informed consent in accordance with the declaration of Helsinki. The cantonal ethics in Zurich approved the experimental protocol prior to start of the study (Req-2019-00417).

Experimental protocol

Before placing the IMU system, the participants were assessed using the FMA-UE test on the affected and non-affected side by a physiotherapist. The experimental protocol was performed on both limbs separately, starting with the non-affected limb.

The sternum and shoulder IMUs were fixed with medical tape. The upper and lower arm, hand and fingers sensors were fixed with the flexible straps. The thumb, index and middle finger IMUs were attached with the force sensitive resistors fixed on the fingertips by the IMU housing's strap. After the set-up, the sensor-to-segment procedure was performed. The therapist helped the participant maintaining the static positions and performing the dynamic movements. Each position was measured for at least five seconds.

The protocol consisted in performing four items from the FMA-UE test to examine movements within and out of the pathological synergies:

Table 3.2: Demographic and clinical characteristics of the participants (N=10)

Characteristic	Value
Sex (male/female)	6/4
Age median (IQR) in years	61.5 (57.5 - 70.0)
BMI median (IQR)	26.5 (23.7 - 29.2)
Arm length median (IQR) in cm	68.5 (62.6 - 76.6)
Dominant hand (left/right)	0/10
Time since stroke median (IQR) in months	31.5 (20.3 - 63.8)
Affected side (left/right)	5/5
FMA-UE median (IQR) / max	33.5 (32.3 - 34.8) / 66
Arm subscore / max	22.0 (22.0 - 24.8) / 36
Wrist subscore / max	6.0 (5.5 - 6.8) / 10
Hand subscore / max	9.5 (6.8 - 11.0) / 14
Coordination subscore / max	2.5 (2.0 - 3.8) / 6

1. *FMA-UE item A2*: movement within the synergies, where the subject is asked to raise the hand to the ipsilateral ear with the forearm fully supinated. The shoulder should abduct at least 90°. It is expected that both the affected and non-affected arms are able to move to this posture. The hypothesis in this movement is that the affected arm might show a smaller range of motion and the inability to reach the desired targeted joint angles. It is expected that the distributed IMU system measures a lower shoulder abduction and elbow flexion angle in the affected arm when compared to the non-affected;

2. *FMA-UE item A3*: movement mixing the flexor and extensor synergies, where the subject is instructed to flex the shoulder 90° and maintain the elbow fully extended. The hypothesis here is that the measured elbow flexion angle is higher when the task is done with the affected arm of the stroke patients. Also, due to the impact of the pathological coupling, the wrist supination angle should be higher in the affected arm. The shoulder flexion angle is expected to be smaller when compared to the non-affected arm;

3. *FMA-UE item A4*: movement out of the pathological synergies, where the subject is asked to abduct the shoulder 90° and keep the elbow fully extended. It is hypothesized that the same behaviour as in the previous item occurs in this one. The measured elbow flexion angle should be higher in the contralesional arm of the patients due to the pathological coupling. A higher wrist supination and a lower shoulder abduction is also expected when the patients performs this item with the affected arm.

4. *FMA-UE item B*: intended to evaluate the range of wrist flexion and extension. The subject is asked to flex the shoulder at least 70° and perform wrist flexion and extension

movements while keeping the elbow extended. The wrist flexion/extension range of motion is expected to be smaller when the task is done with the affected arm. The wrist movement is expected to engage the elbow flexor muscles, so a higher flexion angle in this joint should be seen in the measurements of the contralesional arm.

The participants were sited and performed three repetitions of each item. After the procedure for the non-affected arm, the measurement system was removed, and the affected arm was set up and evaluated according to the same protocol.

3.2.4 Data Analysis

Feature extraction

To characterize the subjects' performance, different features were extracted from measurements.

The joint angles were calculated based on the orientation of each segment. After the alignment of the sensor to the respective limb segment, the estimated orientation represents the anatomical frame of the different segments in relation to the global frame. The anatomical frame has one axis that is longitudinally aligned with the limb segment and another that is perpendicular, pointing in the dorsal direction of the segment, as seen in Figure 3.2. The joint angles are calculated by taking the angle between two axes of different segments, depending on the joint. For the elbow, wrist and fingers flexion/extension angles, the angle was calculated between the two adjacent limb segments. The longitudinal axis of the more distal segment of the joint is firstly projected to the flexion/extension plane of the more proximal segment of the joint. This excludes measuring ulnar or radial deviations or lateral movements of the fingers that do not correspond to flexion or extension of the segment. The shoulder flexion/extension and abduction/adduction is calculated by relating the upper arm frame to the sternum frame. For the flexion angle, the axis aligned with the upper arm is projected onto the body's sagittal plane, which corresponds to the xz-plane of the sternum's frame. The abduction angle is calculated by projecting the same upper arm axis onto the frontal plane, which is defined as the zy-plane of the sternum's frame. Details on the joint angles calculation can be found in section 2.4 of Chapter 2.

An example of the joint angle estimation for one of the tasks can be seen in Figure 3.3. The figure represents the different joint angles of the non-affected arm of one of the patients measured by the system. A positive angle indicates flexion or abduction of a joint and a negative angle extension or adduction. The features used to evaluate the patients' performance are the joint angles measured in the target position of each task (represented with the green shaded area in the figure).

Statistical analysis

The participants were divided into two different groups with different levels of impairment (group 1 and group 2). The groups were created based on the FMA-UE arm subscore. The more affected group (group 1) included subjects with a score of 22 or less ($N = 6$, FMA-UE

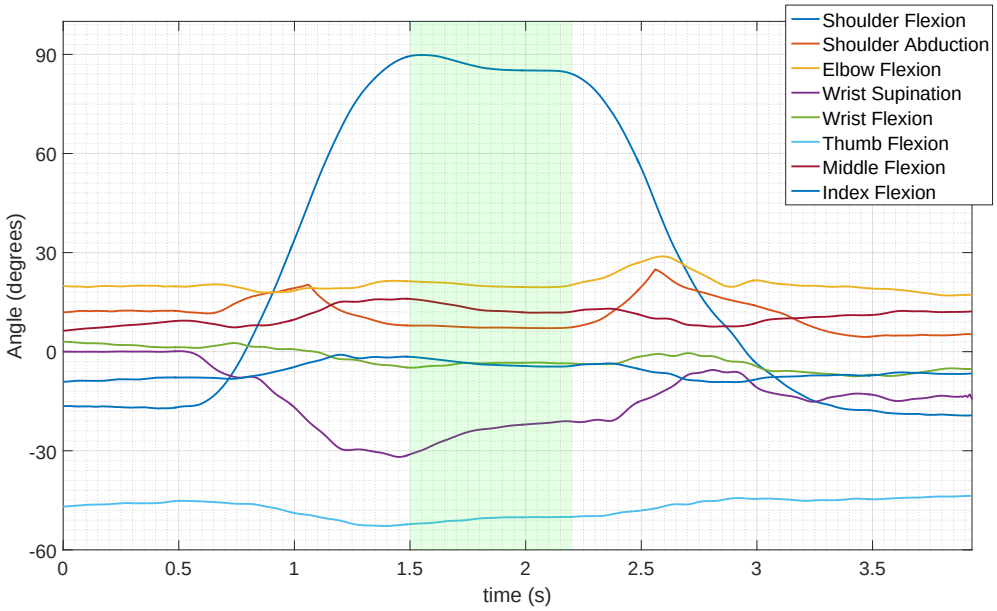

Figure 3.3: Arm joint angles measured in one participant during the second task of the experimental protocol (item A3). The green shaded area indicates the moment where the arm in the target position.

arm subcore median and IQR: 22 (22 - 22)). The less affected group (group 2) was composed by the remaining participants ($N = 4$, FMA-UE arm subscore median and IQR: 25.5 (24.5 - 28.5)/). Within each group, the data from the affected (AF) and non-affected (NAF) arms was separated, creating in total four different groups for the statistical analysis (NAF-1 - non-affected arm of group 1; AF-1 - affected arm of group 1; NAF-2 - non-affected arm of group 2; and AF-2 - affected arm of group 2).

Two different statistical tests were used. Firstly, the Wilcoxon signed rank test was used to analyse differences between the extracted features within the same impairment level group (differences between NAF-1 and AF-1 and between NAF-2 and AF-2). Secondly, the Mann-Whitney U test was used to check differences between the measurements of groups 1 and 2, of the same arm (differences between NAF-1 and NAF-2 and between AF-1 and AF-2).

Both tests are non-parametric due to the small sample size and the low evidence of normally distributed data. All statistic analysis was done with a significance level of 0.05.

3.3 Results

All ten participants were able to complete the experimental protocol. Data from the thumb IMU was discarded for one patient due to malfunctions of the sensor. In one repetition of the fourth item of the protocol, the IMU data had to be excluded due to recording errors. In total, 119 movements were analysed (30 repetitions of tasks 1, 2 and 3 of the protocol and 29 of task 4).

Figure 3.4, 3.5, 3.6 and 3.7 show the joint angles in the target position measured in the

four different groups when subjects performed tasks 1, 2, 3 and 4 respectively. The median and the 25^{th} and 75^{th} percentiles of the measured relevant joint angles of the group are shown in the form of boxplots. The presented joint angles are the ones considered more crucial for evaluating the performance in each task, and allow the visualization of possible pathological synergistic behaviour in the proximal limb segments (shoulder and elbow). Also, the considered relevant joints were based on the observations that the therapist does when scoring the patient with the FMA-UE scale [21]. The desired target joint angles for each task are marked with dashed lines in the figures. Appendix A includes additional figures and analysis of joint angles that were measured as well but are not presented in this chapter.

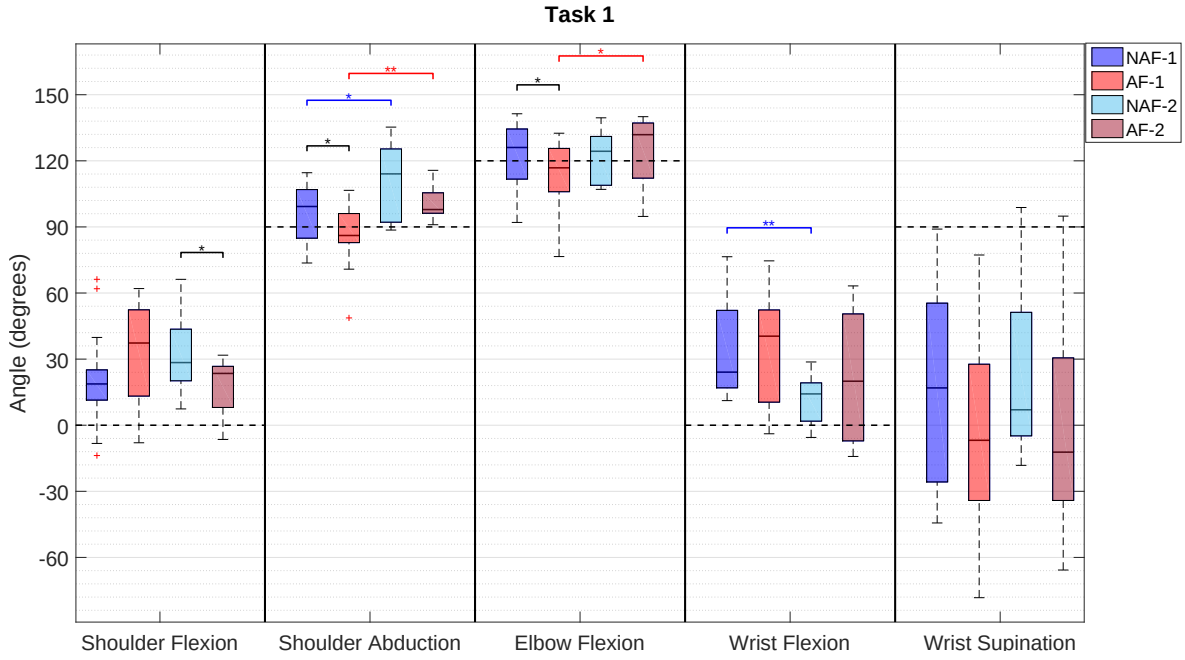

Figure 3.4: Boxplots (median and IQR) of the target angles for the most significant joints evaluated in the first task of the protocol in the four groups. The black dashed lines represent the desired targets for the task. Significant differences between arms of the same group are indicated with a black line. Significant differences between the same arm of different groups are indicated with a blue (for the NAF) or red (for the AF) lines. $*P < 0.05$; $**P < 0.01$; $***P < 0.001$.

For the first task (movement within synergies), it is possible to see that the AF and NAF arms performed similarly. The desired shoulder abduction and elbow flexion target angles were reached by both the AF and NAF limbs in all subjects. The shoulder abduction angle was significantly higher in the NAF limb of the more impaired group when compared to the AF arm of the same group (NAF-1 vs AF-1). In affected arm, these joint angles showed to be significantly higher in group 2 when compared to group 1. The NAF-2 shoulder abduction angle was significantly higher than the NAF-1. The wrist flexion angle did not show any significant difference between the affected and non-affected arms within the same group. The desired wrist supination angle was far from the one measured in all four groups. The dispersion of the wrist supination angle is very high in both arms, not showing significant

differences between either group.

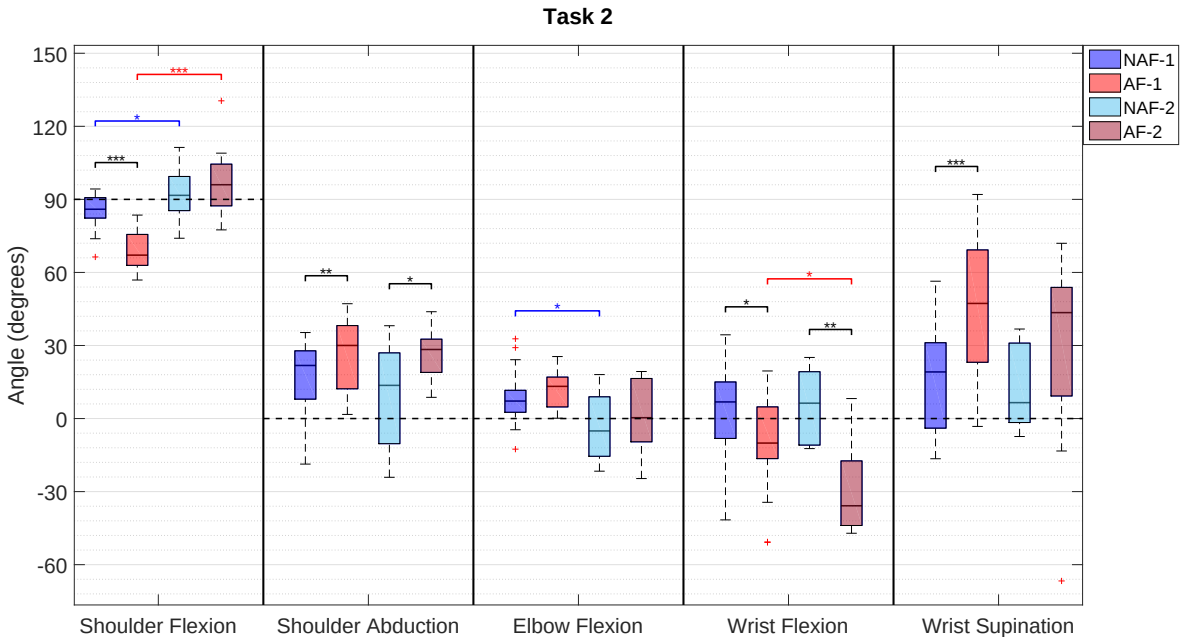

Figure 3.5: Boxplots (median and IQR) of the target angles for the most significant joints evaluated in the second task of the protocol in the four groups. The black dashed lines represent the desired targets for the task. Significant differences between arms of the same group are indicated with a black line. Significant differences between the same arm of different groups are indicated with a blue (for the NAF) or red (for the AF) lines. $*P < 0.05$; $**P < 0.01$; $***P < 0.001$.

In the second task (shoulder flexion movement, mixing synergies), there is a higher deviation from the desired target shoulder flexion angle in the affected arm of the more impaired group of patients. The shoulder flexion angle was significantly higher in the NAF-1 group when compared to the AF-1. However, there is no significant differences between arms of the less affected group. When the two groups are compared, it is seen that the shoulder flexion angle is significantly higher in the AF and NAF arms of group 2. The shoulder abduction angle is significantly higher in the AF-1 and AF-2 groups when compared to the NAF-1 and NAF-2 groups respectively. The median of the elbow flexion angle of the NAF-1 and AF-1 groups is higher than the desired target angle, indicating that the elbow is not fully extended. However, there are no significant differences between arms in the more impaired and less impaired groups of patients. The wrist flexion angle is significantly lower in group AF-2 when compared to group NAF-2 and also when compared to group AF-1. Both groups show significant differences between the affected and non-affected arms of the same group. Finally, the wrist supination angle only shows to be significantly higher in the affected arm of the less impaired group when compared to the non-affected arm of the same group. The difference between both arms in group 2 is not significant.

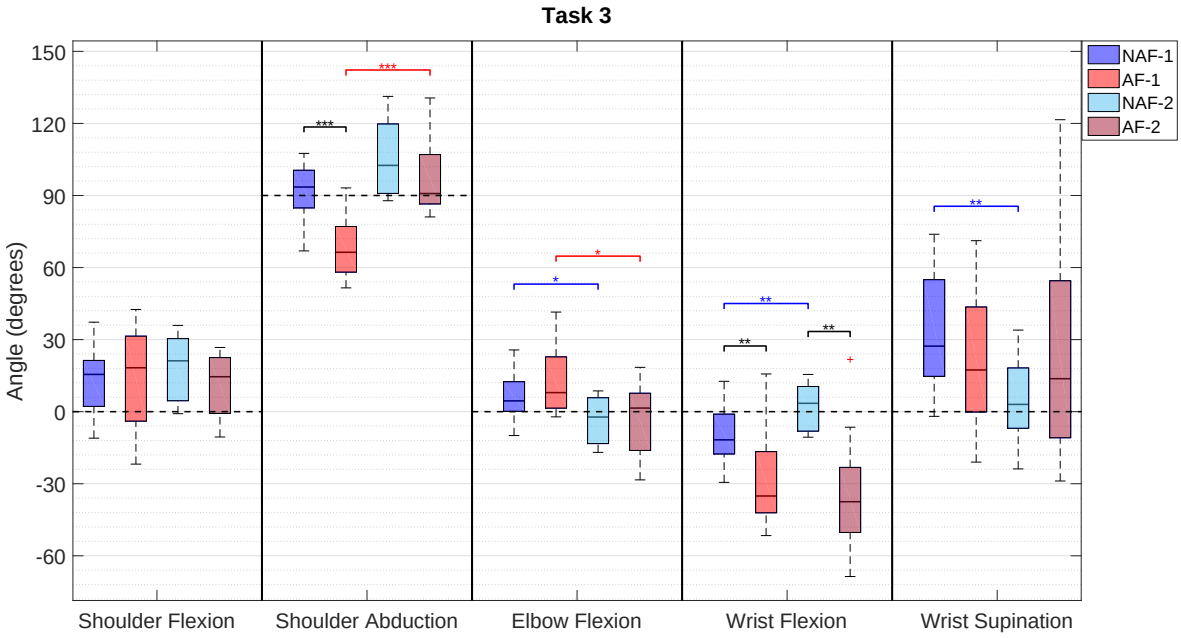

Figure 3.6: Boxplots (median and IQR) of the target angles for the most significant joints evaluated in the third task of the protocol in the four groups. The black dashed lines represent the desired targets for the task. Significant differences between arms of the same group are indicated with a black line. Significant differences between the same arm of different groups are indicated with a blue (for the NAF) or red (for the AF) lines. $*P < 0.05$; $**P < 0.01$; $***P < 0.001$.

During task 3 of the protocol (shoulder abduction, movement out of synergies), a similar behaviour as in the previous task occurs. The affected arm of the more impaired group does not reach the desired target shoulder abduction angle. The measured angle in the AF-1 group is significantly lower than the angle in groups NAF-1 and also than the joint angle in the affected arm of group 2 (AF-2). The difference between arms is not significant in group 2. The elbow flexion angle does not show significant differences between arms of the same group. However, the joint angles of the AF-2 and NAF-2 groups are significantly lower than the ones measured in groups AF-1 and NAF-1 respectively, where the elbow flexion angle is higher than the desired target angle. The wrist is significantly more extended when the task is done with the affected arms when compared to the non-affected arms of the same impairment level groups.

In the last task (wrist flexion/extension), the shoulder flexion angle is significantly lower in the impaired limb when compared to the non-affected one of the more severely impaired group of patients and also when compared to the affected arm of the less impaired group. The desired shoulder flexion angle is not reached only by the AF-1 group. The shoulder abduction angle is significantly higher in the affected arm when compared to the non-affected arm within the same group of subjects. Similarly to the shoulder flexion angle, only the AF-1 shows a significantly higher elbow flexion angle. The wrist flexion and extension angles only show significant differences between groups NAF-1 and AF-1, where the wrist range of

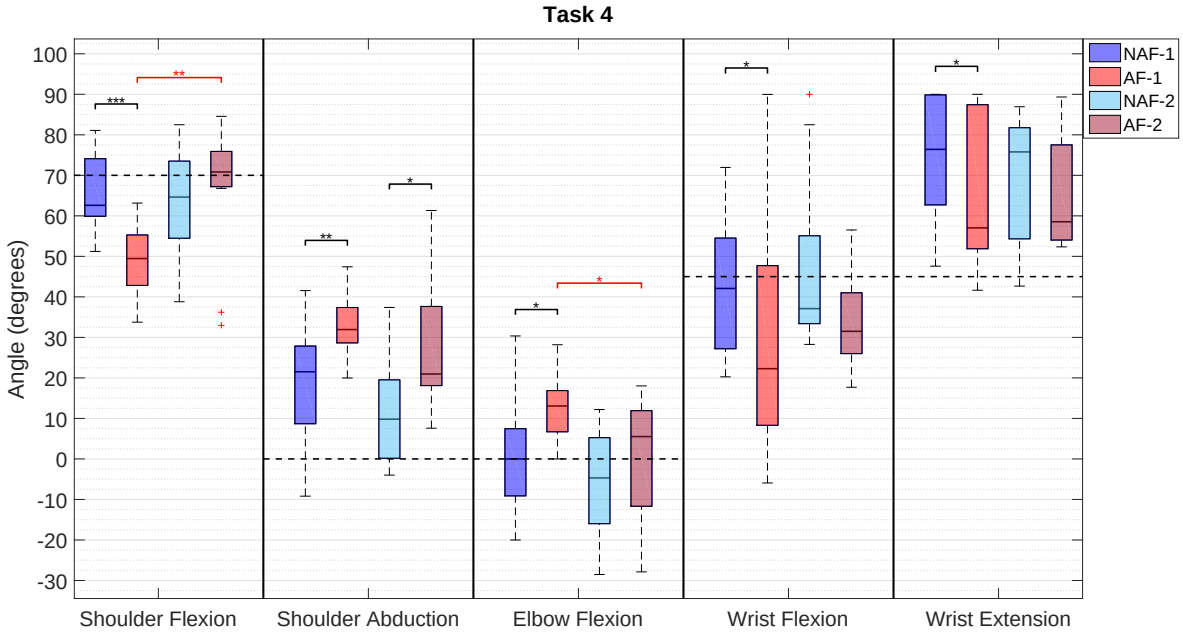

Figure 3.7: Boxplots (median and IQR) of the target angles for the most significant joints evaluated in the fourth task of the protocol in the four groups. The black dashed lines represent the desired targets for the task. Significant differences between arms of the same group are indicated with a black line. Significant differences between the same arm of different groups are indicated with a blue (for the NAF) or red (for the AF) lines. $*P < 0.05$; $**P < 0.01$; $***P < 0.001$.

motion is smaller in the AF-1 group. However, there are no significant differences between the affected arms of the different groups.

3.4 Discussion

Measuring kinematics during clinical motor function assessment scales has not been performed extensively in the past. The majority of studies use kinematic measures in activities of daily living or while performing functional tasks, like reach-to-grasp [9], [48]–[50]. Some studies used inertial measurement units while performing simple movements that include flexion/extension, abduction and supination of limb segments [45], [50]. The four chosen tasks for the protocol of this study are part of the FMA-UE test, and follow the theoretical order of motor function recovery proposed by Twitchel and Brunstrom. The kinematic analysis with the developed distributed IMU measurement system is a minimally invasive technology that uses IMUs for quantification of arm function. By performing the arm-related tasks from the clinical scale, the presence of the described pathological synergies can be analysed via features that describe the movement patterns of the patients. Here, the joint angles of the different segments of the arm are measured. In this study, the ten patients performed the FMA-UE test with the affected and non-affected arms, and, with the system, the orientation of each limb segment, including trunk, shoulder, upper and lower arms, hand, thumb, index

and middle fingers was estimated.

The results presented in Figures 3.4 - 3.7 and the results from the statistical analysis show significant kinematic differences between the affected and non-affected limbs.

The first task movement follows the pathological flexor synergy, where the shoulder abduction is accompanied with elbow flexion and wrist supination. Figure 3.4 shows a similar behaviour in the shoulder and elbow flexion of the AF and NAF arms. The shoulder abduction angle is significantly lower in the affected side, but the median is higher than the desired target angle. These findings suggest that when the movement is done within synergies (abduction of the shoulder accompanied by elbow flexion and wrist supination), the kinematic differences might not be related to the presence of the flexor synergy, but with muscle weakness or paresis, causing the inability to abduct the shoulder against gravity. The lower shoulder and elbow range of motion is only noticed between the affected and non-affected arms of the more impaired group, indicating that less affected patients have a indeed less effects of paresis. The wrist supination angles are below the desired target angle in all groups, having a very high variance in the results. The effects of pathological coupling are inconclusive in the wrist joint.

The second task is intended to mix the flexion and extension synergies. The results show that the shoulder flexion angle is significantly lower in the affected side of the more impaired group. The cause of a lower shoulder flexion can be related to weakness or a compensation strategy to avoid elbow flexion. Figure 3.5 indicates that there is a higher elbow flexion angle in the affected side of all patients. However, the difference is not significant. The subjects were clearly instructed to perform the movement with their elbow completely extended. It is possible that they prioritize the elbow angle and not the shoulder flexion. The shoulder abduction angle is higher in the affected arm of both groups of patients, which is a manifestation of the flexor synergy, where the shoulder flexion is accompanied by abduction. Also, there is more supination of the wrist in the AF arm, which is also a behaviour present in the described pathological flexor synergy [42].

The third task (shoulder abduction movement) shows a significant difference between the affected and non-affected limbs. When the task is done with the affected arm of the more affected group, the shoulder is not sufficiently abducted in order to reach the desired target angle. The pathological synergy behaviour is, however, not clearly visible in this task since the elbow flexion angle does not show significant differences between arms of the same group. Similarly to the previous task, it is possible that patients prioritize the extension of the elbow and prefer not to abduct the shoulder as much in order to not flex the elbow. The flexor synergy is characterized by joint flexion of the wrist and elbow. The results go against the description of this synergy, since the wrist was more extended in the affected arm.

The fourth task, intended to evaluate wrist function, shows expected results, seen in Figure 3.7, where the wrist flexion and extension is significantly higher in the non-affected arm when compared to the affected limb of the more impaired group. The shoulder flexion angle in this movement is not well defined for the subjects. They are instructed to flex the shoulder 70°, which is not easy for the subject to determine where it is. Even so, it appears that the shoulder flexion angle is higher in the non-affected side. The elbow flexion

is significantly higher in the affected limb, as well as the shoulder abduction, which follows the observations of pathological synergies. From the results shown in this study, the wrist range of motion measured in the affected limb is significantly lower than the non-affected arm. It is also visible that if patients attempt to flex or extend the wrist, the elbow is also flexed in the impaired arm, behaviour that is not seen in the non-impaired arm. The presence of the flexor synergy is more clear in this task. It has been observed in the past that wrist and finger motor function is usually the last to recover [19].

The statistical tests done between the upper extremities of the more and less affected groups (group 1 and 2 respectively) suggest that the variation of the level of impairment is related to the features presented in this study, and also to the presence of a more severe pathological synergistic behaviour. A significant decrease in the coupled shoulder flexion or abduction and elbow flexion from group 1 to group 2 can be noticed in tasks 2 and 3. The more impaired group of patients shows a lower shoulder flexion and a higher elbow flexion angle when compared to the less impaired group in task 2 (shoulder flexion movement), indicating a more severe pathological synergistic behaviour in the affected arm. However, the difference between the affected arm's elbow flexion angle of group 1 and 2 is not significant, despite the lower median value. The same happens in task 3 (shoulder abduction movement), where the shoulder abduction angle is smaller and the elbow flexion is higher in group 1. This behaviour is seen between both the affected arms and the non-affected arms of the two groups, although the difference in shoulder flexion and decrease in elbow flexion is smaller in the NAF limb. This suggests that the ipsilesional upper extremity is also affected by stroke. This finding is supported by previous research [53], where it was found that the ipsilesional arm also suffers from less severe motor impairments after stroke. It is also possible that the subject does not perform the movement well with the non-affected arm due to factors not related with brain cell damage, and only due to age-related weakness or low flexibility in the joints. Nevertheless, results show that the difference between the shoulder abduction of the AF and NAF arms in the same group of subjects is significant in group 1 but not in group 2, indicating that the less impaired subjects perform the task similarly with both arms, having less severe pathological muscle coupling. The decreased coupling between elbow flexion and wrist flexion/extension angles is also seen in the fourth task. Less impaired subjects have a lower elbow flexion angle when the wrist is flexed or extended. The wrist range of motion, however, does not vary significantly between the arms of the same group.

Several objective kinematic features have been shown to have a strong correlation with clinical scales [9], [45], [50], [54], [55], such as movement smoothness, peak velocity and hand trajectory. The mentioned studies performed a kinematic objective assessment in reach-to-grasp tasks. Also, a detailed measurement of the different limb segments has not been explored in movements of the clinical FMA-UE test. The relation between the measures shown in the present study and the level of impairment, although it follows the theoretical aspects that qualify motor function in stroke patients, does not have a high statistical power due to the low sample size and the small range of impairment severity in the population. This is also reflected in the high variation of some joint angles measured in patients of the same group. Although there is a general decrease in impairment level measured with

the kinematic features for less affected participants, some specific patients who had a lower FMA-UE score could reach the desired target joint angles of the different tasks with no signs of severe pathological synergistic movement. The recovery of motor function and the presence of specific types of impairments is highly variable between individuals [21]. The fact that the joint angles used in this analysis where only the ones measured when the subject was in the end posture of the task is a limitation of this study. Several other types of features related to the movement profile can indicate the presence of motor function impairments, like movement smoothness and velocity profiles [45], [50], [56]. The measurement of the joint angles at different time points of the task can be of interest as well. In the tasks performed in this experiment, the FMA-UE score is based on the range of motion of the joints and also in the moment where the coupling of the shoulder and elbow starts. This moment is hard to be visually identified in less impaired stroke patients, as well as the smoothness and the velocity profiles. The sensors used in the distributed measurement system developed for this study have the ability to measure these features. A future study should analyse different strategies for quantifying motor function.

Although the results of this study followed the theoretical insights of the disease, some limitations were identified. Different sources of errors could have a negative impact in the arm orientation estimation. The sensor-to-segment calibration procedure was performed before and after the experiment. Although the therapist helped the participants maintaining the required positions or performing the dynamic movements (like the wrist pronation and the hip flexion movements), it was difficult to perform them correctly. More calibration movements would increase the accuracy in the joint angle estimation and the estimated angles would correspond better to reality. The same applies to the global frame definition. Another source of error is the lack of consistency in the initial position for each task. The kinematic reconstruction is based on the orientation of the initial position, defined by the orientation of the sensors related to the global frame before the task execution. This orientation is used to reset the orientation of the sensors and reduce drifts caused by gyroscope and accelerometer bias, noise and possible external factors that affect the measurements (like temperature and sudden movements). If the subject deviates a lot from the initial posture defined in the beginning of the experiment, the orientation estimation of the task will be prone to errors. The lack of a reference system to validate the orientation estimation methods is a drawback of the study. The quality of the measurements was assumed to be acceptable based on trials performed on rigid models of the arm and on healthy subjects (see section 2.5 of Chapter 2).

Nevertheless, the usage of the distributed IMU system developed in this work can increase the impairment's evaluation quality and discard the subjective perspective of the human eye. The complementary use of the system during the FMA-UE test is of interest since it objectively measures the observations done by the therapist during the assessment and provides a detailed analysis of the movement.

3.5 Conclusions

The presented usability study showed that the developed distributed measurement system is capable of distinguishing movements of the affected and non-affected upper extremities of stroke patients. The IMU system can objectively measure important kinematic features to assess motor function of patients when they perform tasks from the FMA-UE test. It was shown that the system can identify the presence of pathological muscle coupling and measure features related to the pathological synergies present in the movement of stroke patients. Also, the severity of the pathological coupling reflected and measured by the arm joint angles is related to the level of impairment of the patients, where the more affected patients show the presence of more severe pathological synergistic behaviour and weakness in the shoulder, elbow and wrist joints. It is concluded that the distributed measuring system is a useful tool for assessing motor function of the upper extremity of stroke patients.

Chapter 4

Quantifying abnormal movement patterns in functional tasks with the use of a distributed inertial measurement unit system in stroke patients

4.1 Introduction

The previous chapter focused on evaluating stroke patients on a motor function level. Despite the prevalence of different impairments, stroke survivors can perform several functional activities to a certain extent [41]. It is important that both the body function and activity level are assessed to get a full comprehensive view on the motor assessment of patients [17], [21]. Stroke patients' independence decreases when performing simple activities of daily living, such as reaching to objects, grasping and moving them. The functional usability of the upper extremities require a more complex coordination of joints. Grasping objects involve complex contextual constraints, like the object's properties and location relative to the body, and the goal of the task influences motor planning and execution [57]. The positioning of the fingers, hand and arm will be sensitive to the goal of the task.

Depending on the level of motor impairments, stroke patients will have the tendency to decrease the use of the paretic limb or to adopt certain movement strategies that lead to a learned bad use of the upper extremity [6]. When a patient with motor deficits due to stroke attempts to voluntarily move the impaired arm, the natural reaction is to use compensatory strategies in order to successfully complete the movement. The presence of pathological coupling of the arm muscles potentiates the use of compensatory strategies [6], [9]. When stroke patients perform reaching tasks, the shoulder flexion or abduction is combined with elbow flexion (flexor synergy) and shoulder extension or adduction is accompanied by elbow extension (extensor synergy). In order to achieve success in the task, patients adopt trunk

movements to compensate for the short reaching distances limited by the inability to fully extend the elbow. The level of hand dexterity also has a high impact in the level of success in activities of daily living. Weakness in the hand causes inability to grasp, lift and hold objects. Loss of independent finger movement and dexterity causes difficulties in grasping objects of different shapes, forcing the person to adopt non-efficient arm postures to perform tasks [31], [58].

As stated in Chapter 1, one of the most commonly used tests to assess the activity level of the upper limb in stroke is the Action Research Arm Test (ARAT) [17]. The ARAT test was firstly designed by Lyle [22] and consists of four different domains that focus on evaluating grasp, grip, pinch and gross movement. It includes 19 items, where each task is rated on a 4-point scale based on the ability and time to perform the movement. The ARAT scale suffers from common limitations as in the FMA test. The subjectiveness of the clinician can induce misclassification of the activity level of the patient if the score criteria does not follow a standardized method [24]. Also, the scale has a floor and ceiling effect and low sensitivity for patients with mild hemiparesis [26]. Objectively quantifying the level of activity in stroke patients becomes of interest to complement the assessment of motor function. The ARAT grasp subscale is intended to evaluate the subjects performance in grasping an object and placing it in different target positions. This movement is performed with different types of predefined objects, varying in size and shape. Usually, the specific weight of the object is not changed and is standardized for each type of object [24].

Several studies with kinematic analysis of the upper extremity in stroke patients while performing activities of daily living or reaching and grasping tasks have shown significant results and encouraged the use of objective measures for assessing quality of movements [9], [27], [44], [48]–[50]. Wearable sensors have gained a significant interest over optical systems, and its relevance has been shown in multiple studies [29], [44], [59]–[62]. One study used accelerometers on the trunk, arm, hand and fingers to predict clinical scores of motor abilities in stroke patients while reaching and performing different activities of daily living [62]. A more recent study used IMUs with both accelerometers and gyroscopes placed in the sternum, upper and lower arms and hand, in order to extract several kinematic features while stroke patients performed the ARAT protocol [63]. However, a system that allows simultaneous orientation estimation of the trunk, arm, hand and fingers has not been done before. The developed distributed kinematic measurement system, in addition to having IMUs placed on the sternum, shoulder, upper and lower arms, hand and thumb, index and middle fingers, it contains force sensitive resistors that measure the linear force applied by the fingertips of the thumb, index and middle fingers.

The main aim of this chapter is to objectively quantify abnormal movement patterns, such as pathological synergies and compensation strategies, in functional reach-grasp-displace tasks with the use of inertial sensors. It is hypothesized that the distributed measurement system can differentiate the movement between the affected and non-affected upper extremities of stroke patients. The effect of pathological muscle coupling in the upper extremity is noticed on the shoulder and elbow. It is expected that when stroke patients attempt to grasp an object, the shoulder is more abducted when the movement is done with the affected

upper extremity than with the non-affected arm. When patients attempt to move the object to a certain target position with their affected arm, due to the fact that the shoulder abductor muscles are activated, the elbow is incapable of extending since there is a coupled activation of the elbow flexor muscles (pathological flexor synergy). The inability to fully extend the elbow is usually accompanied by compensation strategies in order to displace the objects. Stroke patients typically adopt trunk movements in order to successfully transport objects. With the measurement of the sternum's orientation by the distributed IMU system, it is hypothesized that patients that suffer from motor impairments use a higher amplitude of trunk movements towards the direction of the movement when displacing objects with the impaired arm. The level of motor impairment is theoretically directly related to the motor performance of the affected upper extremity. It is expected that patients with a stronger presence of pathological synergistic movements (patients with higher difficulties in extending the elbow) utilize more the trunk compensation strategies than less affected patients.

An additional aim of this study is to analyse the influence of the object's weight and size in the motor performance of the task. It is hypothesized that stroke patients have more difficulties in displacing heavier objects. Heavier objects require a higher muscle activation, potentiating the coupled activation of the arm muscles. The pathological synergistic behaviour is more prevalent and the shoulder and elbow joints are more abducted and flexed respectively. Due to this, the trunk compensation strategies have a higher amplitude when displacing heavier objects. The size of the object is expected to have more impact in the posture of the hand. A natural behaviour is that smaller objects require a higher finger flexion in order to grasp it. Grasping smaller objects also require a higher level of dexterity. On the other side, grasping larger objects requires a higher range of motion to extend the fingers.

In this chapter, kinematics and kinetics are measured in a reach-grasp-displace task that follows the ARAT grasp subscale protocol. The influence of the object's weight and size is explored, as well as the influence of the target position on the motor performance in the affected and non-affected arms of stroke patients.

4.2 Methodology

The measurement system and the kinematic reconstruction followed the same methodology as in Chapter 3. The detailed description of the system can be found in section 3.2.1 and the kinematic reconstruction in Chapter 2. Since this experiment was performed immediately after the FMA-UE protocol of Chapter 3, the sensor-to-segment calibration parameters used were the same.

An additional step was needed for the kinematic reconstruction in this study. The initial orientation of the sensors in this case is different from the one used in the FMA-UE experiment. The participant was asked to do the last two movements of the sensor-to-segment procedure (see table 3.1, which are used to define the global frame). After these movements, the subject was asked to immediately go to the initial position, while still recording the IMU data. With the kinematic reconstruction methods, the orientation of the sensors in the initial position was estimated and used as a reset point for the kinematic reconstruction of each

movement. This was done to avoid drift and errors in the orientation of the sensors (see section 2.1.2 in Chapter 2).

4.2.1 Experimental Design

The participants included in this second study are the ones that were included in Chapter 3. Detailed demographics can be found on table 3.2.

The experimental procedure was based on the grasp subscale protocol of the ARAT. The participants were sited in front of a table and were asked to grasp several blocks and place them in different target positions. They were instructed to start and finish the task with the hand flat on the table. The block was initially placed next to the hand.

Positions: The target positions were based on each subject's arm length. The first position was defined by asking the participants to fully extend their arm to the front (aligned with the shoulder ipsilateral shoulder) while keeping the hand on the table without moving the trunk. The physiotherapist aided if the subjects were not able to fully extended the arm. The second position was set at a 60° horizontal abduction of the arm from the first position. The third and fourth positions are the same as the first and second position, respectively, but at a height of 37 centimetres above the table. Figure 4.1 presents a schematic of the different positions used for the tasks.

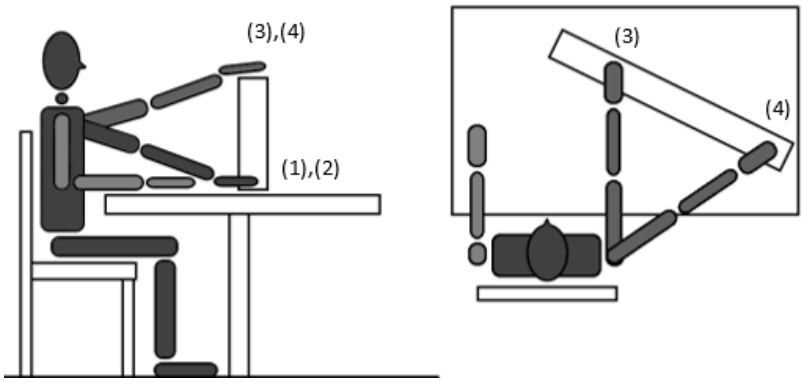

Figure 4.1: Schematic of the four positions used in the ARAT experimental protocol.

Blocks: The experiment consisted in moving six different blocks to the four target positions. Two of the blocks were the standard wooden blocks used in the traditional ARAT: one 10 cm^3 block (referd to as BW) and a 2.5 cm^3 block (referred to as SW). The additional four blocks consisted of two variations in weight per wooden block (a heavier and a lighter version). The lighter blocks are 3D printed out of poly lactic acid (PLA) with low infill to reduce the weight (the 2.5 cm^3 and the 10 cm^3 lighter blocks are referred to as SL and BL respectively). The heavy block were similarly printed, but a lead inner core was inserted to increase the weight (the 2.5 cm^3 and the 10 cm^3 heavier blocks are referred to as SH and BH respectively). The blocks can be seen in Figure 4.2, and the size and weight of each one is described in table 4.1.

In total, 24 combinations of block and position were performed. For each combination, the participant was asked to do three repetitions of the reach-grasp-displace task. The sessions

Block	Size	Weight
BW	10 cm^3	490 g
BH	10 cm^3	1008 g
BL	10 cm^3	108 g
SW	2.5 cm^3	20 g
SH	2.5 cm^3	106 g
SL	2.5 cm^3	6 g

Table 4.1: Size and weight of the blocks used in the experimental protocol.

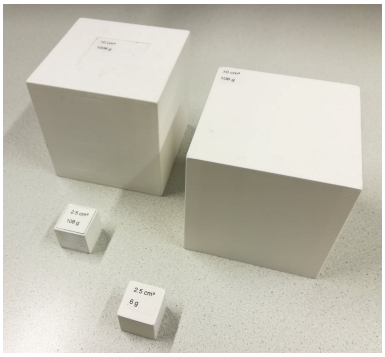

Figure 4.2: Picture of the blocks used in the experimental protocol.

were divided by block. A session consisted in performing the three repetitions in each of the four target positions with one of the blocks. Each participant did six sessions. The order of the blocks was randomized and the subjects did not know the weight of the 3D-printed blocks. For each session, before starting the tasks, the two last movements from the sensor-to-segment procedure (synchronization movements) were performed to reset the global frame and to redefine the orientation of the sensors in the initial position.

4.2.2 Data Analysis

Feature extraction

The features used to characterize the movement were the same as the ones described in section 3.2.4 (details in Chapter 2, section 2.4). An additional feature included in this part is the trunk compensation. The trunk angular compensation was measured as the difference between the inclination of the trunk while performing the movement and its initial inclination. Three different angular compensations were considered: frontal (changes in the inclination on the sagittal plane), lateral (inclination in the frontal plane) and rotational compensation (angular change in the transverse plane).

The arm, hand and fingers features used in the analysis are the joint angles taken in two different time points of the movement. The first time point is when the subject completes the grasping of the block (**grasping action**). The second time point is when the block is placed in the target position (**placing action**). The identification of the time points is based on the observation of the shoulder, elbow and finger joint angles. In some cases, the fingers force data was used to identify the moment when the subject grasps and releases the object, complementing the information about the two time points estimated by the joint angles. An example of the joint angles and trunk compensations measured during one task is presented in Figure 4.3. For the arm and hand joint angles, the grasping and placing action is identified with a green and red dashed line respectively. The trunk compensation is not discriminated between the two moments. The trunk compensation features used in the analysis are the maximum frontal, lateral and rotational angle during the movement.

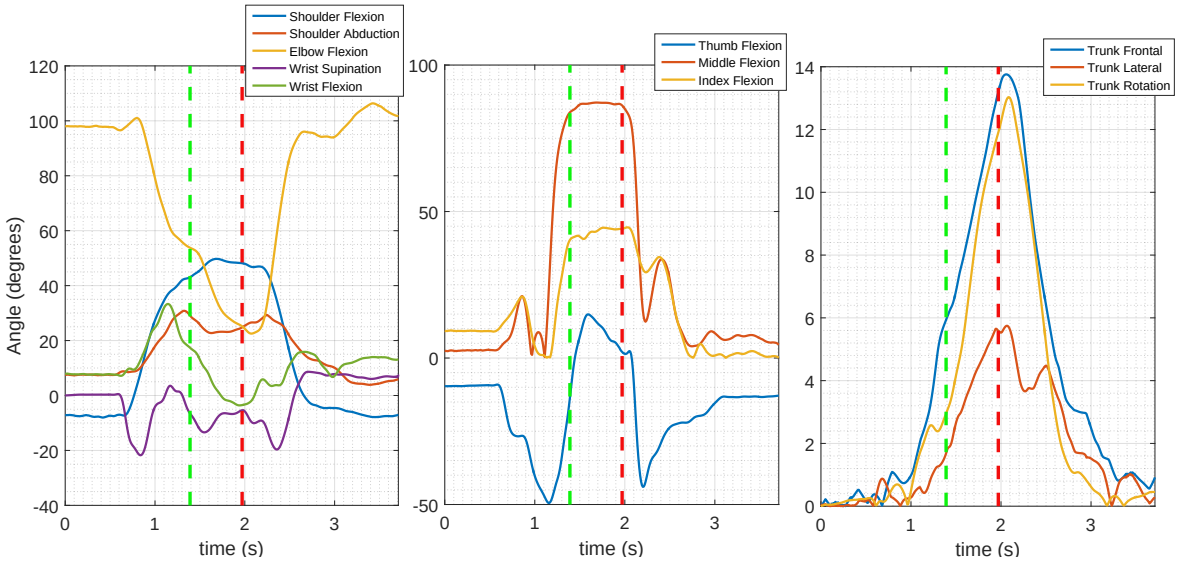

Figure 4.3: Arm joint angles (left), finger joint angles (centre) and trunk compensation (right) measured in one participant during a reach-to-grasp task. The green and red dashed lines indicate the grasping and the placing time points respectively.

Statistical analysis

Similarly to the analysis in Chapter 3, the subjects were divided in two groups based on their level of impairment. The difference is that here, they were divided according to the total FMA-UE score instead of the arm subscore. The more affected group (group 1) included subjects with a score lower than 40 ($N = 4$, FMA-UE score median and IQR: 35.5 (34.5 - 37.5)). The less impaired group (group 2) included subjects with a score of 40 or higher ($N = 6$, FMA-UE score median and IQR: 40.5 (40 - 46)). Each group was separated into affected (AF) and non-affected (NAF) arms, having in total 4 subgroups (NAF-1 - non-affected arm of group 1; AF-1 - affected arm of group 1; NAF-2 - non-affected arm of group 2; and AF-2 - affected arm of group 2).

Different statistical tests were applied to the results. Firstly, to analyse differences between the features of the affected and non-affected arms of the same impairment level group, the Wilcoxon signed rank test was used (more speciffically, differences between NAF-1 and AF-1 and between NAF-2 and AF-2). Differences between the measured features in the same arm but in different groups of impairment were analysed with the Wilcoxon rank sum test (differences between NAF-1 and NAF-2 and between AF-1 and AF-2).

To test differences in the performance of the affected arm of the patients due to the weight and size of the blocks, the subjects were not separated in groups of impairment level. Here, all the measured features of the affected arm were analysed together. Data was separated only by block (six groups corresponding to the measured features in the tasks done with each block). The Kruskal-Wallis test, a non-parametric version of the one-way ANOVA, was used to analyse differences between the measured features of the six different blocks in each position. A post-hoc analysis to discriminate differences in the values of each block was done

using the Bonferroni method.

All statistical tests were performed with a level of significance of 5%.

4.3 Results

Nine of the ten participants were able to perform the complete designed protocol. Due to time restrictions, one of the subjects could not complete the reach-to-grasp tasks for the wooden 10 cm^3 and 2.5 cm^3 blocks. Also, the subject did not perform the synchronization movements in all trials, which lead to errors in the kinematic reconstruction. For these reasons, this subject was excluded from the analysis. After the kinematic reconstruction and joint angle estimation, each angle is taken for the two defined time points. (Legend of the joint angles labels: Sh Flex - shoulder flexion; Sh Abd - shoulder abduction; El Flex - elbow flexion; Wr Sup - wrist supination; Wr Flex - wrist flexion; T Flex - thumb flexion; M Flex - middle finger flexion; I Flex - index finger flexion; Tr Front - trunk frontal compensation; Tr Lat - trunk lateral compensation; Tr Rot - trunk rotational compensation).

Arm, hand and trunk kinematic features

The large number of combinations of target position and block makes it unfeasible to present all the results in plots. Figures 4.4, 4.6 and 4.9 represent the distribution of the calculated features in both the AF and NAF limbs of the two patient groups. Figures 4.4 and 4.6 present boxplots of the upper limb joint angles for the grasping and placing actions respectively. Figure 4.9 presents the trunk compensation angles. Each boxplot includes the measured features in the the tasks performed with all the blocks. The grasping action analysis (Figure 4.4) is not separated for each target position of the protocol, since the blocks where placed in the same position at the start of each task. The figures of the placing action (Figure 4.6) and trunk compensation features (Figure 4.9) contain one subfigure for each of the target positions defined. The statistical analysis is presented by a bar with an asterisk ($*$) on top, indicating significant differences ($* - P < 0.05$; $** - P < 0.01$; $*** - P < 0.001$). The black bars and asterisks represent differences between AF and NAF of the same group. Differences between the NAF arms of different groups (NAF-1 vs NAF-2) are indicated with blue bars and asterisks, and differences between the AF arms of different groups (AF-1 vs AF-2) are indicated with red bars and asterisks.

The multivariate analysis comparing the features of the patients between the different blocks in each target position is presented in tables 4.2, 4.3 and 4.4, where the P-values of the Kruskal-Wallis test are shown. The post-hoc analysis of the affected arm is presented in the form of figures for the relevant comparisons (comparison between blocks with the same size but different weights - BH vs BL; and comparison between blocks with the same weight but with different sizes - BL vs SH). Each figure contains boxplots (median and IQR) of the measured features in each block. The significant differences between pairs of blocks are marked with bars with an asterisk.

The results are organized by grasping action, placing action and trunk compensation

features. In each subsection, the two types of analysis (between each group of patients and between blocks) are presented.

Grasping action

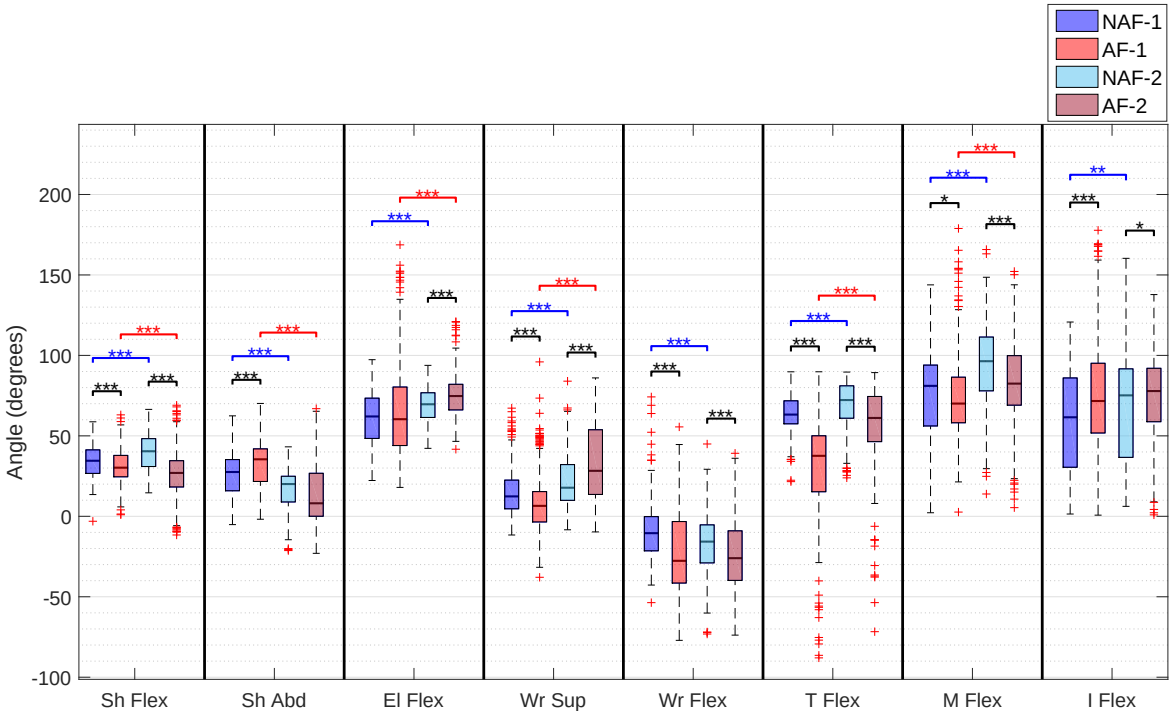

Figure 4.4: Arm joint angles in the grasping action of the experimental tasks of the affected and non-affected arms of the patients in the more and less impaired groups. Significant differences between arms of the same group are indicated with a black line. Significant differences between the same arm of different groups are indicated with a blue (for the NAF) or red (for the AF) lines ($* - P < 0.05$; $** - P < 0.01$; $*** - P < 0.001$).

In the moment where patients grasp the block (Figure 4.4), results indicate that there are significant differences between AF and NAF arms of the same group (NAF-1 vs AF-1 and NAF-2 vs AF-2) in the shoulder, wrist and fingers joint angles. It can be seen that the shoulder is significantly more flexed when patients grasp the object with the affected arm, either in more and less affected patients. The shoulder abduction angle is significantly higher in AF-1 compared to NAF-1 groups, but the difference is not significant between the arms of the less impaired group. In the wrist joint, it is seen that when the grasping is done with the affected arm, the wrist is more extended. At the fingers level, the non-affected hand flexes significantly more the thumb and the middle finger than the affected hand. The index finger is significantly more flexed in the affected hand.

When patients are compared based on their level of impairment, it is seen that both the affected and non-affected arms have different postures. Less impaired subjects appear to have a lower shoulder abduction than more impaired patients when they grasp the object with

either the affected arm or the non-affected. A common higher elbow flexion in both arms in less affected patients was also measured. At the wrist level, less affected patients grasp the objects with a more supinated wrist when compared to more affected patients. It is also seen that both the thumb and middle fingers are significantly more flexed in less affected patients, when grasping with the affected or non-affected arms.

Table 4.2 presents the results of the Kruskal-Wallis analysis of the arm joint angles during the grasping action with the different blocks. The post-hoc analysis of all joint angles of the AF limb is included in Appendix B.2.1.

Table 4.2: P-values of the Kruskal-Wallis test for the arm joint angles of the AF and NAF arms during the grasping action of the different blocks. Bold values indicate a significant difference ($P < 0.05$) between at least two groups (blocks).

	Sh Flex	**Sh Abd**	**El Flex**	**Wr Sup**	**Wr Flex**	**T Flex**	**M Flex**	**I Flex**
NAF	**0.000**	**0.003**	**0.000**	**0.000**	**0.000**	**0.000**	**0.000**	**0.000**
AF	**0.000**	**0.043**	**0.006**	**0.049**	**0.000**	**0.000**	**0.000**	**0.000**

Significant differences are encountered in all joint angles, either between tasks done with the affected or the non-affected arms. This means that at least two blocks cause a different arm posture in the grasping action. The post-hoc analysis on the comparison of the arm posture when patients grasp blocks with the same size but with different weights (weight comparison) and of blocks with the same weight but with different sizes (size comparison) is presented in Figure 4.5.

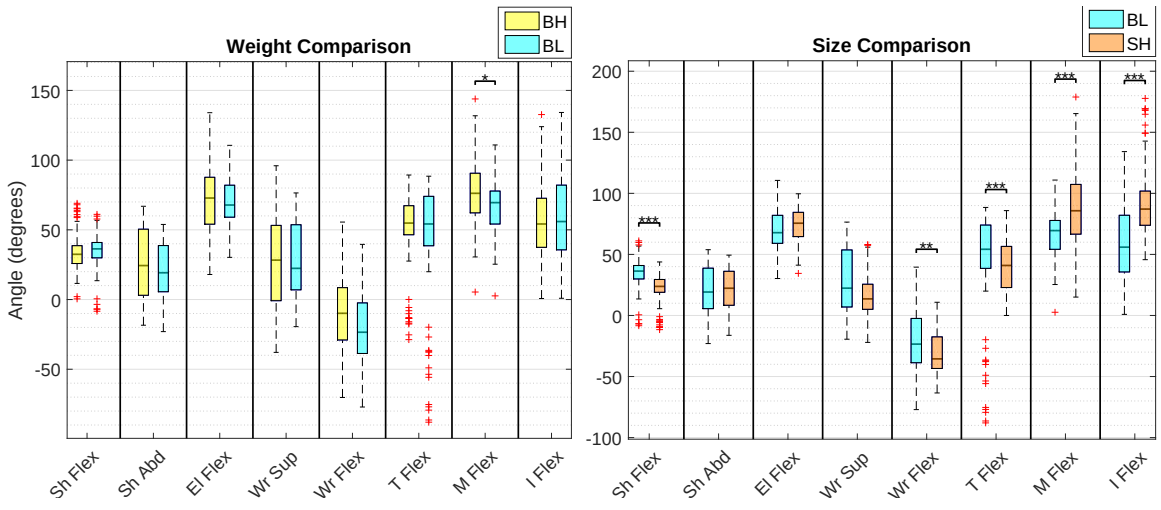

Figure 4.5: Comparison of the arm joint angles in the grasping action of the affected arm of the patients during the experimental tasks with blocks with the same size but different weights (left) and with blocks with the same weight but different sizes (right). Significant differences between arms of the same group are indicated with a black line ($* - P < 0.05$; $** - P < 0.01$; $*** - P < 0.001$).

The grasping posture of the arm varies more when the block has different sizes. When patients grasp the 10 cm^3 block (BL) with the affected arm, they appear to significantly

flex more the shoulder and extend the wrist when compared to the 2.5 cm^3 block (SH). At the more distal joints, the grasping of the small block is done with a significantly higher middle and index fingers flexion but a smaller thumb flexion, as it can be seen in the right plot of Figure 4.5. The wrist supination angle when the subject grasps the block, despite not showing significant differences between the blocks, has a higher median and interquartile range in the 10 cm^3 block when compared to the 2.5 cm^3 block. This indicates that more patients grasp the bigger blocks from the side, with the hand supinated. The smaller block has a lower interquartile range and a median value closer to 0°, indicating that the smaller blocks are grasped from the top.

Placing action features

In the moment when subjects place the block in the target position, the analysis of the measured joint angles is done for each target position of the task (Figure 4.6). From the statistical analysis comparing the AF and NAF arms of the same group, differences at the shoulder, elbow and wrist can be seen when the patients place the blocks in the target position. In all cases, the shoulder and elbow flexion angles are significantly higher when the placement is done with the affected arm than with the non-affected arm in both groups of patients. The elbow flexion angle is significantly smaller in group AF-2 when compared to group AF-1 when the task is done to the target positions 1 and 3 (frontal positions), indicating that the less impaired subjects (from group 2) have the ability to extend more the elbow. However, the shoulder abduction angle is higher in group AF-2, indicating that less affected patients don't abduct the shoulder as much. When the task is done to the target positions 2 and 4 (lateral positions), it is seen that less affected subjects abduct the shoulder significantly more than the more impaired ones. A general overview of the shoulder flexion angle indicates that the affected arm of patients has more difficulties in performing the tasks by flexing the shoulder. In target position 1 (frontal at the table level), the shoulder flexion angle when the placement is done with the affected arm is significantly higher in the less affected patient group when compared to the same arm of the more affected group. This indicates that less impaired patients have a better ability to flex the shoulder. When the placement of the block is done to the lateral target positions (3 and 4), the more affected patients flex more the elbow. The wrist supination angle also shows significant differences in all groups. The placement of the blocks with the affected arm shows to be done with a significantly more supinated wrist than with the non-affected, specially when the target position is on the side of the arm (target positions 2 and 4).

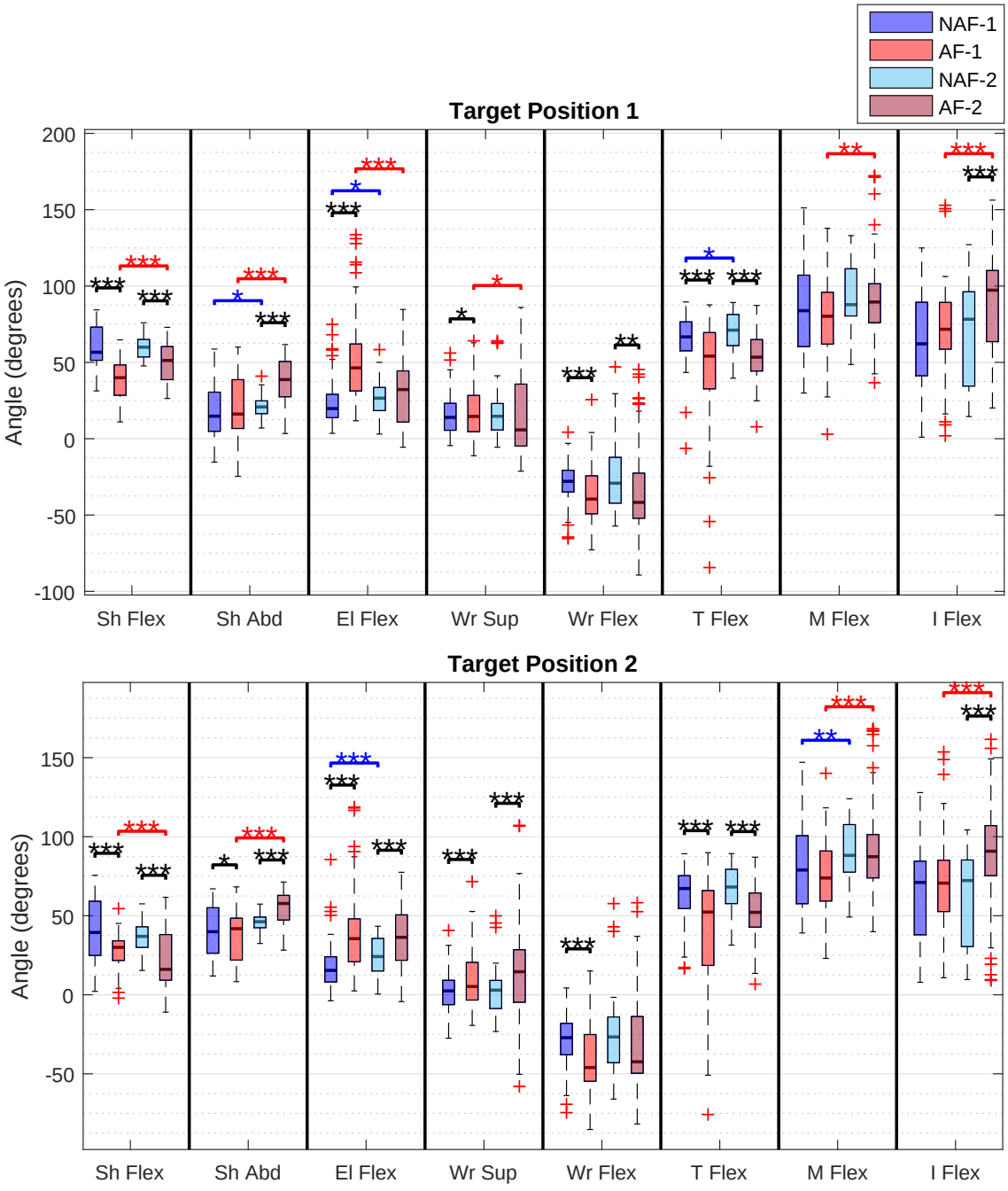
NAF-1
AF-1
NAF-2
AF-2
Target Position 1
Angle (degrees)
200
150
100
50
0
-50
-100
Sh Flex
Sh Abd
El Flex
Wr Sup
Wr Flex
T Flex
M Flex
I Flex
Target Position 2
Angle (degrees)
150
100
50
0
-50
Sh Flex
Sh Abd
El Flex
Wr Sup
Wr Flex
T Flex
M Flex
I Flex

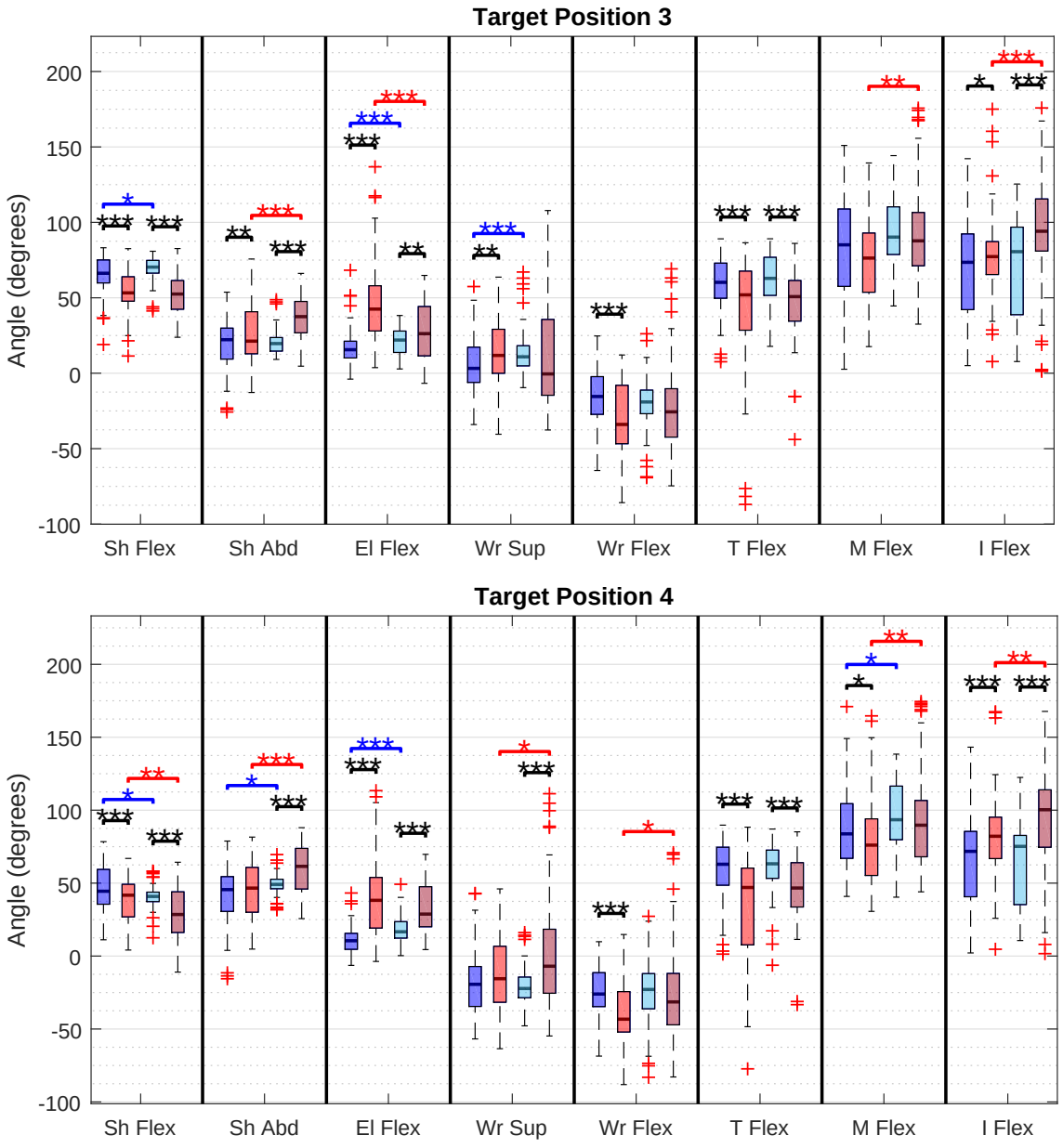

Figure 4.6: Arm joint angles in the grasping action of the affected and non-affected arms of the patients in the more and less impaired groups, in the experimental tasks to each target position. Significant differences between arms of the same group are indicated with a black line. Significant differences between the same arm of different groups are indicated with a blue (for the NAF) or red (for the AF) lines ($* - P < 0.05$; $** - P < 0.01$; $*** - P < 0.001$).

The results of the multivariate analysis of the calculated features in the placing action with different blocks is presented 4.3. It is possible to see that the variability in the joint angles is more significant between the wrist supination, middle and index fingers flexion angles of tasks performed with the different blocks. The post-hoc analysis of all joint angles of the affected arm of all patients in the grasping action is presented in appendix B.2.2.

Table 4.3: P-values of the Kruskal-Wallis test for the arm joint angles of the AF and NAF arms during the placing action of the different blocks. Bold values indicate a significant difference ($P < 0.05$) between at least two groups (blocks).

		Sh Flex	Sh Abd	El Flex	Wr Sup	Wr Flex	T Flex	M Flex	I Flex
Pos 1	NAF	0.955	0.511	**0.012**	**0.001**	**0.000**	0.687	**0.000**	**0.000**
	AF	0.303	0.381	**0.017**	0.271	**0.016**	0.395	**0.000**	**0.000**
Pos 2	NAF	0.976	0.935	0.357	**0.000**	**0.003**	0.275	**0.002**	**0.000**
	AF	0.324	0.954	**0.003**	**0.000**	0.155	0.624	**0.034**	**0.002**
Pos 3	NAF	0.373	0.431	0.404	**0.000**	**0.003**	**0.006**	**0.000**	**0.000**
	AF	**0.003**	**0.013**	0.168	**0.001**	0.236	**0.004**	**0.000**	**0.019**
Pos 4	NAF	0.993	0.993	0.571	**0.000**	0.842	**0.003**	**0.000**	**0.000**
	AF	0.086	0.181	**0.044**	**0.000**	**0.027**	**0.006**	**0.001**	**0.010**

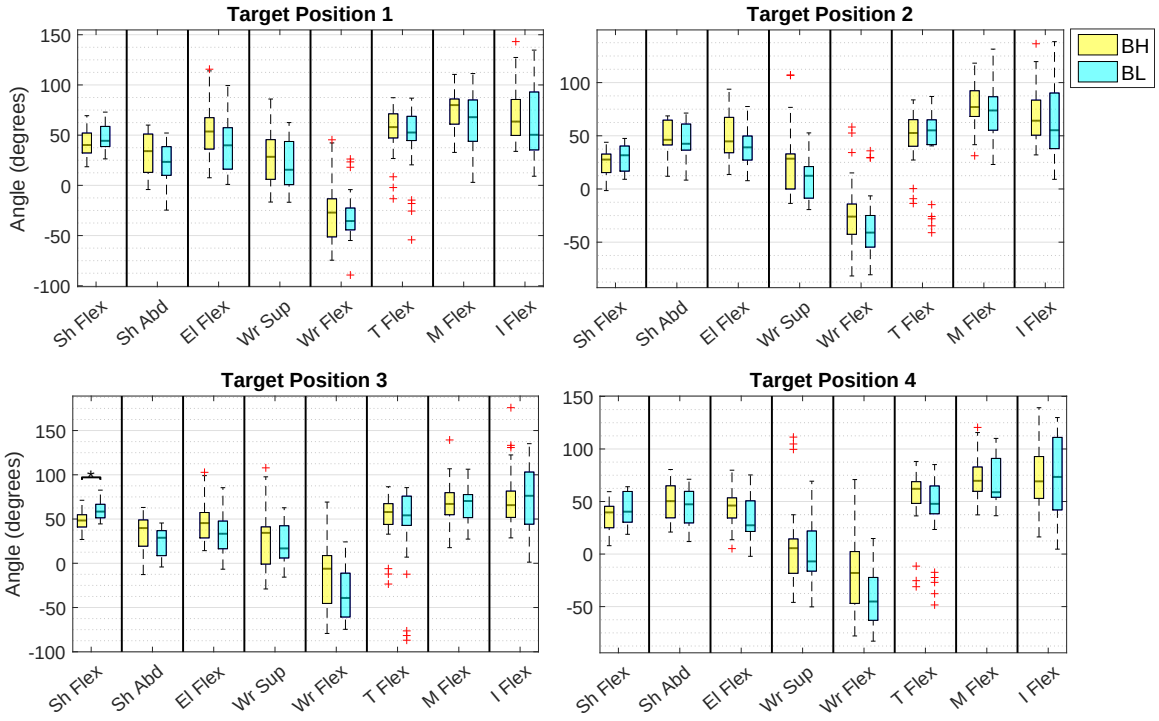

Figure 4.7: Comparison of the arm joint angles in the grasping action of the affected arm of the patients, in the experimental tasks with blocks with the same size but different weights. Significant differences are indicated with a black line ($*-P < 0.05$).

The post-hoc analysis on the comparison of the arm posture when patients grasp blocks with the same size but with different weights (weight comparison) and of blocks with the

same weight but with different sizes (size comparison) is presented in Figures 4.7 and 4.8 respectively.

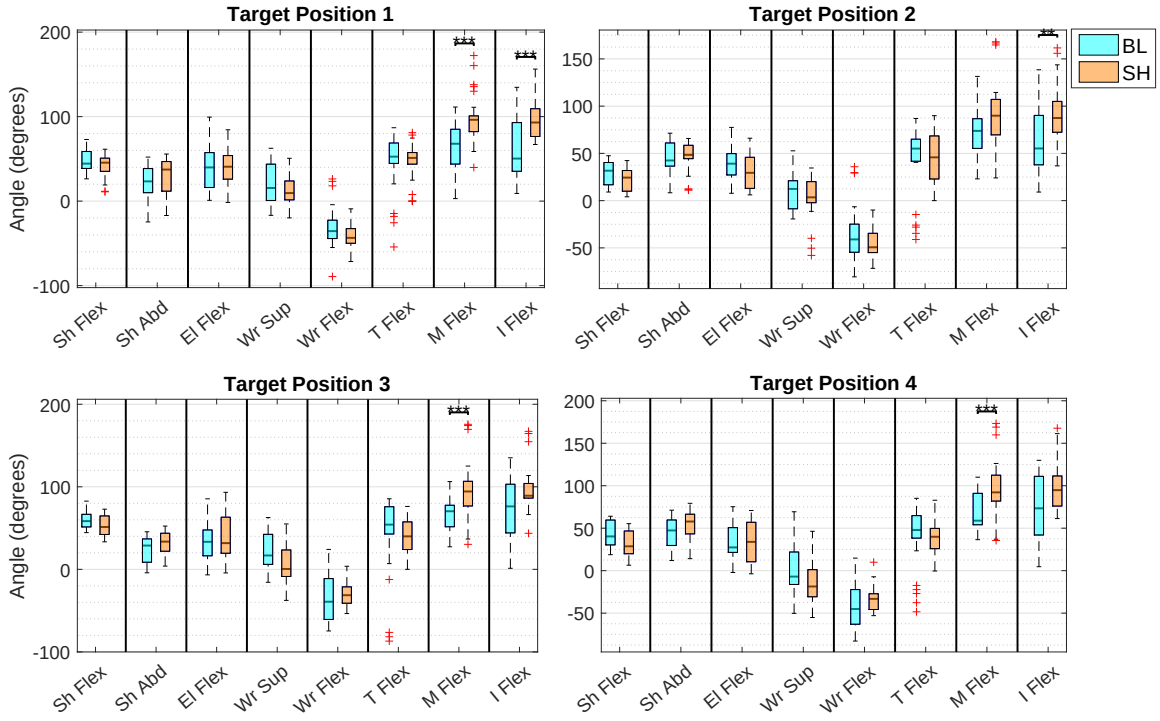

Figure 4.8: Comparison of the arm joint angles in the grasping action of the affected arm of the patients, in the experimental tasks with blocks with the same weight but different sizes. Significant differences are indicated with a black line ($**-P < 0.01$; $***-P < 0.001$).

From Figure 4.7, it is seen that the only significant difference between the placement of blocks with the same size but different weight is in the shoulder flexion angle of the task done to the target position 3, where when patients place the lighter block (BL) the shoulder is significantly more flexed. However, the median values of the shoulder abduction and elbow flexion are lower for the tasks done with the lighter block, despite not being significantly different.

When comparing the effects of the size of the block in the patients' affected arm posture, it is seen from Figure 4.8, similarly to the results from the grasping action, that the index and middle fingers sow to be significantly more flexed when tha task is performed with the 2.5 cm^3 block (SH). The other joint angles do not show significant differences between each block.

Trunk compensation features

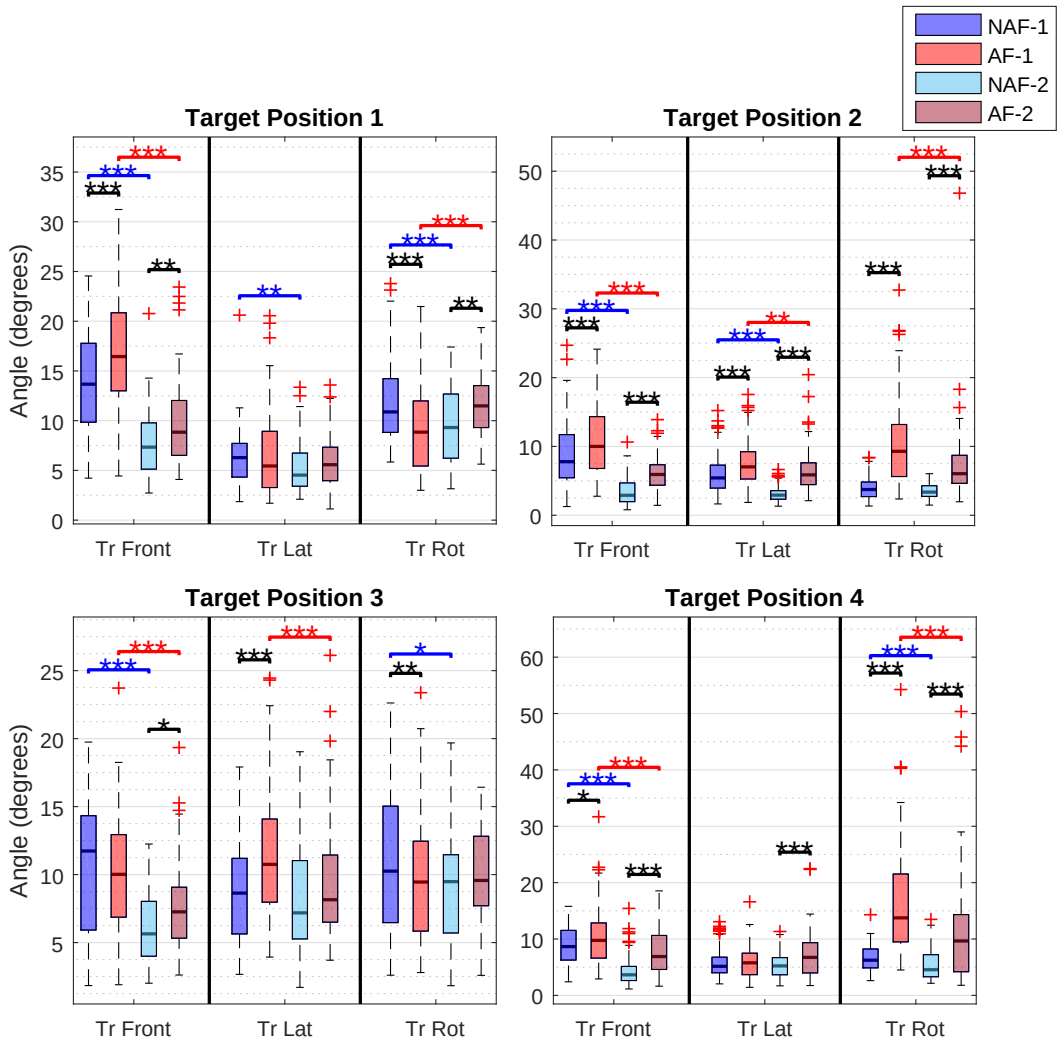

Figure 4.9: Trunk compensation features during the experimental tasks of the affected and non-affected arms of the patients of the more and less impaired groups. Significant differences between arms of the same group are indicated with a black line. Significant differences between the same arm of different groups are indicated with a blue (for the NAF) or red (for the AF) lines ($*-P < 0.05$; $**-P < 0.01$; $***-P < 0.001$).

Depending on the target position, different trunk compensation angles show significant differences between the groups (seen in Figure 4.9). For the first target position, the trunk frontal compensation is significantly higher when the task is done with the AF arm when compared to the NAF of the same group. More affected patients show a significantly higher trunk frontal compensation than less impaired patients, either with the AF and the NAF arms. On the second target position, the frontal, lateral and rotational compensation are significantly more pronounced when the subjects use the AF arm. It is also clearly visible that the amplitude of trunk compensation angles is significantly higher in more affected patients.

The movements performed to the target position 3 only employ a significantly higher trunk lateral compensation when comparing the arms of different patient groups. More affected patients have a higher measured trunk frontal compensation in tasks done with both the AF and NAF arms. The trunk lateral compensation is only significantly higher in group AF-1 when compared to group AF-2. When the task is performed to the target position 4, both the trunk frontal and rotational compensation show significant differences. When the AF arm is used, these features are significantly higher than the NAF of the same group. Similarly to the other target positions, more affected patients use significantly more trunk frontal and rotational compensation in this target position.

The block size and weight also show significant differences in the trunk compensation angles. The results of the multivariate analysis in table 4.4 shows that the trunk frontal and lateral compensation is significantly different between blocks in every target position in movements performed with the AF arm. The trunk rotational compensation is significantly different in both the AF and NAF arms when the displacement of the object is done to the lateral positions (2 and 4) with different blocks. In appendix B.2.3, the post-hoc analysis of the AF arm block variation is presented for all blocks.

Table 4.4: P-values of the Kruskal-Wallis test for the trunk compensation angles of the AF and NAF arms during the tasks with the different blocks. Bold values indicate a significant difference ($P < 0.05$) between at least two groups (blocks).

		Tr Front	**Tr Lat**	**Tr Rot**
Pos 1	NAF	**0.008**	0.106	0.667
	AF	**0.006**	**0.010**	0.782
Pos 2	NAF	**0.004**	**0.016**	**0.010**
	AF	**0.001**	**0.015**	**0.009**
Pos 3	NAF	0.796	0.264	0.510
	AF	**0.000**	**0.002**	0.075
Pos 4	NAF	0.614	0.161	**0.003**
	AF	**0.000**	**0.001**	**0.042**

The post-hoc analysis on the isolated weight and size block variation is presented in Figures 4.10 and 4.11 respectively.

The weight of the block has a significant influence on the level of trunk frontal compensation that the patients use when performing the tasks with the affected arm. Figure 4.10 indicates that patients use significantly more trunk frontal compensation when moving the heavier block (BH) to all target positions.

However, the effect of the size of the block is null. Figure 4.11 indicates that there are no significant differences in any trunk compensation feature between the tasks performed with the smaller and the bigger block.

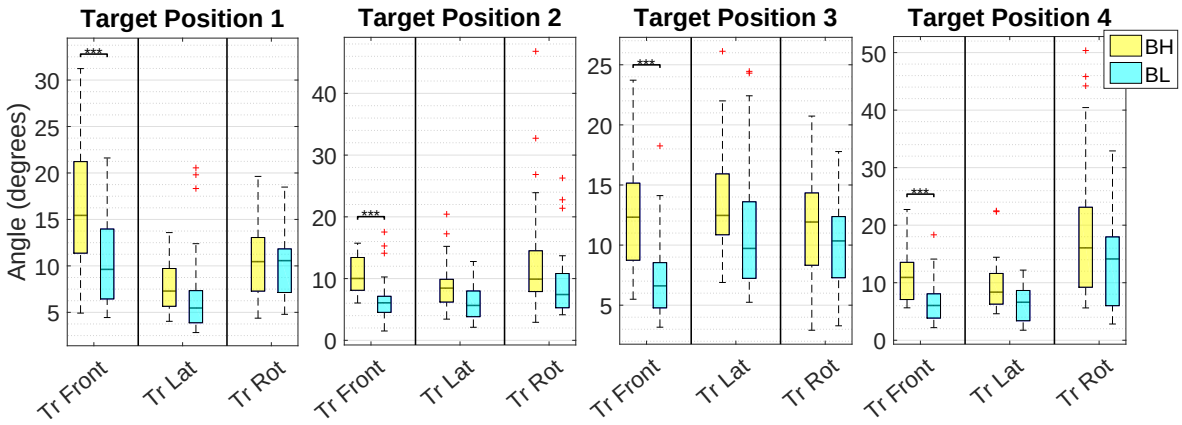

Figure 4.10: Comparison of trunk compensation features during the tasks performed with the affected arm of the patients and with blocks of different weight but the same size. Significant differences are indicated with a black line ($***-P<0.001$).

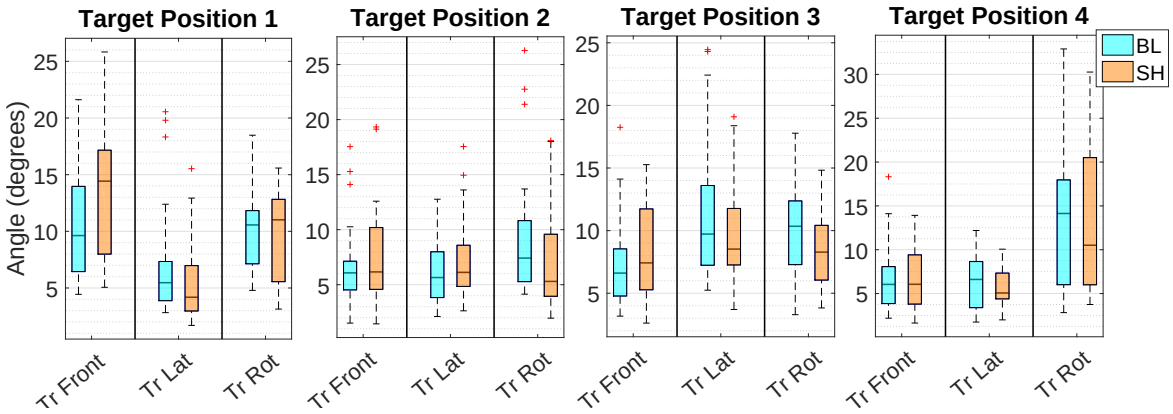

Figure 4.11: Comparison of trunk compensation features during the tasks performed with the affected arm of the patients and with blocks of different size but the same weight.

4.4 Discussion

In the previous chapter, the distributed measurement system was proven to be a useful and objective method to measure the arm and hand movement patterns when stroke patients performed tasks from the FMA-UE protocol. The same methods were applied to analyse the patient's kinematics while they perform functional activities. The reach-grasp-displace movements were analysed separately in two different specific time points of the movement: the moment of grasping the object and the moment when the subjects place the block in the target position. Similarly to Chapter 3, the affected and the non-affected upper extremities of two groups of patients (more and less impaired) were compared within the different tasks.

The statistical results presented in Figures 4.4 and 4.6 show that there are significant

differences between arm joint angles of the AF and the NAF arms of the same group of patients (differences between groups NAF-1 and AF-1, and between groups NAF-2 and AF-2) during the placing action than during grasping of the object. Also, there is a difference in the arm postures when comparing the arms of the less affected patients with the more affected ones.

In the grasping action, the features that show statistical significance are the same, independently of the target position of the task. From the tables of appendix B.1.1 show that the mean of the measured features do not differ between positions. Consistent differences between the AF and NAF of the same group of patients are found in the shoulder, wrist and thumb flexion angles. All these angles are significantly higher when the task is done with the NAF arm. Figure 4.4 shows that in the grasping action, more affected patients abduct more the shoulder than less affected ones. There is also a common increase in the elbow flexion in both AF and NAF arms related to an increase in the FMA-UE score. This shows a reduced presence of the pathological synergistic behaviour in the less affected patients. More impaired stroke patients tend to abduct the shoulder instead of flexing it [6]. The distal joints features show that the wrist supination angle varies between subjects. The more affected patients have the tendency of grasping the blocks without supinating the wrist, and the less impaired ones show a higher supination angle. The higher shoulder abduction and lower wrist supination in the patients with a lower FMA-UE score (more impaired patients) can be related to the increased difficulty of grasping the block. Arm elevation is considered a compensation strategy in order to position the hand and orient it above the block [64]. This goes along with the hypothesis formulated for the grasping of the objects.

During the placing action, the majority of the joint angles show a significant difference between the AF and NAF arms of the same group. In all target positions, the shoulder flexion is significantly lower, and the shoulder abduction and elbow flexion are significantly higher in the AF limb. This behaviour was expected, since the pathological synergistic movement pattern is described as a coupled elbow flexion with shoulder flexion or abduction. The compensatory shoulder movements in reaching have been studied previously, and have shown a possible relation to an abnormal recruitment of the shoulder abductor muscles [65]–[67]. This is visible in the higher shoulder abduction angles measured in the AF arm. The mean values of these joint angles also differ between positions. In the frontal positions (1 and 3), the shoulder flexion angles are higher than the ones in the lateral positions (2 and 4), as seen in Figure 4.6 and in the mean joint angle values of the tables in appendix B.1.2. When the target position is to the front, the shoulder flexion is higher and the shoulder abduction angles are lower than when the target position is to the side. The elbow flexion angles do not vary as much between positions.

The increased elbow flexion and shoulder abduction in the AF arm is accompanied by a higher trunk compensation. Figure 4.9 indicates that the frontal compensation is significantly higher when the task is done with the AF arm. The inability to fully extend the elbow leads to an increased compensatory behaviour from the trunk [9]. However, when the target position is in the front at a higher height (position 3), the frontal compensation is not significantly different between AF and NAF in the more impaired group of patients, suggesting that even

if the task is done with the non-affected limb, patients resort to trunk movements. For the lateral target positions, all the trunk compensation features are significantly higher for the AF arm, mainly the trunk rotation angle. This shows that in order to compensate for the lower shoulder flexion and higher elbow flexion, patients rotate the trunk to the direction of the desired movement. It has been previously shown that the trunk is used to transport the impaired arm and to orient the hand in grasping tasks [68]. A lateral inclination of the trunk towards the movement side is also noticed. The lateral target positions require a wider range of motion of the shoulder and elbow in order to reach them.

The analysis of the difference in features related to different levels of impairment (comparison between groups NAF-1 and NAF-2 and between AF-1 and AF-2), indicate that the shoulder abduction is lower and the elbow flexion angle is higher in the AF arm of more impaired patients. As mentioned before, stroke patients activate shoulder abductor muscles to compensate for the reduced shoulder flexor power [67]. However, the smaller shoulder abduction in the more impaired subjects can be related to the lower range of motion and effects of weakness in the shoulder. The pathological coupling between shoulder and elbow is more pronounced in the more affected patients, since the elbow flexion angle of the affected arm of the more impaired subjects is significantly higher than the less affected patients. The difference in impairment level is visualized with the features extracted from the kinematic measures. The increased effect of pathological coupling in more affected patients is also accompanied by an increased amplitude in the trunk compensation strategies. When the displacement of the object is performed to the frontal positions, it is seen that more affected patients have a significantly higher trunk frontal compensation angle than less affected patients. In the lateral positions, more affected patients use a higher rotational and frontal compensation than less affected patients. The relation between level of impairment with pathological coupling and trunk compensation amplitude is clearly visible in the measured features. This follows the theoretical expectations that more affected patients have the need to use more trunk compensation to position and guide the arm to the target of the reach-to-grasp task. It was expected that if a patient has more difficulties in extending the elbow, they use more the trunk in order to successfully displace the object to the desired target position. The results show that this is verified. These findings suggest that the joint and trunk compensation angles can provide a more detailed description on the increased employment of compensation strategies and its relation to the pathological coupling.

Results from tables 4.2, 4.3 and 4.4 show that the size and weight of the blocks influenced the trunk, arm and hand postures in both the grasping and placing moments.

In the grasping moment, significant differences between the AF and NAF joint angles were found for the shoulder, wrist and finger flexion angles. Figure 4.5 shows that the size of the block influences significantly the posture of the shoulder and hand. For the smaller block, it is natural that the subjects need more finger flexion in order to grasp them. The wrist is more extended when the patient grasps the smaller objects. The lower shoulder flexion and higher wrist extension for the 2.5 cm^3 blocks occurs because the subject does not need to elevate the arm as much as when a larger object is to be grasped. The wrist supination angle does not show significant differences between specific blocks, but the results show that the

range of the measured values is much higher in the bigger blocks. It indicates that there is a more variability on the way subjects grasped the block. A higher supination indicates that the block was grasped from the side.

The results of the block effect on the placing action show that the influence of the weight on the posture of the affected arm is not very significant. From the statistical results presented in Figure 4.7, it can be concluded that the heaviest 10 cm^3 block BH caused a higher elbow flexion angle in all positions. However this difference is not significant. The same behaviour is seen in the shoulder flexion angle, where the tasks done with the lighter block BL present a median angle higher than the tasks performed with the heavy block BH, but not significantly. However, by analysing the effect of the weight of the block on the level of trunk compensation (Figure 4.10), it is concluded that in order to displace a heavier block, patients use significantly more compensation strategies. It was expected that both the trunk and arm posture would have significant differences in the performance of tasks with different weighted objects.

The size of the object only has a significant effect on the posture of the fingers (seen in Figure 4.8), which can be explained by the grasping posture of different sized objects. The trunk compensation strategies are not affected by the size of the object. This factor was expected to only show differences in the grasping posture, which was verified with the results of the measured features.

The quantification of the movement performance in reach-to-grasp tasks shows a very high variability between subjects. This could be due to the heterogeneity of movement patterns between individuals, which can influence the statistical results in this study. By increasing the number of subjects, the statistical power would increase and more solid conclusions can be taken. However, the presence of common pathological stereotypical movements can be seen in stroke patients. Some common limitations with the previous chapter are applicable on this study as well. The kinematic reconstruction can suffer from the same sources of error, such as non-optimal movements for the sensor-to-segment calibration and for the global frame definition. Despite instructing the patients to perform the synchronization movements for the global frame definition (static standing position and trunk flexion) before each trial and go quickly to the starting position (which did not happen in some cases), the errors in the orientation estimation in this transition period affects the whole kinematic reconstruction. Also, it is possible that the patients deviated from the initial position in the beginning of some movements, which can induce additional errors in the joint angle estimation. Ideally, the results obtained in this work should be compared to a reference measurement system, but the amount of sensors and markers would constraint the subjects' movement. However, the time to calibrate and mount such systems is very high, which would make the experimental protocol unfeasible. The potential of the kinematic sensors used for activity performance assessment is the same as the ones stated in Chapter 3, where the information about the velocity profiles and smoothness of movement in the different phases of the reaching and grasping tasks can add valuable insights on the patients' level of impairment [63], [69]. In this chapter, the analysis was restricted to the static postures of the arm and trunk in the grasping time point and the placing time point. It would be of interest to study the behaviour

of the patients throughout the whole movement and not only on these static postures. The behaviour of the shoulder and elbow coupling during the reaching phase and the displacement phase is of interest. The evolution of the trunk compensation in these phases is also of interest. The analysis of the compensation strategies right from the moment when patients start the movement can provide better insights on their motor performance and presence of abnormal arm synergies.

4.5 Conclusion

The overall observation of this study is that the developed distributed measurement system is able to differentiate movement patterns between the affected and non-affected upper extremities of stroke patients. The arm joint angles and trunk compensations measured showed to be relevant in objectively characterizing the movement patterns of stroke patients, and showed significant differences between the affected and non-affected arms and also between patients with different levels of impairment. Signs of pathological synergies are well seen in the kinematic features and the differences between the arms follow the stereotypical abnormal movements observed in stroke patients. When reach-grasp-displace tasks are done with the affected arm, there is a higher shoulder abduction and elbow flexion, directly related to the pathological synergistic behaviour. It was shown that when the task is done with the impaired arm, stroke patients are unable to extend the elbow and, consequently, use more compensation strategies with the trunk in order to reach the desired target positions.

The size and weight of the objects influences the movement patterns and employment of compensation strategies. This study showed that stroke patients tend to adopt different postures when grasping and when placing the objects in the target positions of the tasks. When stroke subjects grasp bigger blocks, they have the tendency to flex more the shoulder and to extend and supinate more the wrist. The hand posture is also different depending on the size of the blocks. The fingers are more flexed when a smaller block is to be grasped. The weight of the block did not show significant differences in the arm posture of the affected arm. However, the trunk compensation measurements are significantly higher when patients displace heavier blocks, indicating that they have more difficulties in the movement.

It can be concluded that kinematic analysis of the upper extremity and trunk of stroke patients provides an objective assessment of the movement profile and can increase the quality of stroke motor activity assessment scales.

Chapter 5

General conclusion

Objective assessment of the upper extremity motor function in stroke patients has gained interest over the years. The development of portable and minimally evasive kinematic measurement systems allowed their use in clinical environments to analyse patients' movement. The presented work showed the usability of a distributed measuring system composed of IMUs for the upper extremity and trunk in evaluating the level of motor impairment in stroke patients.

The study done in Chapter 3 concluded that the joint angles of the upper extremity measured with the system can indeed differentiate movements performed with the affected and the non-affected arms of the patients. The kinematic analysis reflected the presence of pathological muscle coupling and weakness when the patients performed movements from the FMA-UE protocol. Also, the measured objective features vary with the level of impairment of the patients. Significant differences between the shoulder, elbow and wrist joint angles were found between groups of more impaired and less impaired patients. The clinical assessment of stroke patient's motor function can definitely benefit with the use of kinematic features measured with the developed system.

In Chapter 4, the same distributed measuring system was applied in a more functional setup, where reach-to-grasp tasks were performed. The main conclusions were that in functional tasks, the movement patterns of stroke patients were different in the affected and in the non-affected arm. The kinematic features were proven to objectively measure the abnormal synergies that stroke patients perform when employ the use of the impaired arm in functional tasks. The compensation strategies adopted by the patients was also measured and differences when the tasks were done with the affected and non-affected arms were also identified. Furthermore, the influence of the size and weight in the posture of the upper extremity during the grasping and placing actions of the reach-to-grasp movement was identified. The presented kinematic features also differentiate motor performance of groups of patients with different levels of impairments. Significant differences in the arm joint angles were found between each arm of the same group of patients and between groups. The usability of the developed IMU system is of interest for assessing motor activity of stroke patients.

5.1 Recommendations

The presented methods for the movement analysis have some clear limitations that affected the results of this work.

It would be of interest to investigate how the features calculated from the IMUs differ with the inclusion of the magnetometer measurements. The sensors orientation estimation methods developed were based on defined movements in order to define a common reference frame for all the sensors, and consequently, reconstruct the real orientation of the upper limb. Magnetometer sensors are highly susceptible to magnetic disturbances of the environment. It would be interesting to compare the orientation errors of the method presented in this report with methods developed previously that include these types of sensors.

The sensor-to-segment calibration is a procedure that is crucial for the estimation of the orientation of the limb segment. In the experimental protocols, only two repetitions of the calibration protocol were performed. With more repetitions, the accuracy of the extracted features would improve. One of the reasons for not repeating the calibration procedure was the limited time for the experimental protocol. In future studies, if possible, the repetition of the calibration protocol is desirable.

During the experiments, to avoid drift errors in the kinematic reconstruction, the initial orientation of each sensor was recorded in order to reset the arm orientation at the beginning of each individual movement. However, some participants deviated from the initial position. This causes errors in the limb segments orientation estimation, and consequently in the joint angles calculation. A more strict instruction to the patients should be done in the future.

As it was stated in sections 3.4 and 4.4, the analysis of different type of features such as smoothness of the movement, trajectory of each limb segment and velocity profiles can increase the quality of the motor assessment with the IMU system. The data set collected in these experiments should be further analysed with different methods. Also, the relation between the measured joint angles throughout time can provide a better view of the pathological coupling of the different joints at an individual level. It would also be wise to compare the kinematic features of stroke patients with healthy age-matched controls, since the non-affected arm can also show signs of impairment in the more affected patients.

The experimental protocol of the experiments conducted in this work also included measuring muscle activity of seven different muscles in the arm (biceps brachii, triceps lateral and long head, deltoideus medial and anterior head and flexor and extensor capri radialis). Muscle activity in the upper limb of stroke patients has been studied in the past [32]. Electromyography (EMG) measurements have provided insight on the abnormal synergistic movement patterns in stroke patients by quantifying co-activation patterns. Muscle activity measurements were also correlated to clinical measurements, such as the FMA test scores [33]. It was hypothesized that more impaired patients severe co-contractions have a higher degree of muscle weakness, manifestation of pathological synergies and bigger delays in initiation of muscle contractions, all related to the impact in functional activity performance. Thus, including EMG activity in the characterization of the patients' motor function together with the kinematic analysis enlarges the number of objective features to quantify motor impairments.

The usability of the developed distributed multisensory system by therapists is the next step in order to include such technologies in the assessment of motor function and activity of stroke patients in the clinic. Despite showing great potential, the drawbacks of the use of such system are still to be tackled. Until then, the usual clinical assessment scales will continue to be utilized for motor assessment.

Bibliography

[1] J. McKay and G. A. Mensah, *The atlas of heart disease and stroke.* World Health Organization, 2005.

[2] S. Balasubramanian, "Motor impairments following stroke," 2015. [Online]. Available: http://rgdoi.net/10.13140/RG.2.1.3349.6804

[3] V. L. Feigin, B. Norrving, and G. A. Mensah, "Global burden of stroke," *Circulation Research*, vol. 120, no. 3, p. 439–448, Mar 2017.

[4] E. S. Lawrence, C. Coshall, R. Dundas, J. Stewart, A. G. Rudd, R. Howard, and C. D. A. Wolfe, "Estimates of the prevalence of acute stroke impairments and disability in a multiethnic population," *Stroke*, vol. 32, no. 6, p. 1279–1284, 2001.

[5] P. Langhorne, F. Coupar, and A. Pollock, "Motor recovery after stroke: a systematic review," *The Lancet Neurology*, vol. 8, no. 8, p. 741–754, 2009.

[6] P. Raghavan, "Upper limb motor impairment after stroke," *Physical Medicine and Rehabilitation Clinics of North America*, vol. 26, no. 4, p. 599–610, 2015.

[7] L. Dipietro, H. I. Krebs, S. E. Fasoli, B. T. Volpe, J. Stein, C. Bever, and N. Hogan, "Changing motor synergies in chronic stroke," *Journal of Neurophysiology*, vol. 98, no. 2, p. 757–768, 2007.

[8] C. G. Canning, L. Ada, and N. J. O'Dwyer, "Abnormal muscle activation characteristics associated with loss of dexterity after stroke," *Journal of the Neurological Sciences*, vol. 176, no. 1, p. 45–56, 2000.

[9] M. C. Cirstea and M. F. Levin, "Compensatory strategies for reaching in stroke," *Brain*, vol. 123, no. 5, p. 940–953, 2000.

[10] C. J. Winstein, J. Stein, R. Arena, B. Bates, L. R. Cherney, S. C. Cramer, F. Deruyter, J. J. Eng, B. Fisher, R. L. Harvey, and et al., "Guidelines for adult stroke rehabilitation and recovery," *Stroke*, vol. 47, no. 6, 2016.

[11] P. Langhorne, J. Bernhardt, and G. Kwakkel, "Stroke rehabilitation," *The Lancet*, vol. 377, no. 9778, p. 1693–1702, 2011.

[12] W. H. Organization, *International classification of functioning, disability and health World Health Organization (ICF).* World Health Organization, 2001.

[13] P. W. Duncan, "Outcome measures in stroke rehabilitation," *Neurological Rehabilitation Handbook of Clinical Neurology*, p. 105–111, 2013.

[14] M. A. Murphy, C. Resteghini, P. Feys, and I. Lamers, "An overview of systematic reviews on upper extremity outcome measures after stroke," *BMC Neurology*, vol. 15, no. 1, Nov 2015.

[15] C. Bushnell, J. P. Bettger, K. M. Cockroft, S. C. Cramer, M. O. Edelen, D. Hanley, I. L. Katzan, S. Mattke, D. M. Nilsen, T. Piquado, and et al., "Chronic stroke outcome measures for motor function intervention trials," *Circulation: Cardiovascular Quality and Outcomes*, vol. 8, no. 6 suppl 3, 2015.

[16] M. F. Levin, J. A. Kleim, and S. L. Wolf, "What do motor "recovery" and "compensation" mean in patients following stroke?" *Neurorehabilitation and Neural Repair*, vol. 23, no. 4, p. 313–319, May 2008.

[17] L. Santisteban, M. Térémetz, J.-P. Bleton, J.-C. Baron, M. A. Maier, and P. G. Lindberg, "Upper limb outcome measures used in stroke rehabilitation studies: A systematic literature review," *Plos One*, vol. 11, no. 5, Jun 2016.

[18] A. Fugl-Meyer, L. Jääskö, I. Leyman, S. Olsson, and S. Steglind, "The post-stroke hemiplegic patient. 1. a method for evaluation of physical performance," *Scandinavian journal of rehabilitation medicine*, vol. 7, no. 1, p. 13—31, 1975. [Online]. Available: http://europepmc.org/abstract/MED/1135616

[19] T. E. Twitchell, "The restoration of motor function following hemiplegia in man," *Brain*, vol. 74, no. 4, p. 443–480, 1951.

[20] S. Brunnstrom, "Motor testing procedures in hemiplegia: Based on sequential recovery stages," *Physical Therapy*, vol. 46, no. 4, p. 357–375, Jan 1966.

[21] D. J. Gladstone, C. J. Danells, and S. E. Black, "The fugl-meyer assessment of motor recovery after stroke: A critical review of its measurement properties," *Neurorehabilitation and Neural Repair*, vol. 16, no. 3, p. 232–240, 2002.

[22] R. C. Lyle, "A performance test for assessment of upper limb function in physical rehabilitation treatment and research," *International Journal of Rehabilitation Research*, vol. 4, no. 4, p. 483–492, 1981.

[23] D. Carroll, "A quantitative test of upper extremity function," *Journal of Chronic Diseases*, vol. 18, no. 5, p. 479–491, 1965.

[24] N. Yozbatiran, L. Der-Yeghiaian, and S. C. Cramer, "A standardized approach to performing the action research arm test," *Neurorehabilitation and Neural Repair*, vol. 22, no. 1, p. 78–90, Apr 2007.

[25] T. Platz, C. Pinkowski, F. V. Wijck, I.-H. Kim, P. D. Bella, and G. Johnson, "Reliability and validity of arm function assessment with standardized guidelines for the fugl-meyer test, action research arm test and box and block test: a multicentre study," *Clinical Rehabilitation*, vol. 19, no. 4, p. 404–411, 2005.

[26] C.-L. Koh, I.-P. Hsueh, W.-C. Wang, C.-F. Sheu, T.-Y. Yu, C.-H. Wang, and C.-L. Hsieh, "Validation of the action research arm test using item response theory in patients after stroke," *Journal of Rehabilitation Medicine*, vol. 38, no. 6, p. 375–380, Jan 2006.

[27] A. Schwarz, C. M. Kanzler, O. Lambercy, A. R. Luft, and J. M. Veerbeek, "Systematic review on kinematic assessments of upper limb movements after stroke," *Stroke*, vol. 50, no. 3, p. 718–727, 2019.

[28] A. I. Cuesta-Vargas, A. Galán-Mercant, and J. M. Williams, "The use of inertial sensors system for human motion analysis," *Physical Therapy Reviews*, vol. 15, no. 6, p. 462–473, 2010.

[29] C. P. Walmsley, S. A. Williams, T. Grisbrook, C. Elliott, C. Imms, and A. Campbell, "Measurement of upper limb range of motion using wearable sensors: A systematic review," *Sports Medicine - Open*, vol. 4, no. 1, 2018.

[30] S. Lambrecht, S. Nogueira, M. Bortole, A. Siqueira, M. Terra, E. Rocon, and J. Pons, "Inertial sensor error reduction through calibration and sensor fusion," *Sensors*, vol. 16, no. 2, p. 235, 2016.

[31] E. G. Cruz, H. C. Waldinger, and D. G. Kamper, "Kinetic and kinematic workspaces of the index finger following stroke," *Brain*, vol. 128, no. 5, p. 1112–1121, Feb 2005.

[32] J. P. A. Dewald, P. S. Pope, J. D. Given, T. S. Buchanan, and W. Z. Rymer, "Abnormal muscle coactivation patterns during isometric torque generation at the elbow and shoulder in hemiparetic subjects," *Brain*, vol. 118, no. 2, p. 495–510, 1995.

[33] J. Chae, G. Yang, B. Park, and I. Labatia, "Muscle weakness and cocontraction in upper limb hemiparesis: Relationship to motor impairment and physical disability," *Neurorehabilitation and Neural Repair*, vol. 16, no. 3, p. 241–248, Jan 2002.

[34] S. O. H. Madgwick, A. J. L. Harrison, and R. Vaidyanathan, "Estimation of imu and marg orientation using a gradient descent algorithm," *2011 IEEE International Conference on Rehabilitation Robotics*, 2011.

[35] B. Kirking, M. El-Gohary, and Y. Kwon, "The feasibility of shoulder motion tracking during activities of daily living using inertial measurement units," *Gait and Posture*, vol. 49, p. 47–53, 2016.

[36] W. Kong, S. Sessa, M. Zecca, and A. Takanishi, "Anatomical calibration through post-processing of standard motion tests data," *Sensors*, vol. 16, no. 12, p. 2011, 2016.

[37] H. Luinge, P. Veltink, and C. Baten, "Ambulatory measurement of arm orientation," *Journal of Biomechanics*, vol. 40, no. 1, p. 78–85, 2007.

[38] L. Ricci, D. Formica, L. Sparaci, F. Lasorsa, F. Taffoni, E. Tamilia, and E. Guglielmelli, "A new calibration methodology for thorax and upper limbs motion capture in children using magneto and inertial sensors," *Sensors*, vol. 14, no. 1, pp. 1057–1072, 2014.

[39] S. W. Shepperd, "Quaternion from rotation matrix," *Journal of Guidance and Control*, vol. 1, no. 3, p. 223–224, 1978.

[40] J. B. Kuipers, *Quaternions and rotation sequences: a primer with applications to orbits, aerospace, and virtual reality.* Princeton University Press, 2007.

[41] S. M. Hatem, G. Saussez, M. D. Faille, V. Prist, X. Zhang, D. Dispa, and Y. Bleyenheuft, "Rehabilitation of motor function after stroke: A multiple systematic review focused on techniques to stimulate upper extremity recovery," *Frontiers in Human Neuroscience*, vol. 10, 2016.

[42] A. J. C. Mcmorland, K. D. Runnalls, and W. D. Byblow, "A neuroanatomical framework for upper limb synergies after stroke," *Frontiers in Human Neuroscience*, vol. 9, 2015.

[43] C. E. Lang, M. D. Bland, R. R. Bailey, S. Y. Schaefer, and R. L. Birkenmeier, "Assessment of upper extremity impairment, function, and activity after stroke: foundations for clinical decision making," *Journal of Hand Therapy*, vol. 26, no. 2, p. 104–115, 2013.

[44] A. D. L. Reyes-Guzmán, I. Dimbwadyo-Terrer, F. Trincado-Alonso, F. Monasterio-Huelin, D. Torricelli, and A. Gil-Agudo, "Quantitative assessment based on kinematic measures of functional impairments during upper extremity movements: A review," *Clinical Biomechanics*, vol. 29, no. 7, p. 719–727, 2014.

[45] Y. Li, X. Zhang, Y. Gong, Y. Cheng, X. Gao, and X. Chen, "Motor function evaluation of hemiplegic upper-extremities using data fusion from wearable inertial and surface emg sensors," *Sensors*, vol. 17, no. 3, p. 582, 2017.

[46] H. G. Kortier, V. I. Sluiter, D. Roetenberg, and P. H. Veltink, "Assessment of hand kinematics using inertial and magnetic sensors," *Journal of NeuroEngineering and Rehabilitation*, vol. 11, no. 1, p. 70, 2014.

[47] M. Kok, J. D. Hol, and T. B. Schön, "Using inertial sensors for position and orientation estimation," *Foundations and Trends® in Signal Processing*, vol. 11, no. 1-2, p. 1–153, 2017.

[48] M. A. Murphy, C. Willén, and K. S. Sunnerhagen, "Responsiveness of upper extremity kinematic measures and clinical improvement during the first three months after stroke," *Neurorehabilitation and Neural Repair*, vol. 27, no. 9, p. 844–853, 2013.

[49] ——, "Kinematic variables quantifying upper-extremity performance after stroke during reaching and drinking from a glass," *Neurorehabilitation and Neural Repair*, vol. 25, no. 1, p. 71–80, Sep 2010.

[50] J. Li, B. Pan, T. Jin, Z. Huang, S. Ye, J. Wu, Z. Huang, B. Xie, C. Luo, C. Wang, and et al., "A single task assessment system of upper-limb motor function after stroke," *Technology and Health Care*, vol. 24, no. s2, 2016.

[51] A. S. Klochkov, A. E. Khizhnikova, M. A. Nazarova, and L. A. Chernikova, "Pathological upper limb synergies of patients with poststroke hemiparesis," *Neuroscience and Behavioral Physiology*, vol. 48, no. 7, p. 813–822, 2018.

[52] L. C. Miller and J. P. Dewald, "Involuntary paretic wrist/finger flexion forces and emg increase with shoulder abduction load in individuals with chronic stroke," *Clinical Neurophysiology*, vol. 123, no. 6, p. 1216–1225, 2012.

[53] E.-L. Bustrén, K. S. Sunnerhagen, and M. A. Murphy, "Movement kinematics of the ipsilesional upper extremity in persons with moderate or mild stroke," *Neurorehabilitation and Neural Repair*, vol. 31, no. 4, p. 376–386, 2017.

[54] S. K. Subramanian, J. Yamanaka, G. Chilingaryan, and M. F. Levin, "Validity of movement pattern kinematics as measures of arm motor impairment poststroke," *Stroke*, vol. 41, no. 10, p. 2303–2308, 2010.

[55] C. Duret, O. Courtial, and A. G. Grosmaire, "Kinematic measures for upper limb motor assessment during robot-mediated training in patients with severe sub-acute stroke," *Restorative Neurology and Neuroscience*, vol. 34, no. 2, p. 237–245, 2016.

[56] M. A. Murphy and C. K. Häger, "Kinematic analysis of the upper extremity after stroke – how far have we reached and what have we grasped?" *Physical Therapy Reviews*, vol. 20, no. 3, p. 137–155, 2015.

[57] M. A. Murphy, M. C. Baniña, and M. F. Levin, "Perceptuo-motor planning during functional reaching after stroke," *Experimental Brain Research*, vol. 235, no. 11, p. 3295–3306, Dec 2017.

[58] M. Térémetz, F. Colle, S. Hamdoun, M. A. Maier, and P. G. Lindberg, "A novel method for the quantification of key components of manual dexterity after stroke," *Journal of NeuroEngineering and Rehabilitation*, vol. 12, no. 1, Feb 2015.

[59] L. V. Dokkum, I. Hauret, D. Mottet, J. Froger, J. Métrot, and I. Laffont, "The contribution of kinematics in the assessment of upper limb motor recovery early after stroke," *Neurorehabilitation and Neural Repair*, vol. 28, no. 1, p. 4–12, 2013.

[60] G. Uswatte, W. L. Foo, H. Olmstead, K. Lopez, A. Holand, and L. B. Simms, "Ambulatory monitoring of arm movement using accelerometry: An objective measure of upper-extremity rehabilitation in persons with chronic stroke," *Archives of Physical Medicine and Rehabilitation*, vol. 86, no. 7, p. 1498–1501, 2005.

[61] A. Parnandi, E. Wade, and M. Maja, "Motor function assessment using wearable inertial sensors," *2010 Annual International Conference of the IEEE Engineering in Medicine and Biology*, 2010.

[62] T. Hester, R. Hughes, D. M. Sherrill, B. Knorr, M. Akay, J. Stein, and P. Bonato, "Using wearable sensors to measure motor abilities following stroke," *International Workshop on Wearable and Implantable Body Sensor Networks (BSN06)*.

[63] E. Repnik, U. Puh, N. Goljar, M. Munih, and M. Mihelj, "Using inertial measurement units and electromyography to quantify movement during action research arm test execution," *Sensors*, vol. 18, no. 9, p. 2767, 2018.

[64] A. Roby-Brami, S. Jacobs, N. Bennis, and M. F. Levin, "Hand orientation for grasping and arm joint rotation patterns in healthy subjects and hemiparetic stroke patients," *Brain Research*, vol. 969, no. 1-2, p. 217–229, 2003.

[65] M. C. Cirstea, A. B. Mitnitski, A. G. Feldman, and M. F. Levin, "Interjoint coordination dynamics during reaching in stroke," *Experimental Brain Research*, vol. 151, no. 3, p. 289–300, Jan 2003.

[66] J. Roh, W. Z. Rymer, E. J. Perreault, S. B. Yoo, and R. F. Beer, "Alterations in upper limb muscle synergy structure in chronic stroke survivors," *Journal of Neurophysiology*, vol. 109, no. 3, p. 768–781, Jan 2013.

[67] P. H. Mccrea, J. J. Eng, and A. J. Hodgson, "Saturated muscle activation contributes to compensatory reaching strategies after stroke," *Journal of Neurophysiology*, vol. 94, no. 5, p. 2999–3008, 2005.

[68] S. M. Michaelsen, S. Jacobs, A. Roby-Brami, and M. F. Levin, "Compensation for distal impairments of grasping in adults with hemiparesis," *Experimental Brain Research*, vol. 157, no. 2, 2004.

[69] T. S. Patterson, M. D. Bishop, T. E. Mcguirk, A. Sethi, and L. G. Richards, "Reliability of upper extremity kinematics while performing different tasks in individuals with stroke," *Journal of Motor Behavior*, vol. 43, no. 2, p. 121–130, 2011.

Appendix A

Additional Results of Chapter 2

A.1 Kinematic features

The analysis done in Chapter 3 separates the measured data into two groups of patients (more and less impaired, based on the FMA-UE score). In this appendix, the overall distribution of the measured joint angles in all 10 patients is presented and only separated between affected and non-affected arms to understand if, despite the level of impairment of the patients, the pathological synergies can be identified as well. Additionally, the finger flexion angles are added and analysed too. Figures A.1, A.2, A.3 and A.4 present the median, 25th and 75th quartiles of the joint angles measured in all patients in the form of boxplots, for each task of the protocol. Table A.1 presents the mean and standard deviation of the same measured joint angles that are presented in the figures.

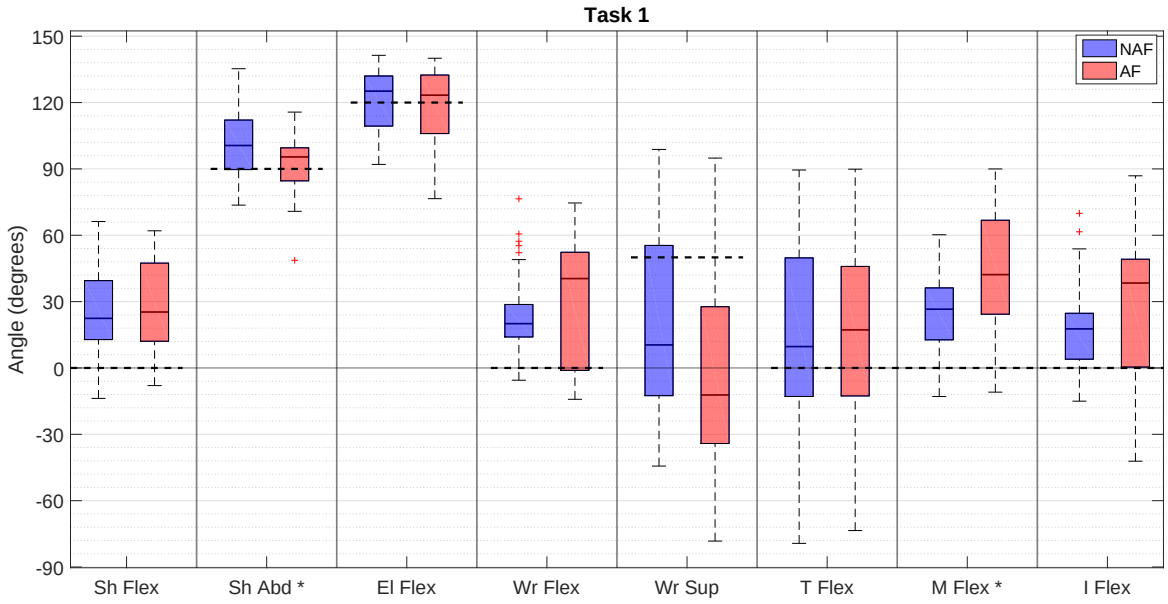

Figure A.1: Boxplots (median and IQR) of the joint angles of the NAF and AF arm in all ten patients for task 1 of the protocol. Statistical significant differences between the AF and NAF arms are represented by an $*$ following the joint angle label (Wilcoxon signed rank test with $P < 0.05$).

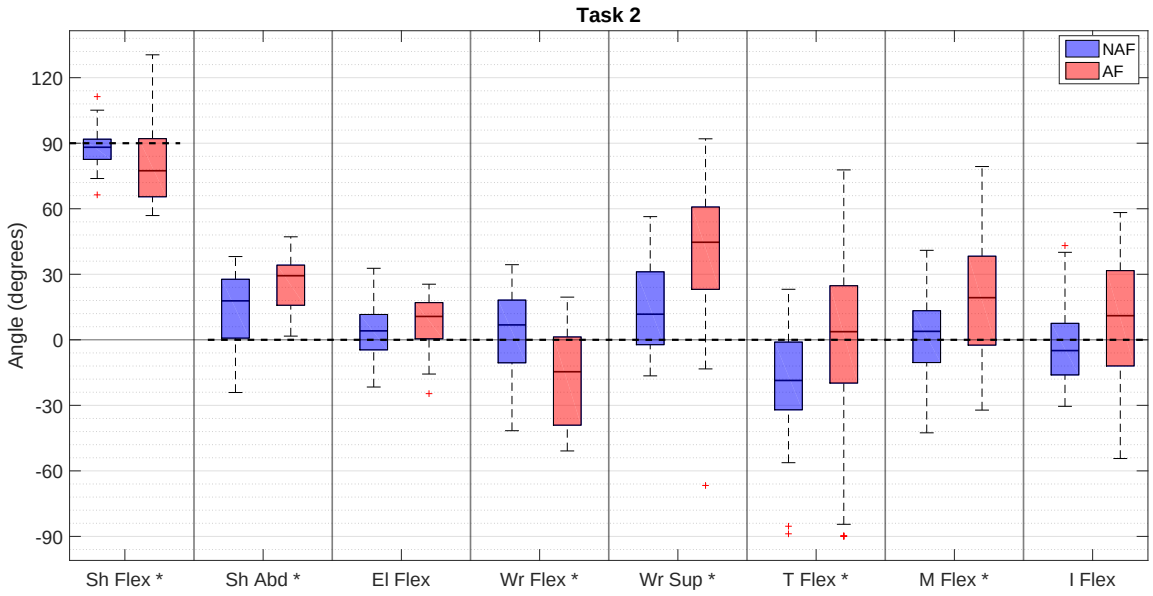

Figure A.2: Boxplots (median and IQR) of the joint angles of the NAF and AF arm in all ten patients for task 2 of the protocol. Statistical significant differences between the AF and NAF arms are represented by an $*$ following the joint angle label.

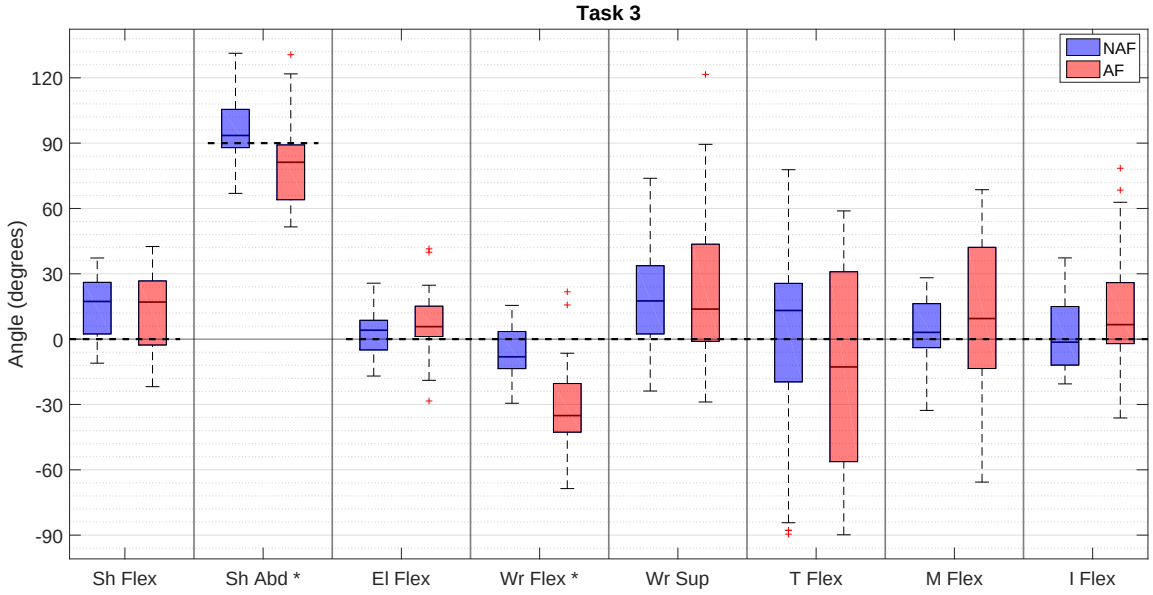

Figure A.3: Boxplots (median and IQR) of the joint angles of the NAF and AF arm in all ten patients for task 3 of the protocol. Statistical significant differences between the AF and NAF arms are represented by an $*$ following the joint angle label.

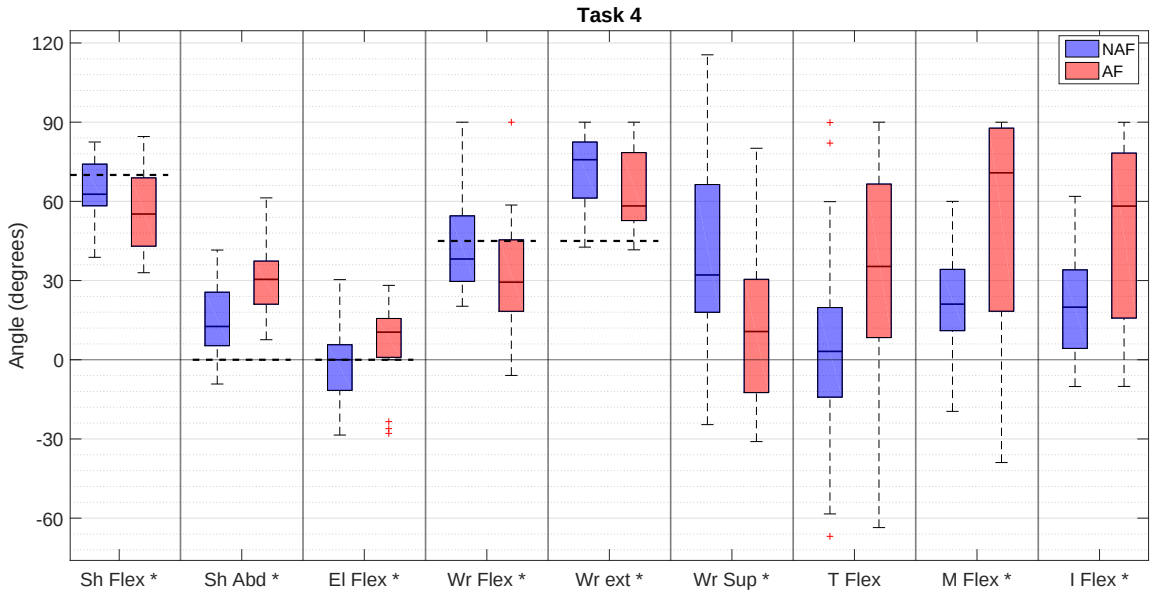

Figure A.4: Boxplots (median and IQR) of the joint angles of the NAF and AF arm in all ten patients for task 4 of the protocol. Statistical significant differences between the AF and NAF arms are represented by an $*$ following the joint angle label.

Table A.1: Mean and standard deviation of the arm joint angles (in degrees) of the AF and NAF limbs measured in the target posture of each task. Bold values indicate a significant difference between the AF and NAF arms (Wilcoxon signed rank test with $P < 0.05$).

		Sh Flex	Sh Abd	El Flex	Wr Flex	Wr Sup	Wr Ext	T Flex	M Flex	I Flex
Task 1	NAF	25.5 ± 19.9	**101.8 ± 16.5**	121.2 ± 14.3	24.5 ± 19.9	34.0 ± 37.7	-	-49.1 ± 39.2	**24.3 ± 19.5**	18.5 ± 21.2
	AF	26.2 ± 19.8	**92.2 ± 13.5**	118.5 ± 16.8	28.7 ± 27.2	19.5 ± 49.5	-	-52.7 ± 35.3	**42.3 ± 24.5**	28.0 ± 35.6
Task 2	NAF	**87.8 ± 9.4**	**13.2 ± 18.1**	3.5 ± 13.4	**4.2 ± 18.6**	**-6.0 ± 18.7**	-	-28.7 ± 58.9	**1.4 ± 19.9**	-2.9 ± 18.6
	AF	**80.6 ± 17.4**	**26.7 ± 12.4**	8.0 ± 12.1	**-18.0 ± 21.4**	**-28.4 ± 36.1**	-	-50.2 ± 26.9	**18.8 ± 27.2**	9.7 ± 30.6
Task 3	NAF	14.7 ± 13.7	**97.0 ± 15.4**	2.4 ± 10.7	**-5.6 ± 12.7**	-10.1 ± 22.2	-	-50.3 ± 30.1	3.7 ± 15.3	1.8 ± 16.2
	AF	13.7 ± 17.3	**80.1 ± 20.3**	6.3 ± 15.5	**-31.1 ± 20.5**	-14.6 ± 37.5	-	-58.7 ± 40.6	12.3 ± 34.2	11.8 ± 26.3
Task 4	NAF	**64.9 ± 10.6**	**15.5 ± 14.4**	**-1.4 ± 13.8**	**43.5 ± 17.6**	**62.4 ± 29.0**	**72.5 ± 14.6**	-18.1 ± 45.3	**21.9 ± 18.7**	**19.6 ± 19.7**
	AF	**56.0 ± 15.0**	**31.2 ± 12.4**	**7.2 ± 13.4**	**30.4 ± 21.0**	**42.2 ± 31.6**	**65.2 ± 15.6**	-25.5 ± 41.5	**55.1 ± 38.1**	**49.6 ± 33.8**

The results for the statistical tests in this analysis go in accordance with the ones found in Chapter 3. In task 1, the shoulder abduction angle is significantly smaller in the affected arm, showing that the affected arm suffers from weakness. In tasks 2 and 3, a significantly smaller shoulder flexion and shoulder abduction in each task respectively is observed in the affected side. The elbow flexion angle is higher in the affected side but not significantly in both tasks. The affected side shows to have more effects of pathological coupling of the upper extremity muscles. The affected arm's wrist is more extended in both tasks. In task 4, it is possible to see a bigger effect of the pathological coupling. The shoulder flexion is significantly smaller, and the shoulder abduction and elbow flexion angles are significantly

higher in the affected arm of the patients. Thw wrist range of motion is significantly smaller in the impaired limb. The middle and index fingers were more flexed in general for all tasks done with the affected arm, but in some cases, not significantly. The fingers are not regarded as a priority evaluation point in the FMA-UE scale, but the level of finger flexion can indicate more severe impairments and the presence of pathological synergies. In task 4, both the index and middle finger flexion angle was significantly higher in the AF arm. Inability to control independent finger flexion is well documented [51], [52].The results show that in the impaired arm, when the wrist is flexed or extended, the index and middle fingers are jointly flexed as well.

Overall, the level of pathological synergies observed and measured with the joint angles is significantly higher in the affected upper extremity of stroke patients. By not separating the patients in groups based on the level of impairment, it is possible to see that the measured joint angles have a higher variance. Nevertheless, the same conclusions from Chapter 3 can be applied in this analysis.

Appendix B

Additional Results of Chapter 3

B.1 Detailed results of the kinematic features

A more detailed analysis was performed to check for significant differences between the features in the two upper extremities for every combination of block and target position. The tables shown in this section present the mean and standard deviation of the features measured in all nine patients for each block and for each target position. Four tables are presented (one for each target position) for the grasping action and another four for the placing moment. The values in bold indicate that the Wilcoxon signed rank test showed a significant difference ($P < 0.05$) between AF (affected) and NAF (non-affected).

B.1.1 Grasping action joint angles

Table B.1: Mean and standard deviation of the arm joint angles (in degrees) measured during the grasping action for the tasks in the target position 1. Bold values indicate a significant difference between AF and NAF arms (Wilcoxon signed rank test, $P < 0.05$).

Pos 1		Sh Flex	Sh Abd	El Flex	Wr Sup	Wr Flex	T Flex	M Flex	I Flex
BW	NAF	**43.0 ± 11.9**	21.9 ± 15.6	66.9 ± 12.5	-16.5 ± 13.5	**-2.3 ± 10.9**	**69.1 ± 12.8**	72.5 ± 23.1	**31.5 ± 12.1**
	AF	**31.5 ± 12.8**	25.4 ± 20.5	75.7 ± 27.7	-18.3 ± 30.7	**-14.0 ± 26.0**	**57.9 ± 14.3**	78.2 ± 27.8	**64.0 ± 42.5**
BH	NAF	42.4 ± 10.6	22.6 ± 19.3	67.0 ± 14.5	-18.5 ± 20.6	-11.3 ± 18.3	**68.2 ± 13.9**	82.9 ± 21.7	39.1 ± 21.8
	AF	35.8 ± 11.0	25.8 ± 23.6	72.9 ± 23.8	-26.8 ± 28.7	-9.8 ± 30.8	**50.6 ± 27.7**	71.6 ± 23.9	53.4 ± 32.9
BL	NAF	**45.4 ± 9.1**	23.0 ± 17.4	61.6 ± 14.9	-21.4 ± 19.9	-4.0 ± 14.8	**68.0 ± 16.9**	69.0 ± 22.6	**32.6 ± 16.0**
	AF	**37.1 ± 11.4**	23.0 ± 21.3	69.4 ± 18.1	-25.6 ± 29.4	-13.3 ± 24.1	**53.3 ± 31.7**	70.6 ± 21.3	**56.5 ± 33.9**
SW	NAF	32.6 ± 9.0	20.1 ± 10.3	69.7 ± 11.1	-13.3 ± 9.2	**-13.6 ± 12.3**	**65.3 ± 15.0**	86.1 ± 30.8	80.0 ± 15.5
	AF	26.7 ± 11.1	21.4 ± 17.5	67.3 ± 13.1	-16.4 ± 17.3	**-28.2 ± 16.6**	**40.5 ± 22.9**	82.7 ± 20.9	82.0 ± 18.6
SH	NAF	**34.3 ± 11.1**	25.0 ± 8.8	68.4 ± 16.5	-11.4 ± 10.3	-21.1 ± 11.3	**67.3 ± 11.5**	95.9 ± 32.2	93.3 ± 21.7
	AF	**22.3 ± 10.5**	22.2 ± 18.1	72.8 ± 13.1	-18.4 ± 15.8	-28.3 ± 17.8	**41.8 ± 21.2**	86.0 ± 32.1	88.5 ± 21.7
SL	NAF	**31.8 ± 8.2**	20.0 ± 14.5	70.7 ± 13.2	-12.1 ± 8.7	**-9.3 ± 24.4**	**64.2 ± 14.2**	82.9 ± 34.3	76.5 ± 22.5
	AF	**23.5 ± 9.3**	24.0 ± 15.3	69.0 ± 11.8	-18.1 ± 16.0	**-27.6 ± 17.5**	**47.0 ± 26.6**	79.6 ± 26.6	83.2 ± 20.0

Table B.2: Mean and standard deviation of the arm joint angles (in degrees) measured during the grasping action for the tasks in position 2. Bold values indicate a significant difference between AF and NAF arms (Wilcoxon signed rank test, $P < 0.05$).

Pos 2		Sh Flex	Sh Abd	El Flex	Wr Sup	Wr Flex	T Flex	M Flex	I Flex
BW	NAF	**42.9 ± 10.1**	21.4 ± 13.4	**62.5 ± 12.0**	-18.8 ± 12.0	**-3.6 ± 10.9**	**71.7 ± 10.7**	75.8 ± 18.6	**31.9 ± 12.9**
	AF	**34.5 ± 15.4**	25.6 ± 21.0	**74.6 ± 30.3**	-20.2 ± 28.1	**-14.7 ± 20.7**	**47.4 ± 37.9**	81.1 ± 24.1	**61.8 ± 41.9**
BH	NAF	**43.5 ± 7.3**	23.3 ± 16.9	62.6 ± 14.5	-25.0 ± 20.7	-11.6 ± 17.7	**69.2 ± 13.0**	85.6 ± 21.5	45.4 ± 25.9
	AF	**35.6 ± 12.0**	25.8 ± 24.2	68.6 ± 27.6	-24.7 ± 29.7	-9.5 ± 23.0	**51.0 ± 25.1**	80.9 ± 22.0	58.0 ± 20.0
BL	NAF	**45.7 ± 8.8**	24.2 ± 12.3	58.2 ± 13.2	-21.9 ± 13.2	**-1.1 ± 15.1**	**68.5 ± 13.0**	**81.1 ± 16.8**	**33.3 ± 14.8**
	AF	**36.2 ± 13.2**	21.5 ± 19.8	66.1 ± 19.5	-28.4 ± 24.6	**-15.1 ± 28.9**	**50.1 ± 33.2**	**69.1 ± 16.4**	**61.2 ± 33.6**
SW	NAF	30.3 ± 8.7	17.3 ± 10.8	68.5 ± 13.0	-14.7 ± 9.0	**-24.9 ± 12.9**	**64.5 ± 12.6**	97.2 ± 30.5	90.5 ± 10.6
	AF	26.7 ± 10.8	20.2 ± 16.8	65.0 ± 13.6	-17.1 ± 15.8	**-32.5 ± 17.6**	**41.9 ± 23.8**	83.0 ± 26.5	86.4 ± 18.7
SH	NAF	**33.1 ± 8.3**	21.8 ± 8.9	66.7 ± 15.1	-12.6 ± 10.1	-23.3 ± 15.0	**67.8 ± 10.7**	**105.1 ± 29.7**	100.9 ± 15.4
	AF	**22.9 ± 13.2**	21.7 ± 18.9	71.9 ± 16.1	-17.4 ± 18.2	-33.2 ± 19.2	**41.7 ± 23.8**	**89.4 ± 35.0**	97.3 ± 26.9
SL	NAF	**32.7 ± 10.4**	20.0 ± 14.0	66.9 ± 13.9	**-12.7 ± 12.0**	**-16.9 ± 26.9**	**64.6 ± 14.8**	90.6 ± 33.1	86.9 ± 11.6
	AF	**22.5 ± 9.3**	23.1 ± 16.7	67.6 ± 11.5	**-18.9 ± 14.4**	**-29.4 ± 17.2**	**43.4 ± 24.1**	79.8 ± 18.9	86.7 ± 18.3

Table B.3: Mean and standard deviation of the arm joint angles (in degrees) measured during the grasping action for the tasks in position 3. Bold values indicate a significant difference between AF and NAF arms (Wilcoxon signed rank test, $P < 0.05$).

Pos 3		Sh Flex	Sh Abd	El Flex	Wr Sup	Wr Flex	T Flex	M Flex	I Flex
BW	NAF	**42.3 ± 12.5**	24.7 ± 13.3	**65.0 ± 11.7**	-19.9 ± 17.9	**-4.9 ± 13.2**	**71.3 ± 10.9**	76.8 ± 20.3	**36.1 ± 20.4**
	AF	**31.4 ± 16.2**	28.4 ± 19.1	**81.3 ± 32.7**	-28.4 ± 34.8	**-20.9 ± 25.0**	**46.7 ± 42.8**	85.9 ± 27.0	**79.2 ± 40.0**
BH	NAF	**39.8 ± 9.0**	21.1 ± 15.4	64.2 ± 14.0	-38.6 ± 19.3	-17.4 ± 22.1	**71.4 ± 11.8**	87.4 ± 19.3	56.0 ± 28.7
	AF	**32.1 ± 13.1**	27.2 ± 24.4	74.3 ± 32.6	-28.6 ± 29.2	-8.9 ± 28.9	**52.1 ± 27.3**	79.0 ± 19.7	55.7 ± 30.2
BL	NAF	**43.5 ± 8.2**	24.4 ± 11.7	**59.9 ± 15.3**	-29.7 ± 16.6	-4.8 ± 19.5	**63.3 ± 15.3**	**78.3 ± 20.3**	**40.9 ± 17.4**
	AF	**32.9 ± 14.9**	19.1 ± 21.7	**69.6 ± 20.1**	-29.5 ± 27.4	-20.3 ± 32.4	**39.9 ± 51.3**	**66.1 ± 14.5**	**57.0 ± 28.8**
SW	NAF	30.2 ± 9.1	17.6 ± 9.4	70.3 ± 13.0	-10.8 ± 8.0	**-21.9 ± 13.3**	**63.3 ± 11.1**	89.8 ± 26.5	81.9 ± 20.1
	AF	27.5 ± 11.6	19.4 ± 18.8	65.8 ± 13.8	-16.4 ± 16.7	**-33.2 ± 17.6**	**37.0 ± 22.7**	81.7 ± 22.9	82.7 ± 15.7
SH	NAF	**32.3 ± 11.0**	21.5 ± 7.5	68.5 ± 16.3	-13.3 ± 7.7	-23.5 ± 11.4	**68.4 ± 12.9**	101.0 ± 23.4	95.7 ± 13.2
	AF	**22.4 ± 10.7**	20.4 ± 15.1	72.4 ± 16.2	-17.4 ± 17.7	-29.8 ± 19.6	**38.6 ± 22.4**	85.4 ± 32.6	92.2 ± 28.3
SL	NAF	**31.1 ± 9.6**	20.3 ± 12.3	69.5 ± 12.7	**-12.0 ± 9.7**	**-19.8 ± 21.0**	**63.4 ± 13.5**	**94.8 ± 32.0**	84.7 ± 17.7
	AF	**21.5 ± 8.3**	23.0 ± 17.5	69.3 ± 11.0	**-18.9 ± 17.3**	**-28.0 ± 17.0**	**45.1 ± 23.3**	**80.1 ± 25.9**	84.9 ± 18.0

Table B.4: Mean and standard deviation of the arm joint angles (in degrees) measured during the grasping action for the tasks in position 4. Bold values indicate a significant difference between AF and NAF arms (Wilcoxon signed rank test, $P < 0.05$).

Pos 4		Sh Flex	Sh Abd	El Flex	Wr Sup	Wr Flex	T Flex	M Flex	I Flex
BW	NAF	**39.9 ± 10.0**	23.7 ± 11.3	**61.6 ± 10.8**	-29.5 ± 16.4	**-10.0 ± 14.5**	**72.8 ± 13.0**	74.3 ± 25.9	**37.1 ± 18.1**
	AF	**28.7 ± 14.8**	26.7 ± 21.8	**82.1 ± 32.2**	-27.1 ± 35.6	**-25.2 ± 27.9**	**47.2 ± 43.9**	83.1 ± 29.8	**76.0 ± 35.9**
BH	NAF	39.3 ± 9.2	22.4 ± 13.9	**61.4 ± 13.1**	-42.3 ± 20.2	-14.4 ± 15.1	**71.6 ± 14.8**	75.9 ± 29.4	47.3 ± 27.6
	AF	33.0 ± 15.5	28.3 ± 21.8	**77.2 ± 29.0**	-24.8 ± 36.2	-6.0 ± 26.6	**51.5 ± 30.3**	77.7 ± 20.2	52.5 ± 23.7
BL	NAF	**42.6 ± 10.6**	23.6 ± 12.8	**56.7 ± 14.8**	-36.3 ± 15.4	**-7.8 ± 17.3**	**66.1 ± 18.3**	**78.1 ± 25.5**	**43.0 ± 20.3**
	AF	**32.8 ± 14.3**	16.4 ± 21.1	**68.9 ± 20.9**	-27.5 ± 26.0	**-25.5 ± 35.1**	**39.3 ± 52.7**	**61.1 ± 18.6**	**57.5 ± 28.3**
SW	NAF	31.4 ± 8.4	16.2 ± 10.5	66.8 ± 12.6	**-10.3 ± 8.2**	**-23.6 ± 13.8**	**62.2 ± 14.8**	**102.1 ± 19.8**	84.4 ± 15.5
	AF	27.0 ± 11.6	19.1 ± 20.3	64.9 ± 13.7	**-15.8 ± 14.0**	**-35.4 ± 17.1**	**38.6 ± 22.5**	**79.5 ± 26.1**	84.4 ± 17.4
SH	NAF	**33.1 ± 8.4**	19.9 ± 10.1	65.6 ± 17.1	-11.1 ± 10.0	-26.7 ± 15.3	**68.5 ± 11.8**	**106.6 ± 31.4**	96.3 ± 16.0
	AF	**20.9 ± 12.6**	20.4 ± 15.4	73.0 ± 16.9	-16.0 ± 18.1	-31.9 ± 19.2	**34.8 ± 22.8**	**84.1 ± 36.6**	91.1 ± 31.9
SL	NAF	**31.9 ± 9.8**	17.6 ± 15.7	66.2 ± 15.0	-13.4 ± 10.4	**-20.0 ± 21.2**	**63.1 ± 17.3**	92.8 ± 30.1	84.7 ± 12.6
	AF	**22.0 ± 9.6**	23.5 ± 18.0	68.7 ± 12.4	-17.0 ± 16.1	**-28.6 ± 19.2**	**44.7 ± 24.8**	76.4 ± 24.7	84.4 ± 18.6

B.1.2 Placing action joint angles

Table B.5: Mean and standard deviation of the arm joint angles (in degrees) measured during the placing action for the tasks in position 1. Bold values indicate a significant difference between AF and NAF arms (Wilcoxon signed rank test, $P < 0.05$).

Pos 1		Sh Flex	Sh Abd	El Flex	Wr Sup	Wr Flex	T Flex	M Flex	I Flex
BW	NAF	**60.9 ± 11.6**	**16.1 ± 15.7**	**22.7 ± 13.0**	-17.8 ± 10.1	-19.8 ± 13.8	**69.4 ± 11.5**	75.4 ± 18.1	**34.1 ± 14.3**
	AF	**42.5 ± 15.7**	**30.1 ± 18.6**	**47.2 ± 33.1**	-16.2 ± 26.1	-29.0 ± 26.6	**52.8 ± 31.2**	80.0 ± 21.5	**71.9 ± 41.3**
BH	NAF	**58.5 ± 13.1**	21.6 ± 17.1	**32.2 ± 14.8**	-22.6 ± 19.3	-24.6 ± 14.2	**69.8 ± 11.6**	86.9 ± 20.8	**45.5 ± 23.7**
	AF	**42.3 ± 13.3**	30.4 ± 21.6	**55.7 ± 27.8**	-25.8 ± 25.7	-26.1 ± 33.8	**53.6 ± 25.2**	76.0 ± 19.1	**71.5 ± 28.3**
BL	NAF	**60.2 ± 9.0**	20.4 ± 11.4	**22.3 ± 9.7**	-21.2 ± 14.2	-21.6 ± 15.3	**66.0 ± 21.7**	74.9 ± 18.3	**40.5 ± 11.3**
	AF	**47.1 ± 13.6**	21.6 ± 21.3	**40.3 ± 27.2**	-20.7 ± 23.9	-30.6 ± 24.7	**45.7 ± 35.2**	64.5 ± 24.8	**62.5 ± 36.1**
SW	NAF	**60.3 ± 9.4**	17.1 ± 11.6	**22.1 ± 15.0**	**-11.1 ± 10.9**	**-32.9 ± 10.8**	**65.6 ± 12.9**	96.4 ± 26.0	87.9 ± 12.1
	AF	**47.5 ± 14.0**	24.2 ± 19.5	**30.3 ± 21.0**	**-10.7 ± 19.0**	**-45.0 ± 13.5**	**45.1 ± 22.4**	94.7 ± 20.0	87.7 ± 16.8
SH	NAF	**57.6 ± 11.5**	23.8 ± 15.6	**27.5 ± 12.3**	-11.8 ± 10.7	-37.6 ± 11.7	**70.1 ± 11.1**	107.3 ± 27.2	99.5 ± 11.9
	AF	**42.0 ± 13.3**	28.5 ± 22.0	**39.7 ± 22.9**	-14.4 ± 17.2	-40.4 ± 14.9	**47.3 ± 23.1**	98.5 ± 28.7	99.2 ± 25.4
SL	NAF	**61.0 ± 11.0**	**18.3 ± 12.9**	**20.3 ± 10.4**	-9.6 ± 7.7	**-27.9 ± 23.9**	**66.3 ± 14.3**	91.8 ± 31.5	81.9 ± 15.6
	AF	**40.2 ± 12.6**	**31.6 ± 20.1**	**35.7 ± 18.9**	-12.9 ± 14.8	**-42.2 ± 13.5**	**51.3 ± 25.0**	91.8 ± 31.0	87.7 ± 17.9

Table B.6: Mean and standard deviation of the arm joint angles (in degrees) measured during the placing action for the tasks in position 2. Bold values indicate a significant difference between AF and NAF arms (Wilcoxon signed rank test, $P < 0.05$).

Pos 2		Sh Flex	Sh Abd	El Flex	Wr Sup	Wr Flex	T Flex	M Flex	I Flex
BW	NAF	**39.7 ± 16.9**	41.9 ± 15.8	**19.6 ± 12.5**	**-6.1 ± 7.8**	**-20.5 ± 12.1**	**68.3 ± 13.7**	74.1 ± 16.3	**32.5 ± 14.7**
	AF	**24.9 ± 17.2**	45.9 ± 16.0	**42.8 ± 30.5**	**-17.8 ± 13.6**	**-33.7 ± 29.8**	**47.2 ± 39.2**	79.8 ± 25.4	**73.3 ± 45.2**
BH	NAF	**39.8 ± 18.9**	42.7 ± 12.4	**23.9 ± 14.9**	-13.8 ± 16.3	-29.2 ± 17.7	**67.6 ± 12.5**	81.3 ± 21.0	**46.7 ± 25.2**
	AF	**24.8 ± 12.4**	46.0 ± 18.7	**49.9 ± 21.9**	-26.6 ± 32.2	-26.4 ± 35.8	**49.3 ± 25.0**	76.7 ± 20.6	**68.6 ± 24.1**
BL	NAF	**39.5 ± 15.4**	43.1 ± 12.7	**22.7 ± 9.2**	-4.1 ± 9.7	-23.3 ± 18.1	**59.8 ± 19.7**	78.3 ± 16.9	**35.3 ± 11.3**
	AF	**28.4 ± 12.3**	43.7 ± 18.3	**40.4 ± 20.2**	-11.5 ± 20.5	-35.3 ± 30.5	**43.3 ± 37.2**	70.9 ± 22.1	**64.9 ± 37.0**
SW	NAF	**41.2 ± 17.4**	41.6 ± 13.1	**16.6 ± 12.0**	3.2 ± 11.4	**-34.8 ± 13.2**	**64.3 ± 11.4**	93.4 ± 25.2	83.3 ± 8.1
	AF	**27.2 ± 16.2**	44.2 ± 16.4	**27.6 ± 17.4**	-0.5 ± 15.5	**-41.9 ± 19.0**	**45.4 ± 22.6**	88.3 ± 25.4	84.4 ± 14.8
SH	NAF	**38.1 ± 11.8**	45.8 ± 7.8	**20.5 ± 12.7**	**5.1 ± 11.0**	-34.9 ± 17.2	**68.8 ± 13.5**	99.9 ± 30.1	93.8 ± 13.8
	AF	**22.4 ± 12.0**	46.8 ± 16.5	**31.3 ± 19.1**	**-3.4 ± 23.0**	-43.9 ± 18.6	**45.3 ± 27.3**	91.5 ± 35.5	91.7 ± 28.4
SL	NAF	**38.7 ± 16.3**	42.6 ± 14.0	**21.3 ± 17.4**	**3.8 ± 12.8**	**-25.5 ± 28.9**	**63.8 ± 14.9**	84.4 ± 28.0	81.1 ± 7.4
	AF	**18.8 ± 15.6**	46.9 ± 14.4	**31.9 ± 13.8**	**-4.8 ± 13.8**	**-39.9 ± 18.3**	**48.0 ± 22.5**	88.8 ± 32.1	85.0 ± 16.1

Table B.7: Mean and standard deviation of the arm joint angles (in degrees) measured during the placing action for the tasks in position 3. Bold values indicate a significant difference between AF and NAF arms (Wilcoxon signed rank test, $P < 0.05$).

Pos 3		Sh Flex	Sh Abd	El Flex	Wr Sup	Wr Flex	T Flex	M Flex	I Flex
BW	NAF	**62.4 ± 13.9**	**24.0 ± 12.8**	**17.8 ± 15.7**	-7.9 ± 18.0	**-6.8 ± 14.0**	65.3 ± 13.8	73.6 ± 20.0	**37.9 ± 19.5**
	AF	**50.7 ± 17.3**	**34.9 ± 18.4**	**46.7 ± 31.6**	-18.0 ± 31.7	**-28.6 ± 37.8**	51.6 ± 35.3	82.9 ± 31.8	**88.3 ± 47.1**
BH	NAF	**66.0 ± 13.5**	23.0 ± 14.7	**22.6 ± 13.0**	-27.2 ± 20.6	-21.7 ± 23.0	**68.1 ± 14.7**	**89.4 ± 18.2**	58.9 ± 30.3
	AF	**48.6 ± 11.8**	33.2 ± 21.7	**47.0 ± 23.3**	-27.3 ± 34.8	-13.0 ± 40.1	**52.2 ± 28.1**	**67.6 ± 24.8**	73.6 ± 34.5
BL	NAF	**66.8 ± 9.7**	20.4 ± 14.7	**15.3 ± 6.9**	-17.0 ± 14.6	**-14.2 ± 19.4**	52.4 ± 20.7	65.6 ± 28.6	**44.7 ± 27.0**
	AF	**61.4 ± 11.9**	22.3 ± 15.5	**35.6 ± 24.3**	-23.1 ± 22.5	**-33.7 ± 29.0**	40.7 ± 49.2	64.8 ± 21.6	**73.7 ± 38.5**
SW	NAF	**69.6 ± 6.2**	**14.7 ± 15.4**	**18.2 ± 8.1**	-4.8 ± 9.9	**-21.3 ± 13.1**	**57.9 ± 15.6**	95.0 ± 22.8	82.5 ± 18.7
	AF	**59.1 ± 12.1**	**25.4 ± 15.2**	**31.0 ± 24.3**	-1.8 ± 22.4	**-32.7 ± 15.2**	**35.8 ± 21.4**	92.0 ± 24.6	87.1 ± 14.7
SH	NAF	**68.5 ± 11.6**	**19.4 ± 14.2**	**20.2 ± 9.7**	-3.2 ± 9.8	**-20.5 ± 17.6**	**64.6 ± 14.4**	102.8 ± 30.0	96.3 ± 19.7
	AF	**52.7 ± 12.6**	**32.7 ± 14.0**	**36.9 ± 28.7**	-5.0 ± 21.7	**-29.2 ± 15.6**	**39.6 ± 23.1**	95.9 ± 36.1	96.6 ± 27.4
SL	NAF	**68.9 ± 7.3**	**18.0 ± 11.7**	**18.9 ± 7.9**	-2.0 ± 8.8	**-20.3 ± 16.0**	**57.5 ± 16.7**	98.4 ± 30.7	89.0 ± 17.9
	AF	**49.5 ± 16.4**	**36.4 ± 19.9**	**35.7 ± 21.0**	-5.1 ± 18.1	**-29.6 ± 14.8**	**45.3 ± 21.5**	93.6 ± 31.7	88.4 ± 17.2

Table B.8: Mean and standard deviation of the arm joint angles (in degrees) measured during the placing action for the tasks in position 4. Bold values indicate a significant difference between AF and NAF arms (Wilcoxon signed rank test, $P < 0.05$).

Pos 4		Sh Flex	Sh Abd	El Flex	Wr Sup	Wr Flex	T Flex	M Flex	I Flex
BW	NAF	43.1 ± 16.1	43.2 ± 23.0	**14.1 ± 9.2**	**9.1 ± 14.3**	**-22.5 ± 18.9**	**66.3 ± 13.9**	75.2 ± 17.1	**39.7 ± 19.8**
	AF	34.1 ± 20.0	51.6 ± 21.3	**46.0 ± 28.7**	**-6.9 ± 36.7**	**-41.4 ± 35.7**	**44.5 ± 39.1**	84.9 ± 33.0	**97.1 ± 40.7**
BH	NAF	**43.2 ± 15.2**	46.8 ± 15.2	**16.7 ± 9.9**	-1.5 ± 19.3	-28.4 ± 21.9	**68.9 ± 15.6**	84.0 ± 23.2	**56.0 ± 30.4**
	AF	**34.5 ± 14.7**	51.9 ± 17.7	**43.2 ± 17.4**	-9.2 ± 40.0	-15.1 ± 40.4	**52.1 ± 30.2**	73.9 ± 20.0	**71.1 ± 30.7**
BL	NAF	44.9 ± 12.1	44.8 ± 12.7	**12.1 ± 7.8**	**18.5 ± 11.8**	**-25.8 ± 21.9**	51.4 ± 23.5	80.0 ± 24.6	**40.9 ± 24.4**
	AF	42.6 ± 14.1	44.5 ± 17.2	**35.4 ± 22.0**	**1.1 ± 30.6**	**-39.3 ± 31.7**	41.5 ± 38.2	66.9 ± 21.7	**76.5 ± 38.1**
SW	NAF	**45.8 ± 13.3**	**43.4 ± 15.2**	**13.5 ± 10.2**	29.0 ± 11.1	**-23.4 ± 16.1**	**58.6 ± 12.8**	102.0 ± 17.8	**75.8 ± 12.4**
	AF	**37.8 ± 15.6**	**50.4 ± 17.8**	**29.0 ± 17.6**	20.3 ± 23.5	**-34.2 ± 18.5**	**33.7 ± 24.3**	90.6 ± 33.3	**87.1 ± 15.3**
SH	NAF	**42.1 ± 11.1**	**47.9 ± 11.1**	**14.9 ± 10.5**	**30.4 ± 11.4**	-25.8 ± 19.0	**63.7 ± 18.1**	111.6 ± 27.8	94.9 ± 21.5
	AF	**30.8 ± 14.9**	**54.4 ± 16.8**	**33.8 ± 24.0**	**14.2 ± 23.6**	-33.2 ± 16.0	**36.0 ± 20.2**	98.2 ± 33.6	98.6 ± 30.3
SL	NAF	**44.9 ± 14.3**	**45.1 ± 14.3**	**14.6 ± 11.7**	29.9 ± 19.2	**-21.0 ± 21.3**	**54.4 ± 20.9**	96.2 ± 24.0	85.2 ± 11.5
	AF	**27.5 ± 19.1**	**58.0 ± 16.8**	**29.5 ± 16.8**	22.8 ± 21.7	**-31.4 ± 17.8**	**41.2 ± 23.3**	91.9 ± 36.9	86.9 ± 19.2

B.1.3 Trunk compensation angles

Table B.9: Mean and standard deviation of the trunk compensation angles (in degrees) for the tasks in all target positions. Bold values indicate a significant difference between AF and NAF arms (Wilcoxon signed rank test, $P < 0.05$).

		Pos 1			**Pos 2**		
		Tr Front	**Tr Lat**	**Tr Rot**	**Tr Front**	**Tr Lat**	**Tr Rot**
BW	NAF	**8.9 ± 4.7**	5.0 ± 2.2	10.3 ± 2.6	**4.7 ± 3.0**	**3.7 ± 2.2**	**3.8 ± 1.4**
	AF	**11.9 ± 5.1**	6.0 ± 2.8	10.7 ± 3.7	**7.5 ± 3.5**	**5.7 ± 2.6**	**9.6 ± 6.2**
BH	NAF	**11.7 ± 5.4**	**5.9 ± 1.9**	10.4 ± 3.8	**5.7 ± 2.2**	**4.9 ± 2.0**	**4.4 ± 1.2**
	AF	**16.0 ± 6.5**	**7.8 ± 2.7**	10.5 ± 4.1	**10.5 ± 3.0**	**8.6 ± 3.9**	**13.3 ± 9.6**
BL	NAF	9.2 ± 4.4	5.3 ± 2.3	10.5 ± 5.0	**4.3 ± 2.8**	**4.3 ± 2.7**	**3.9 ± 1.5**
	AF	10.6 ± 4.8	7.1 ± 4.9	9.9 ± 3.5	**6.7 ± 3.8**	**6.2 ± 3.0**	**9.2 ± 5.8**
SW	NAF	11.5 ± 4.7	6.2 ± 3.6	**11.9 ± 4.4**	**6.8 ± 4.6**	**4.5 ± 3.3**	**3.3 ± 1.2**
	AF	13.3 ± 5.4	5.1 ± 2.7	**9.4 ± 3.5**	**9.5 ± 5.2**	**7.8 ± 3.2**	**7.3 ± 4.3**
SH	NAF	14.1 ± 6.4	7.1 ± 3.2	12.0 ± 5.4	9.1 ± 6.1	**5.8 ± 3.2**	**3.9 ± 1.4**
	AF	13.5 ± 5.7	5.7 ± 3.8	10.0 ± 4.1	7.5 ± 4.6	**7.3 ± 3.7**	**7.5 ± 4.7**
SL	NAF	**11.8 ± 5.3**	5.4 ± 2.1	11.0 ± 4.7	**8.2 ± 6.0**	**5.4 ± 3.0**	**3.4 ± 1.6**
	AF	**16.3 ± 7.0**	6.1 ± 4.0	10.9 ± 4.6	**10.5 ± 6.9**	**7.4 ± 3.1**	**8.2 ± 3.9**

		Pos 3			**Pos 4**		
		Tr Front	**Tr Lat**	**Tr Rot**	**Tr Front**	**Tr Lat**	**Tr Rot**
BW	NAF	7.9 ± 4.3	8.4 ± 4.6	11.2 ± 4.3	**7.3 ± 3.7**	6.3 ± 2.8	**7.1 ± 2.7**
	AF	9.5 ± 3.1	10.1 ± 4.0	10.4 ± 4.1	**11.5 ± 6.2**	7.0 ± 3.7	**16.6 ± 12.0**
BH	NAF	**9.1 ± 4.8**	**9.7 ± 3.4**	11.0 ± 5.4	**7.2 ± 3.7**	**6.1 ± 2.5**	**7.2 ± 2.7**
	AF	**12.3 ± 4.3**	**13.5 ± 4.5**	11.3 ± 4.4	**11.8 ± 5.0**	**9.6 ± 4.7**	**19.8 ± 13.6**
BL	NAF	8.4 ± 3.9	**8.4 ± 4.4**	9.8 ± 5.9	5.9 ± 3.1	5.4 ± 2.0	**5.8 ± 2.6**
	AF	7.5 ± 3.8	**11.3 ± 5.3**	10.0 ± 3.5	7.0 ± 3.9	6.5 ± 3.0	**13.3 ± 8.2**
SW	NAF	8.0 ± 4.8	7.4 ± 3.4	9.5 ± 4.6	**6.2 ± 3.8**	4.9 ± 2.8	**5.1 ± 2.4**
	AF	7.7 ± 3.6	8.9 ± 2.7	9.6 ± 4.2	**9.4 ± 2.9**	5.7 ± 2.8	**11.6 ± 6.5**
SH	NAF	9.4 ± 5.2	8.9 ± 3.9	9.2 ± 4.8	7.8 ± 4.7	6.0 ± 2.6	**5.5 ± 2.1**
	AF	8.0 ± 3.9	9.7 ± 4.1	8.3 ± 3.2	6.7 ± 3.4	5.7 ± 2.3	**13.1 ± 8.1**
SL	NAF	9.0 ± 4.7	8.2 ± 3.8	9.7 ± 4.8	6.5 ± 4.0	5.2 ± 2.0	**5.1 ± 2.2**
	AF	9.1 ± 3.9	9.5 ± 4.1	8.7 ± 3.7	7.8 ± 3.1	5.3 ± 2.5	**10.0 ± 4.8**

B.2 Block variation analysis

The following section presents the detailed results of the post-hoc analysis on the effect of each block in the arm and trunk postures of the affected limb during the grasping and placing actions of the reach-grasp-displace tasks done in the experimental protocol of Chapter 4.

B.2.1 Block variation during the grasping action

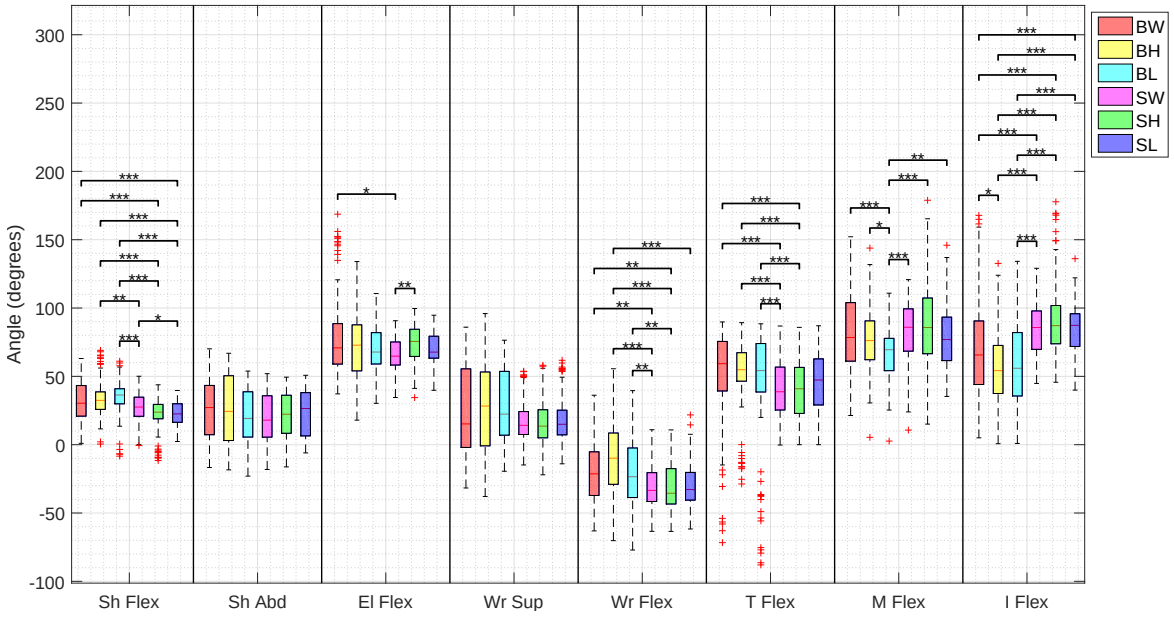

Figure B.1: Arm joint angles of the AF arm for the reach-grasp-displace tasks with each block. Statistical significant mean differences are calculated with Bonferroni method. *- $P < 0.05$; **- $P < 0.01$; ***- $P < 0.001$

B.2.2 Block variation during the placing action

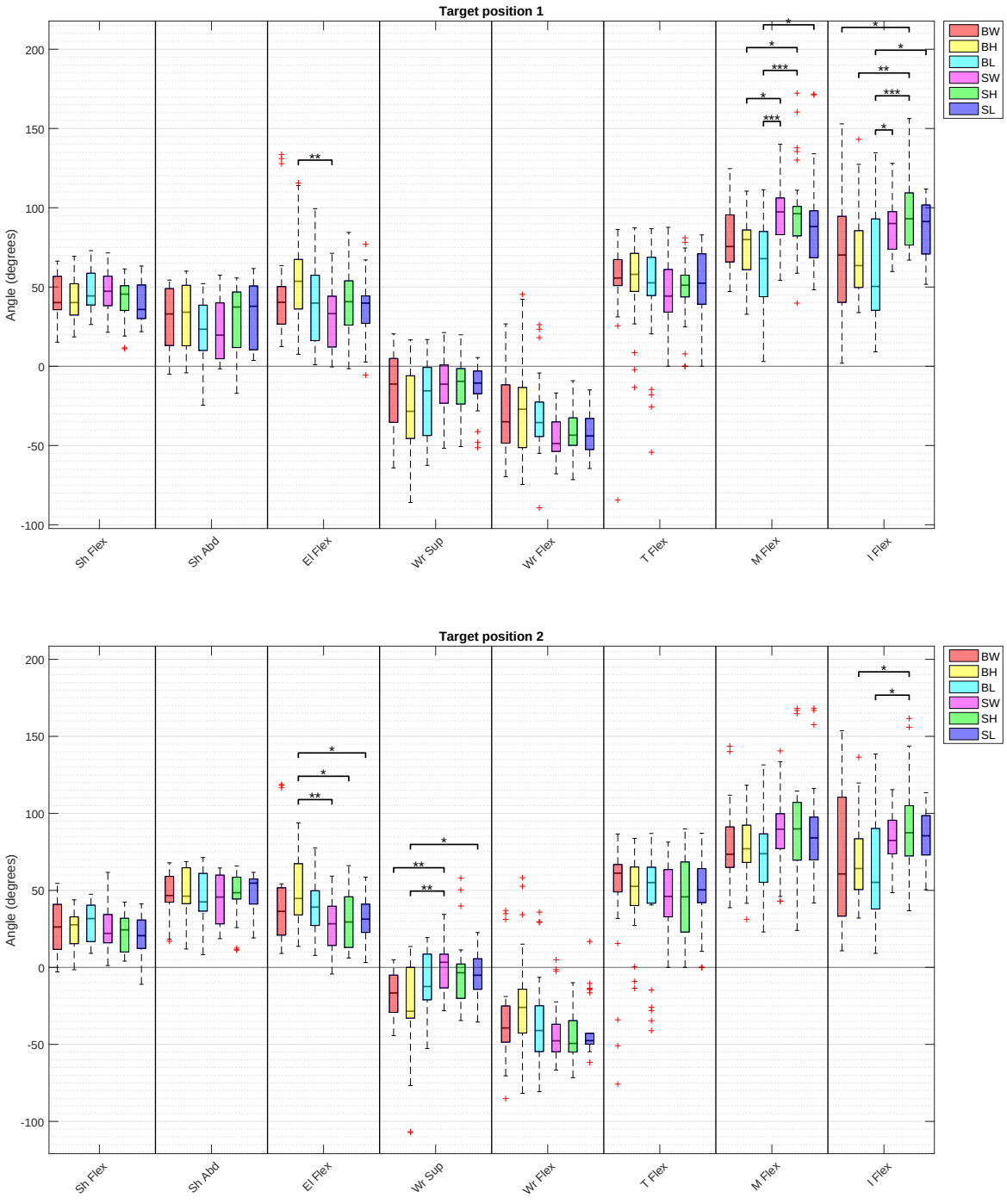

Figure B.2: Arm joint angles of the AF arm for each task separated in blocks, for the target positions 1 and 2. Statistical significant mean differences are calculated with Bonferroni method. *- $P < 0.05$; **- $P < 0.01$; ***- $P < 0.001$

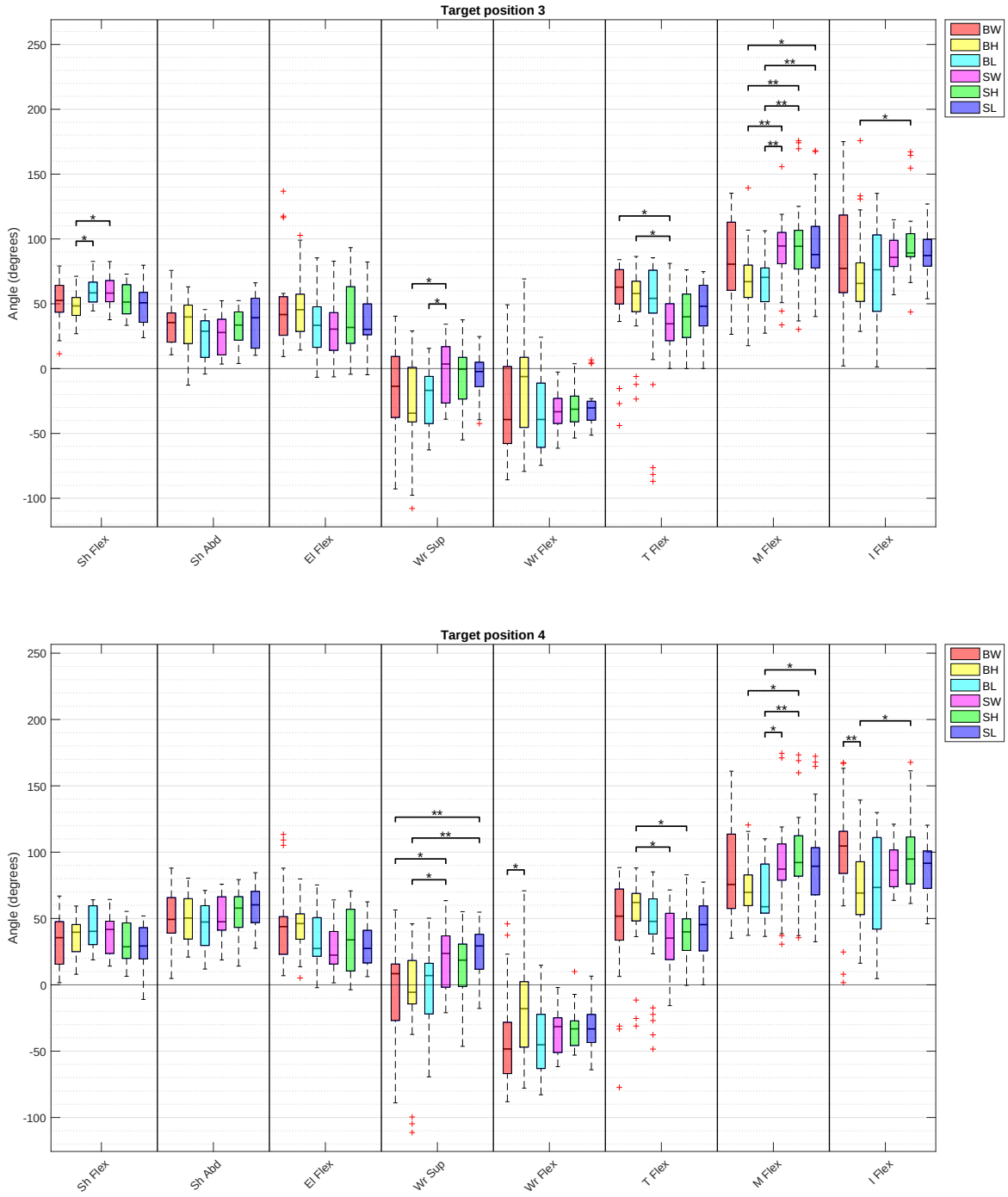

Figure B.3: Arm joint angles of the AF arm for each task separated in blocks, for the target positions 3 and 4. Statistical significant mean differences are calculated with Bonferroni method. *- $P < 0.05$; **- $P < 0.01$; ***- $P < 0.001$

B.2.3 Block variation in the trunk compensation

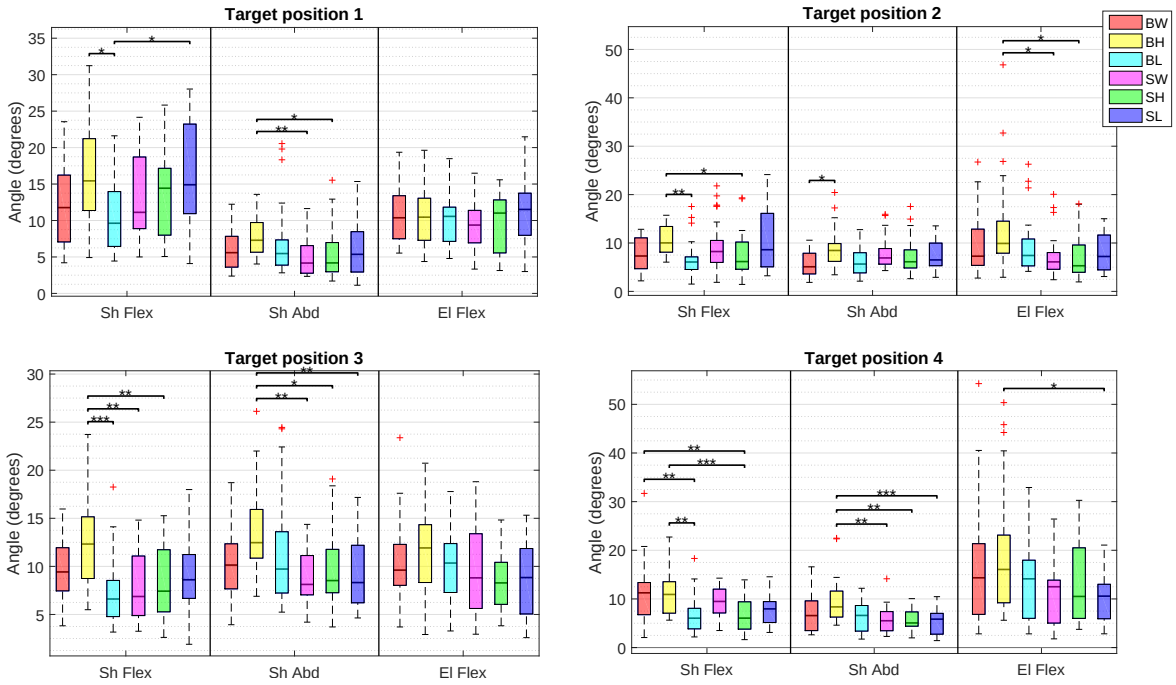

Figure B.4: Trunk compensation angles of the AF arm for each task separated in blocks, for all the target positions. Statistical significant mean differences are calculated with Bonferroni method. *- $P < 0.05$; **- $P < 0.01$; ***- $P < 0.001$